Relating the midbrain dopaminergic system to hippocampal cell assembly dynamics associated with spatial memory function

Doctor of Philosophy (D. Phil.) Thesis

Colin McNamara
Magdalen College

2015

MRC Anatomical Neuropharmacology Unit
Department of Pharmacology
University of Oxford

Abstract

Relating the midbrain dopaminergic system to hippocampal cell assembly dynamics associated with spatial memory function

Colin McNamara, Magdalen College
Thesis submitted for the degree of Doctor of Philosophy, Trinity Term 2015

Central to the understanding of memory is a detailed understanding of the processes contributing to how some information is retained as memories, yet other information is not. Relevant to this is the question, does value and saliency information coded by dopaminergic neurons of the ventral tegmental area (VTA) affect hippocampal memory function and how might this arise? In order to address this question, I performed large scale extracellular recordings combined with optogenetic activation of dopaminergic neurons in mice. Tetrodes were located in the VTA and pyramidal cell layer of the CA1 subfield of the dorsal hippocampus. Midbrain dopaminergic neurons were made to express a chimeric protein formed of the light activated ion channel channelrhodopsin-2 and enhanced yellow florescent protein (ChR2-eYFP) through injection of a Cre activated viral construct in the VTA of DAT-IRES-$Cre^{+/-}$ mice. Mice explored familiar and novel open fields in the presence or absence of photostimulation. Periods of sleep and rest were recorded before and after each exploration in order to calculate the reactivation strength of hippocampal waking firing activity during subsequent sleep; a process thought to aid the stabilisation of representations enhancing their retention as memories. ChR2-eYFP expressing axons were present in the dorsal hippocampus demonstrating a direct dopaminergic projection from the midbrain to the hippocampus. Units isolated from midbrain tetrodes showed a sustained increase in mean firing rate during exploration of a novel over a familiar environment, indicating they have the potential to drive sustained dopamine release in target structures in response to such a sustained novelty cue. Hippocampal reactivation strength after exploration of a novel environment was higher than that seen after exploration of a familiar environment and this was further enhanced by burst mode photoactivation of dopaminergic neurons at their cell bodies in the VTA or at the afferent dopaminergic fibres in the dorsal CA1. A second group of mice performed a spatial learning task on a maze dubbed the 'crossword maze'. Photostimulation during learning trials did not increase the rate of learning but it did increase performance in a probe test held one hour after the end of the learning trials. Additionally, there was enhanced reinstatement of the hippocampal spatial representation during the probe test and it was preceded by enhanced reactivation of the newly formed representation in the intervening rest period. These findings reveal that midbrain dopaminergic neurons, encoding salient information about an environment, promote hippocampal network dynamics associated with memory persistence, thus modulating hippocampal memory function according to the value of the information to be remembered.

Acknowledgments

I would like to thank my primary supervisor Dr. David Dupret for all that he has taught me in guiding me through all parts of this project, from hands on training in the complex techniques used in this work, to developing my high-level scientific thinking and everything in between including data analysis. I am truly grateful for this remarkable training which I may now bring forward to my future scientific work. I would also like to thank my second supervisor Prof. Peter J. Magill for his valuable input, guidance and training throughout this work.

I wish to thank visiting masters student Caroline Etienne for helping with quantification of ChR2-eYFP expression levels and 3D reconstruction of ChR2-eYFP expressing axonal segments in the dorsal hippocampus. I also wish to thank Natalia Campo-Urriza and Dr. Stephanie Trouche for help with some of the data collection (crossword maze and open field control animals). Thanks to those involved in the initial development of the crossword maze task (including the experiments with PV-IRES-Cre mice): Dr. Alvaro Tejero-Cantero, Steven Cuell and Natalia Campo-Urriza. I would also like to thank Dr. Alvaro Tejero-Cantero and Dr. Stephanie Trouche for their general guidance.

Thank you to unit members and support staff for their help and input: Liz Norman, Jane Janson, Dr. Paul Dodson, Dr. Linda Katona, Gido van de Ven, Anna-Kristin Kaufmann, Abhilasha Joshi, Kristina Wagner, Lisa Conyers, Katharine Whitworth, Gareth Hazell, Mary Gilgunn-Jones, Jo Stocker, Agnieszka Swiejkowska and director Prof. Peter Somogyi. Thanks to Dr. Sarah Threlfell for providing the initial DAT-IRES-Cre mice. I also wish to acknowledge the use of computer programs established by Prof. Jozsef Csicsvari and past members of his lab.

Finally, I would like to take this opportunity on a personal level to acknowledge and thank those who have made it possible for me to get to this point. I dedicate this thesis to my family and Linda for their loving support, and also to Marie Stubbings and the Dyslexia Support Centre Limerick for her incredible guidance, teaching and support enabling my survival through primary, secondary and degree level education.

My D. Phil. studies have been funded by a Medical Research Council Doctoral Training Award.

Contents

Figures

Tables

Abbreviations

A

AAV2	adeno-associated virus serotype two
ANOVA	analysis of variance

C

CA1-3	cornu ammonis 1-3
CCK	cholecystokinin
ChR2-eYFP	channelrhodopsin-2 fused to enhanced yellow fluorescent protein
CLi	caudal linear nucleus
CPP	conditioned place preference
CS	conditioned stimulus
CV	coefficient of variation
CV2	coefficient of variation 2

D

DA	dopaminergic
DAPI	4',6-diamidino-2-phenylindole
DAT	dopamine transporter protein
DBH	dopamine-beta-hydroxylase
DNMTS	delayed nonmatching-to-sample

E

EF1a	elongation factor 1-alpha promoter

G

GABA	gamma-amino butyric acid
GFP	green fluorescent protein
GIRK-2	G protein-coupled inward rectifying potassium channel

I

IF	interfascicular nucleus
IFRC	instantaneous firing rate counts
IRES	internal ribosome entry site
ISI	inter spike intervals

L

L-DOPA	L-3,4-dihydroxyphenylalanine
LFP	local field potential
LTP	long term potentiation

M

MAO	monoamine oxidase
mdDA	meso-diencephalic dopaminergic
MRI	magnetic resonance imaging
mRNA	messenger ribonucleic acid

N

NDS	normal donkey serum
NET	norepinephrine transporter
NMDA	N-methyl-D-aspartate receptor
NPY	neuropeptide y

O

O-LM	oriens-lacunosum moleculare

P

PBS	phosphate buffer saline
PFC	prefrontal cortex
PFS	place field similarity
PIF	parainterfascicular nucleus
PN	paranigral nucleus
PV	parvalbumin

R

REM	rapid eye movement
RLi	rostral linear nucleus
RMS	root mean square
RRF	retrorubral field

S

SD	standard deviation
SNc	substantia nigra pars compacta
SWR	sharp wave ripple

T

TH	tyrosine hydroxylase

V

VGAT	vesicular GABA transporter
VGluT2	vesicular glutamate transporter 2
VIP	vasoactive intestinal polypeptide
VMAT2	vesicular monoamine transporter 2
VTA	ventral tegmental area
VTAR	ventral tegmental area rostrodorsal part

W

WPRE	woodchuck hepatitis post-transcriptional regulatory element

Chapter 1 General introduction

1.1 Introduction

The focus of this thesis is on relating activity in two brain areas: (1) the cornu ammonis one (CA1) subfield of the hippocampus; and (2) the dopaminergic nuclei of the midbrain, particularly the ventral tegmental area (VTA). The hippocampus consisting of archicortex is among the most phylogenetically old of cortical areas. It derives from the medial regions of the telencephalon and is located at the base of the medial temporal lobe in humans. It is established as having an important role in declarative memory formation and is also believed to be a substrate for the allocentric representation of space (Eichenbaum and Cohen, 2014; Moser et al., 2015; O'Keefe and Nadel, 1978; O'Neill et al., 2010; Squire et al., 2004). On the other hand, the action potential firing of midbrain dopaminergic neurons, and particularly those of the VTA, is associated with salience, value and expectation mismatch (Cohen et al., 2012; Lak et al., 2014; Schultz et al., 1997). Midbrain dopaminergic neurons also play an important role in voluntary movement, although such functions are more closely associated with neurons of the substantia nigra pars compacta (Roeper, 2013). Of particular interest in studying these two brain areas are the questions; does value and saliency information coded in VTA affect hippocampal memory function and if so, how and over what time scales can this arise? A detailed understanding of this is important for understanding the neuronal processes contributing to how some information is retained as memories while other information is not, and hence, is central to understanding memory function in the brain.

In this chapter, I will first outline the structure, network properties and known functions of the hippocampus, and similarly for midbrain dopaminergic nuclei, before introducing some of the existing work relating the two brain areas. Finally, I will conclude the introductory chapter with an outline of the aims of this thesis.

1.2 Anatomical organisation of the hippocampal formation

The hippocampal formation consists of a number of cytoarchitectonically-distinct brain regions located in the medial temporal lobe in humans which form a functional system (Andersen et al., 2006; Shepherd, 2004). It includes the dentate gyrus, hippocampus proper also called cornu ammonis (abbreviated CA which can in turn be broken into three subfields, CA1-3), subiculum, presubiculum, parasubiculum, and entorhinal cortex. The strongest anatomical evidence to support the grouping of these brain areas into a functional group is the presence of a set of cascading strong excitatory projections which form a looping circuit extending from one area to the next. These projections were first described by Ramón y Cajal (1909) and are depicted in his drawing shown in Figure 1.1. The predominantly unidirectional nature of this substantial excitatory pathway running through the hippocampal formation, with relatively modest reciprocal connections, sets it aside from most other connectivity between cortical areas which is largely reciprocal in nature (Andersen et al., 1971; Felleman and Van Essen, 1991).

Of all the areas in the hippocampal formation, the entorhinal cortex is the only which unambiguously possesses the multilayer structure of a neocortical area. It is also widely connected with the rest of neocortex forming particularly abundant connections to perirhinal and parahippocampal (primates) or postrhinal (nonprimates) cortices (Burwell and Amaral, 1998a, b; Burwell et al., 1995; Canto et al., 2008). As such, the entorhinal cortex acts as the main entry point of sensory information into the hippocampal formation and the main means through which the processed output of the hippocampal formation is returned to the neocortex. It is therefore reasonable to consider entorhinal cortex as the start point in the loop of strong excitatory projections which extend through the hippocampal formation through the dentate gyrus, CA3, CA1 and the subiculum before returning to entorhinal cortex. In fact, entorhinal cortex sends strong projections forward to all stages of the loop however it only receives strong return projections from the final stages (CA1 and subiculum). In addition, the projections from the dentate gyrus to CA3, CA3 to CA1 and CA1 to the subiculum all lack a sizeable reciprocal connection although some return fibres are present (Andersen et al., 2006; Ishizuka et al., 1990; Shepherd, 2004).

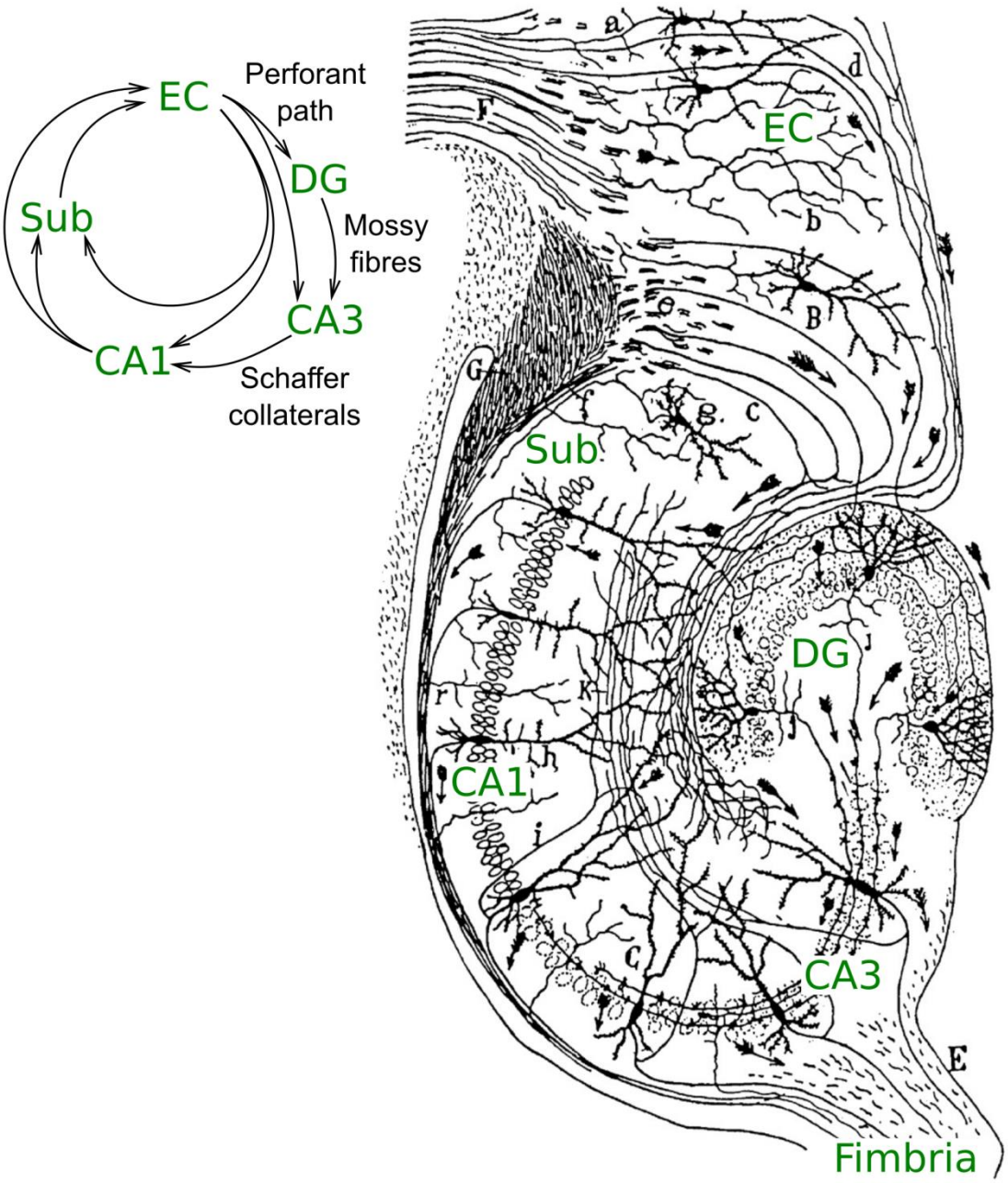

Figure 1.1 *Drawing of the hippocampus by Ramón y Cajal*
Drawing by Ramón y Cajal [(1909) page 753] showing the cascade of excitatory projections which form a looping circuit extending through the areas of the hippocampal formation. Added green labels: EC, entorhinal cortex; DG, dentate gyrus; CA1, cornu ammonis one; CA3, cornu ammonis three, Sub, subiculum. Note, the simplified schematic of connections depicting some of the large excitatory projections was added here and the CA2 subfield is omitted.

The first downstream target within the hippocampal formation from entorhinal cortex is the dentate gyrus. Entorhinal cortex gives rise to a large excitatory projection terminating in the molecular layer of the dentate gyrus forming synapses primarily on the dendritic spines of dentate granule cells. The axons forming this projection described by Ramón y Cajal, perforate

through the subiculum and hippocampal fissure to reach the dentate gyrus giving rise to the name perforant path. The majority of perforant path axons arise from cells in the superficial layers of the entorhinal cortex, particularly layer II, however some do originate in the deeper layers V and VI (Steward and Scoville, 1976).

The dentate gyrus in turn sends projection fibres exclusively to the CA3 subfield of the hippocampus proper (Andersen et al., 1971; Blackstad et al., 1970; Claiborne et al., 1986; Gaarskjaer, 1978; Swanson et al., 1978). The axons that form this projection, named 'mossy fibres', originate from the dentate granule cells and terminate on the proximal (near the cell body) dendrites of CA3 pyramidal neurons, forming complex synapses. Presynaptic terminals, located on extensions from the main axon called mossy fibre expansions, form synapses with intricately branched spines of the CA3 pyramidal neurons called thorny excrescences (Amaral and Dent, 1981). The mossy fibres also form synapses with CA3 interneurons via filopodial extensions (Acsády et al., 1998). Additionally, the CA3 subfield is directly innervated by perforant path fibres originating in entorhinal cortex which form synapses with CA3 pyramidal neurons at the distal tuft of their apical dendrites. The laminar origin and numbers of synaptic contacts of this projection are similar to those formed by perforant path fibres in dentate gyrus (Witter, 1993).

The next area in the cascade of connections is the CA1 subfield of the hippocampus proper. Pyramidal cells in CA3 send axon collaterals that form synapses with the dendrites of CA1 pyramidal neurons (Schaffer collaterals) as well as heavily projecting back into the CA3 subfield (associational connections) (Ishizuka et al., 1990; Li et al., 1994). As with previous areas in the cascade, CA1 pyramidal cells receive a direct projection from the entorhinal cortex to the distal tufts of their apical dendrites. However, in the case of CA1, this projection predominantly originates from layer III of entorhinal cortex, as opposed to layer II which gives rise to the perforant path projection to CA3 and the dentate gyrus (Witter, 1993). In addition, CA1 is the first brain area along the loop of cascading connections to have a strong direct reciprocal connection back to entorhinal cortex. Pyramidal cells in CA1 heavily project to both the subiculum and to the deep layers (layers V and VI) of entorhinal cortex (Cenquizca and Swanson, 2007; Naber et al., 2001; O'Mara et al., 2001; Witter et al., 1988). There are also direct CA1 projections to the dentate gyrus, presubiculum, parasubiculum and a wide range of

neocortical areas including visual, auditory, somatosensory, gustatory, main and accessory olfactory and visceral areas, as well as the basolateral amygdalar complex and the agranular insular and orbital areas (Cenquizca and Swanson, 2007). In contrast to CA3 pyramidal neurons, CA1 pyramidal neurons lack extensive associational connections, although some local interconnectivity is present (Amaral et al., 1991; Deuchars and Thomson, 1996; Takács et al., 2012).

The final brain areas in the hippocampal formation, the subiculum, presubiculum and parasubiculum, form a continuum between CA1 and entorhinal cortex. The subiculum is considered to have a three layer structure like the hippocampus proper however the pyramidal layer cell bodies are more dispersed. Conversely, the presubiculum and parasubiculum have a more multilayer structure resembling neocortex. Like CA1, from where it receives a strong input connection continuing the cascade of strong excitatory projections, the subiculum also has a large reciprocal connection with entorhinal cortex predominately receiving input from layer III and projecting back to layer V (Andersen et al., 2006; Kloosterman et al., 2003; O'Mara et al., 2001). The subiculum projects to the presubiculum and parasubiculum but this projection is perhaps best thought of as part of a number of projections distributing the processed information from the subiculum to a range of cortical and subcortical structures as opposed to a strong continuation of a feedforward cascade running through the hippocampal formation (Andersen et al., 2006). In fact, the subiculum is considered the main output region of hippocampal allocortex because it widely projects throughout neocortex in addition to innervating the entorhinal cortex (O'Mara et al., 2001; Verwer et al., 1997; Wyass and Van Groen, 1992). The presubiculum and parasubiculum project to many other parts of the hippocampal formation including a prominent projection to entorhinal cortex and a relatively strong projection from the parasubiculum to the dentate gyrus (Caballero-Bleda and Witter, 1993; Köhler, 1985), justifying their inclusion in the functional grouping of the hippocampal formation.

Two additional points are worth noting about the cascade of strong excitatory projections through the hippocampal formation. First, for each projection along the cascade (perhaps with the exception of the mossy fibres), small regions of the projecting region can influence large regions of the downstream target. That is, small regions of entorhinal cortex project to a large

number of dentate granule cells and similarly divergent projections are present from CA3 to CA1 and from CA1 to subiculum. This is potentially both divergent and convergent. It can allow information from a small input node to widely influence a large number of output nodes. Equally, a small output node can potentially bind information from a large number of disparate input nodes. The exact extent to which this occurs is still unclear and requires further investigation. The second point is that despite this high level of interconnectivity between regions of the hippocampal formation, there is still a broad topographical organisation maintained across all stages of the parallel projections of the loop, such that pathways originating in superficial layers of the entorhinal cortex return to the deep layers of the same portion of entorhinal cortex. This potentially allows for many parallel processing streams, with each returning to their cortical substrate of origin in a closed loop.

There are two additional fibre bundles associated with the hippocampus (Wyss et al., 1980). The first consists of the dorsal and ventral commissures that connect to the contralateral hippocampus. The second, and most relevant aspect of hippocampal structure in relation to this thesis, is created by both afferent and efferent fibres from the hippocampus which run along the ventricular surface to create a thin layer called the alveus. The alveus fibres gather together to create a fibre tract called the fimbria. The continuation of this fibre bundle descends into the forebrain before splitting into the rostrally directed precommissural fornix and a caudally directed postcommissural fornix. The precommissural fornix carries connections to and from the septal nuclei and nucleus accumbens. The postcommissural fornix extends towards the diencephalon and midbrain hosting connections with the hypothalamus, thalamus and the midbrain (Andersen et al., 2006). The postcommissural fornix runs adjacent to the medial forebrain bundle (Franklin and Paxinos, 2008) which contains dopaminergic fibres projecting from the midbrain up to the forebrain providing a point where dopaminergic fibres could potentially cross over into the fornix and continue to the hippocampus.

1.3 Anatomical organisation of the hippocampus proper

The hippocampus proper or, from now on, simply the ‘hippocampus’, is formed of archicortex which, in comparison to the six or more layers of neocortex, is considered to be a three-layer cortical structure. The basic structure of hippocampal cortex has long been described by

anatomists such as Arantius, Duvernoy and De Garengeot and it was particularly well documented by Ramón y Cajal (Amaral and Lavenex, 2006; Ramon y Cajal, 1893). The cell bodies of nearly all principal cells in the hippocampus are tightly packed together forming the middle layer and they send their processes out on either side of this layer into the outer two layers. The cell bodies of the many types of GABAergic interneurons in the hippocampus are located across all three layers. However, the selective projection of many of the pathways described in the previous section onto the various levels of the principal cell dendrites mean that it is more useful to divide the hippocampal substrate into more than three strata or layers (Amaral and Lavenex, 2006).

Before describing these layers it is first necessary to define a reference system. Because the hippocampus is formed of a folding of the cortical tissue around the subcortical white matter back onto itself, the reference system often used by anatomists reflects this, with the layer near the white matter being described as 'deep' and the layer near the pia and hippocampal fissure being referred to as 'superficial'. This is the most consistent across the continuum from neocortex into the hippocampus through the parasubiculum, presubiculum and subiculum, and will be the reference system of choice here, despite being sometimes counterintuitive from the point of view of introducing an electrode into the brain. Such an electrode will reach deep hippocampal layers in dorsal rodent CA1 before more superficial layers due to the folding of cortex under itself forming the hippocampus.

Perpendicular to the superficial-deep axis, and running along the flattened out cortical cortex from neocortex at one end to the dentate gyrus at the other, the hippocampus can be broken into three cytoarchitectonically-distinct subfields as already mentioned. The CA1 subfield is located adjacent to neocortex and borders the subiculum whereas the CA3 subfield is located adjacent to the dentate gyrus. The CA2 subfield is smaller than, and located between, the other two subfields. The final axis running perpendicular to both these axes along the curvature of the hippocampus from the septal to temporal poles is often broken into two, at least when describing the rodent brain, with the septal end referred to as 'dorsal' hippocampus and temporal end referred to as 'ventral' hippocampus. This final division is not based on a cytoarchitectonic distinction but there is evidence from lesion studies of differing regional function along the septal to temporal axis of the hippocampus, perhaps arising from

the differing connections with extrahippocampal brain areas such as greater connectivity of ventral CA1 with the amygdala and the hypothalamus–pituitary–adrenal (HPA) axis (Bannerman et al., 2004).

Returning to the layers of hippocampal cortex, the principal cells of the hippocampus are often referred to as 'pyramidal neurons' reflecting the shape of their cell bodies, and the layer containing the stomata of the principal cells is called stratum pyramidale. Stratum pyramidale is tightly packed with cell bodies in CA1, but slightly more loosely packed in CA2 and CA3, allowing determination of the border between CA1 and CA2. Stratum oriens is located deep to stratum pyramidale and contains the basal dendrites of the pyramidal neurons with which some of the CA3 to CA3 associational fibres or the CA3 to CA1 Schaffer collaterals form synapses. Deep of stratum oriens, located between the hippocampus and the subcortical white matter, is a thin fibre-containing layer called the alveus. Immediately superficial to stratum pyramidale in CA3, but not in CA2 or CA1, thus delineating the CA3/CA2 border, is a layer that has a somewhat clear appearance in fresh tissue resulting in the name stratum lucidum. This is the site of the dense mossy fibre projection from dentate gyrus into CA3, where the mossy fibre expansions form synapses with the thorny excrescences on the proximal dendrites of CA3 pyramidal neurons. Superficial to stratum lucidum in CA3, and stratum pyramidale in CA1 and CA2, is stratum radiatum where the bulk of the associational fibres (in the case of CA3) and Schaffer collaterals (in the case of CA1) form synapses onto the apical dendrites of the pyramidal neurons. Finally, located near the hippocampal fissure is the most superficial layer of the hippocampus proper called stratum lacunosum-moleculare. It contains the synapses formed by projections from the neocortex, particularly from entorhinal cortex, and the perforant path projection onto the apical tufts of pyramidal neurons.

1.4 The hippocampal formation and memory

The initial evidence implicating the medial temporal lobe including the hippocampal formation in memory function and particularly the formation of new explicit memories came from studies of patients with bilateral lesions in medial temporal lobe structures (Penfield and Milner, 1958; Scoville and Milner, 1957). The best known of these cases is that of the patient H.M. who received a bilateral medial temporal lobe resection at the age of twenty seven in an

attempt to control epileptic seizures (Scoville and Milner, 1957; Squire, 2009a). After the procedure H.M. still appeared to have intact working memory, could hold normal conversations, retained any skills he had learned previously and could recall events and facts from his past. However, he was not able to form new memories for explicit information or events once they had lapsed from immediate memory, nor could he remember events or information from the period leading up to the procedure. For instance, he could remember a three digit number for as long as fifteen minutes through continuous rehearsal, yet once his attention was shifted to a different topic, he would not only fail to recall the number but would forget the entire event (Squire, 2009a). Remarkably, H.M. was still able to learn new skills such as drawing a star while viewing his hand through a mirror. He showed excellent retention over three days of this learned visuo-motor skill despite being unable to recall the ten learning trials (Corkin, 1968; Squire, 2009a). These early lesion studies provided the first evidence that memory was not a single faculty, and different types of learning and memory abilities could be localised to separate brain structures. The terms declarative or explicit memories are often used to describe the type of memory which is dependent on medial temporal lobe structures and which H.M. was unable to retain. Memory types apparently independent of medial temporal lobe function are often termed nondeclarative memories, a term which encompasses a number of different types of memory or learning such as skill, habit, and emotional learning, as well as simple conditioning, priming and perceptual learning. The various different types of nondeclarative memory have been associated with structures throughout the brain including the basal ganglia, amygdala, neocortex and cerebellum (Squire, 2009b).

Both the post-operative report and a subsequent magnetic resonance imaging (MRI) study acknowledge that the extent of damage to H.M. was not limited to the hippocampal formation. The lesion was bilaterally symmetrical and included medial temporal polar cortex, most of the amygdaloid complex and approximately half of the rostrocaudal extent of the intraventricular portion of the hippocampal formation including most of the entorhinal cortex (Corkin et al., 1997). However, combined information from lesion studies across many patients with lesions varying in extent and location suggests that the effects on explicit memory formation experienced by H.M. were, in the main, due to the damage to structures of the

hippocampal formation including associated neocortical areas, and not the damage to other areas such as the amygdaloid complex (Kirwan et al., 2008; Penfield and Milner, 1958; Squire, 2009a; Zola-Morgan et al., 1986). Additionally, the memory impairment seen in H.M. was more dramatic than that seen in patients with smaller lesions implying that damage to a large extent of the hippocampal formation including neocortical areas is required to experience a full deficit in explicit memory formation.

A final important insight about medial temporal lobe function that can be gained by the case of H.M. is that he was impaired in forming new long term declarative memories; however he was able to remember declarative memories acquired before the surgery (Marslen-Wilson and Teuber, 1975; Milner et al., 1968; Squire, 2009a). This suggests, firstly, that structures external to the hippocampal formation can support the storage and recall of the memories, and secondly, that an intact hippocampal formation is required for the acquisition and incorporation of declarative type memories into these structures. There has been much debate about whether H.M. was capable of retaining truly episodic memories from childhood. However, studies probing the finer detail of this were conducted more than fifty years after the lesions (Steinvorth et al., 2005), and follow up MRI studies from this time showed cortical thinning and atrophy of deep grey matter structures suggesting the earlier reports, while less detailed, may be more relevant (Salat et al., 2006). Furthermore, a study involving other patients with medial temporal lobe damage found autobiographical memory to be impaired when memories were taken from the recent past but intact when taken from the distant past (Kirwan et al., 2008). In any case, whether or not truly episodic memories can be supported by structures external to the hippocampal formation, evidence to date indicates that such structures can store and facilitate the recall of declarative memories, including semantic information about events as well as arbitrary facts. Furthermore, the incorporation of such information into areas beyond the hippocampal formation is often facilitated through activity in the hippocampal formation (including entorhinal cortex), and damage to the hippocampal formation reduces facility for such memory formation (Manns et al., 2003). In fact, for the purpose of association with a locus of storage in disparate brain areas, dissociating declarative memories based on the quality of the remembered information into episodic (memory for events that are specific to a time and place) or semantic (learning and remembering facts) may

not be the most optimal, and thus, it may be more appropriate to dissociate on the basis of learning from multiple learning events or learning from a single or very small number of events (Squire et al., 2004).

The remarkable insight into memory function provided by the study of patients such as H.M. has prompted many animal studies investigating the mechanisms at play in the various structures of the hippocampal formation. The design of animal behavioural experiments to accurately capture the specifics of declarative memory has proven challenging and, although the various tasks conceived for monkeys and rodents have provided insights, they come with much methodological debate (Morris, 2006). The task that received early popularity was the delayed nonmatching-to-sample with trial-unique cues, abbreviated as DNMTS (Alvarez et al., 1994; Mishkin, 1978; Overman et al., 1990; Squire, 2004). Results from DNMTS studies in primates with medial temporal lobe lesions supported the findings in human patients showing deficits at longer delay intervals but with intact performance at shorter working memory type interval lengths. The extents of the lesions in these studies were also large, typically incorporating cortex surrounding the hippocampal formation as well as parts of the amygdala (Alvarez et al., 1994; Mishkin, 1978). However, Alvarez and colleagues (1994) targeted the hippocampus proper, dentate gyrus, subiculum, posterior half of entorhinal cortex, and parahippocampal cortex while sparing the amygdala. These studies also agreed with the finding in human patients that a large lesion encompassing a number of medial temporal lobe structures was required to produce profound deficits in performance. Further experiments, using selective lesions to distinct components of the medial temporal lobe aimed at more tightly defining the locus of declarative memory function, or attempting to attribute an independent contribution for the various brain areas, have largely produced unclear results, instead shifting focus back onto the importance of task design (Morris, 2006). Some of these studies found that lesions to neocortical areas adjacent to the hippocampus produced a larger deficit in DNMTS performance than lesions to the hippocampus proper (Meunier et al., 1993; Murray and Mishkin, 1998; Suzuki et al., 1993), whereas others show impairment after hippocampal lesions (Beason-Held et al., 1999). Whether these findings are reflective of what would happen in the case of more complex declarative memory is currently an open question.

Experiments with rodents have provided many insights into the role of the hippocampus in memory and the guidance of behaviour. Many of these experiments, in addition to building on findings from patients like H.M., were guided by two important findings dating from this time period; place cells and long term potentiation. 'Place cell' is a term used to describe the remarkable finding that many hippocampal cells fire action potentials selectively at one or a few locations in the environment (O'Keefe and Dostrovsky, 1971), and is discussed further in the next section. Long term potentiation (LTP) is the activity-dependent persistent strengthening of synaptic efficacy (Bliss and Collingridge, 1993). This synaptic property, whereby transmission efficacy is increased when the pre- and post-synaptic cell are active at the same time, had been previously proposed by Donald Hebb as a means through which learning and memory could be supported in the brain (Hebb, 1949). Changes in synaptic efficacy produced by LTP and its converse, long term depression (LTD) are present throughout the brain and their study in hippocampal networks provides a means to conceptualise some of the mechanisms at play in the hippocampal support of memory. Indeed, LTP was first identified in the mammalian brain at the synapses formed between perforant path fibres and dentate gyrus granule cells (Bliss and Lømo, 1973).

Two tasks that have been extensively utilised in investigations of hippocampal memory function in rodents are the Morris water maze (Morris, 1984) and the radial arm maze. Spatial reference memory can be tested in both tasks, whereas, depending on the rule used for reward delivery, the radial arm maze can also be used to test spatial working memory by requiring the animal to track in which arms it has already received a reward (Schmitt et al., 2003). Rodent hippocampal lesion studies have showed impaired spatial reference memory in the water maze (Morris et al., 1982; Morris et al., 1990). Interestingly, however, studies in transgenic animals attempting to attribute spatial memory to LTP in the hippocampus have produced a complex and controversial picture. The induction of LTP in hippocampal slice preparations is dependent on functional NMDA receptors, an ionotropic glutamate receptor subtype (Collingridge et al., 1983). After many experiments and much methodological debate over studies using pharmacological manipulation and early transgenic lines (Bannerman et al., 2014), recent experiments with animals lacking the GluN1 subunit (essential for NMDA receptor formation) in CA1 pyramidal cells and dentate gyrus granule cells showed impaired

spatial reference memory on the radial maze but normal spatial reference memory in the Morris water maze (Bannerman et al., 2012). These findings, in addition to demonstrating the complexities of interpreting such data, indicate a role for multiple processes and the involvement of other brain areas in memory function relating to these tasks.

Taken together, the studies discussed above provide good evidence that CA1 plays an important role in memory function, especially for memories involving a single experience. However, much of the data also suggests that multiple processes are at play and points to important roles for other brain areas, further suggesting that many aspects of memory emerge from complex interactions across multiple brain areas.

1.5 A spatial map within the brain

In the early seventies, amongst the significant interest in the memory functions of the hippocampal formation, John O'Keefe and researchers at University College London began extracellular recordings from the hippocampus proper, and made the remarkable observation that a large proportion of the recorded cells preferentially fired action potentials in a manner dependent on the location of the animal in the environment (O'Keefe, 1976; O'Keefe and Dostrovsky, 1971). A given hippocampal cell would increase its firing rate when the animal was in a particular region of the environment, and each of the cells had a different preferred firing location. They named the cells which showed this property 'place cells', and the region of space in which such a cell shows an increase in firing is often referred to as the 'place field' of that cell. Since the reference frame for the firing of the cells was not relative to the animal, but instead correlated with absolute locations in the external space, O'Keefe and Nadel (1978) proposed that the hippocampus hosted an allocentric representation of space, and that the activity of hippocampal cells provided the brain with a 'cognitive map' of the environment, which had similar properties to that previously hypothesised by Tolman (1948), who formed the theory on the basis of behavioural experiments.

The properties of place cells have been the topic of intense study since their discovery, and even more so after the advent of recording techniques using tetrodes combined with principal component based analysis, allowing the isolation of spiking activity from multiple individual neurons recorded simultaneously (Abeles and Goldstein, 1977; Csicsvari et al., 1999; Gray et

al., 1995; Harris et al., 2000; McNaughton et al., 1983). Such recordings, paired with systems to track the position of the animal and careful experimental design, have demonstrated that when a rodent is exposed to an environment such as an open field or linear track, the different place cells form place fields distributed throughout the environment (Muller et al., 1987; Wilson and McNaughton, 1993). The locations of the various place fields are such that the entire environment is covered and many of the place fields overlap. It is possible to predict the position of an animal based solely on spiking activity of multiple hippocampal cells using an algorithm when the predictive algorithm is first trained on a portion of the data including the position of the animal (Brown et al., 1998; Zhang et al., 1998). Many place cells maintain the location of their place fields across repeated exposures to the same environment (Thompson and Best, 1990). Importantly, the relative position of the place fields are rearranged in different environments, such that cells which fire in similar regions of one environment (i.e. have overlapping place fields) could fire at opposite ends of a different environment (Muller and Kubie, 1987; Wilson and McNaughton, 1993). The change of the relative firing locations of hippocampal place cells between experiences in different environments, or when the properties of an environment are changed, is often referred to as 'remapping' (Muller, 1996). Furthermore, a cell can be very active during exploration of one environment and less active in another. Such a change in mean firing rate or infield firing rate of the various place cells between environments is often referred to as 'rate remapping' (Leutgeb et al., 2005). When an animal enters a new, never before experienced environment, place fields are present at the very beginning of exploration; however, they do become better defined over the first minutes of exploration (Frank et al., 2004; Hill, 1978).

On first evidence, the fact that the activity of place cells appeared to be largely coding the current position of the animal within the environment seemed at odds with the strong evidence for the hippocampus as important for declarative memory. However, the two lines of evidence are in fact compatible especially when considering the details of both observations. The activity of place cells is not limited to current experience. In radial maze, spatial alternation and T maze tasks, the activity of place cells has been shown to reflect the locations which the animal has come from, the paths the animal is about to take and errors made by the animal, activity seemingly suitable to play a role in a declarative memory system (Ferbinteanu

and Shapiro, 2003; Frank et al., 2000; Johnson and Redish, 2007; O'Keefe and Speakman, 1987; Wood et al., 2000). When a rat or mouse first starts exploring a novel environment, place cells show stable place fields from the very initial moments of exploration (Frank et al., 2004; Hill, 1978). However, there is growing evidence that aspects of the map evolve with the animal's experience in the environment, in a manner dependent on the animal's experiences in the environment and attention to the features of the environment (Frank et al., 2004; Monaco et al., 2014; Wilson and McNaughton, 1993). Additionally, experiences in familiar environments can cause a partial reorganisation of the spatial map with place fields reflecting new goal locations or actions within the environment such as head scans (Dupret et al., 2010; Hok et al., 2007; Hollup et al., 2001; Markus et al., 1995; Monaco et al., 2014). There is also much evidence that modulation of the infield firing rate of place cells with stable place fields can code for events or trial-dependent features representing information beyond simply physical location, thus again attesting to potential suitability as a component of episodic memory encoding (Allen et al., 2012; Leutgeb et al., 2005).

Hippocampal cells also fire in relation to non-spatial features of the environment, including odours (Igarashi et al., 2014; Manns et al., 2007), tactile information (Young et al., 1994) and, importantly, the tracking of time (Hampson et al., 1993; MacDonald et al., 2013; MacDonald et al., 2011). Response properties relating to non-spatial variables were perhaps not so readily recorded in studies reporting only place-related activity since, in many of these studies, the animal was not engaged in tasks that required such non-spatial information. Cells that show responses relating to non-spatial information also show coding of spatial representations, highlighting the flexibility of representation and potential for association available in the hippocampal network (MacDonald et al., 2011). Such flexibility is perhaps a key component of a flexible, highly associative declarative memory system.

A further observation from large scale extracellular recordings linking cognitive map theories of the hippocampus to the idea that the hippocampus is a key component of a declarative memory system is that of hippocampal reactivation (Carr et al., 2011; O'Neill et al., 2010; Skaggs and McNaughton, 1996). Hippocampal reactivation or replay is a term often used to describe the observation that during waking experience, and to a greater extent during subsequent slow-wave sleep, activity matching that present during previous wakening

experience is replayed in the hippocampal network. This is true no matter whether assessed in terms of firing relationships between cells, the place field relationships between cells or the sequential firing of a number of cells (Carr et al., 2011; Davidson et al., 2009; Diba and Buzsaki, 2007; Karlsson and Frank, 2009; Lee and Wilson, 2002; O'Neill et al., 2010; O'Neill et al., 2006; Skaggs and McNaughton, 1996). This activity potentially aids the strengthening of weak connections reflecting both spatial and non-spatial information established during new experiences, thereby aiding their retention as memories, and may also provide a means of forming associations relating to those memories (Ego-Stengel and Wilson, 2010; Girardeau et al., 2009). Much of this activity occurs during local field potential events called sharp wave ripples and is detailed in the next section (and will be returned to in later chapters).

1.6 Field potentials in the hippocampus

In addition to revealing the spiking activity of neurons, extracellular recordings from the brain show many slower variations in field potential at the electrode occurring over various time frames, providing an additional means to study and characterise brain function (Buzsáki, 2006; Buzsáki et al., 2012; Green and Arduini, 1954). Local field potentials in the hippocampus are particularly large in amplitude, in part due to the highly regular laminar structure, with different inputs causing synaptic currents in discrete somatodendritic compartments, thus creating localised current sources and sinks (Buzsáki, 2002; Buzsáki et al., 2012). The hippocampal local field potential (LFP) shows prominent features in a number of frequency bands which correlate with behavioural and brain states. In the mouse, theta band is typically taken as 5 to 12 Hz, gamma as 30 to 100 Hz or higher and ripple band as 140 to 250 Hz, although the definition of the frequency range encompassed by each band depends on the species under study in order to capture slight cross-species variations (Buzsáki et al., 2003).

Theta-band LFP oscillations are prominent when the animal is actively exploring the environment and during rapid eye movement (REM) sleep (Buzsáki, 2002; Green and Arduini, 1954; Vanderwolf, 1969). Theta rhythmic activity is thought to be coordinated by a network of long-range projections to areas of the hippocampal formation that arise from a variety of subcortical structures, including glutamatergic, cholinergic or GABAergic projections from the medial septum, thalamus, hypothalamus and raphe nuclei, with the medial septum playing a

central role (Bland, 1986; Freund and Antal, 1988; Léránth and Frotscher, 1987; Pan and McNaughton, 2004; Petsche et al., 1962; Vertes, 1997). Coherence in theta rhythmic activity between distributed brain networks is associated with enhanced information coupling (Fujisawa and Buzsáki, 2011; Jones and Wilson, 2005; Young and McNaughton, 2009). In CA1, pronounced theta-frequency oscillations in the LFP arise from a periodically active current source at the perisomatic region of the pyramidal neurons, complemented by a phase-shifted periodically-active current sink at the distal apical tuft (Buzsáki, 2002). The current source in the perisomatic region is produced by activation of outward synaptic currents mediated by theta rhythmic GABA release from local CA1 interneurons (Brankačk et al., 1993; Lapray et al., 2012; Montgomery et al., 2009). The complementary current sink in the distal apical tuft arises from inward synaptic currents due to theta rhythmic excitatory afferents from entorhinal cortex (Brankačk et al., 1993; Mizuseki et al., 2009; Montgomery et al., 2009). While theta activity is abolished by both lesions and pharmacological manipulation of medial septum, it is still unclear to what extent theta-frequency activity arises due to pacemaker type drive originating solely from medial septum, or is due to recurrent connections between the hippocampus proper and septum (Lawson and Bland, 1993; Lee et al., 1994; Leung et al., 1994). Other factors which may play important roles in generation of theta-frequency activity include the intrinsic oscillatory properties of local interneurons and excitatory recurrent collaterals in CA3 (Buzsáki, 2002). One of the strongest pieces of evidence suggesting theta-frequency oscillations reflect chunks of functionally-relevant computations is the observation that the firing of a place cell occurs at an earlier phase in each successive theta cycle as the animal moves through that cell's place field (O'Keefe and Recce, 1993; Skaggs et al., 1996). As the animal first enters the place field, the place cell fires on the late ascending phase of theta. When the animal is in the middle of the place field, the place cell fires aligned to the theta trough, and when the animal is exiting the place field, the cell fires on the descending phase. The activity in each theta cycle is thus a sequence of first, where the animal is heading, next, where it is, and finally, where it was. Some interneurons also show theta phase precession; firing at successively earlier phases of successive theta cycles (Maurer et al., 2006).

Gamma-band LFP oscillations have been postulated to reflect a number of functions in perception and memory. Some have suggested gamma-frequency activity is important in the

binding of sensory information across cortical areas which represent diverse components of perception like colour, shape, motion and location into a single precept (Gray, 1994; Singer, 1993). It is also believed to participate in memory (Fell et al., 2001) encoding and retrieval as well as being implicated in the support of attention and working memory (Fries et al., 2001; Yamamoto et al., 2014). Furthermore, it is interesting to note that the period of gamma oscillations matches the optimal window for Hebbian-like plasticity in CA1 pyramidal neurons (Magee and Johnston, 1997), the membrane time constant of pyramidal neurons (Spruston and Johnston, 1992) and the optimal time window for CA1 pyramidal cell spike time prediction from simultaneous peer activity (Harris et al., 2003). In CA1, gamma-band LFP oscillations are smaller in amplitude than theta-band oscillations and tend to occur with greater amplitude during theta activity, often showing amplitude modulation by theta phase (Csicsvari et al., 2003; Schomburg et al., 2014). Recently, high-channel count (up to 256) recordings using silicon probes from multiple regions of the hippocampus have allowed fine scale interrogation of gamma oscillations in CA1 (Lasztóczi and Klausberger, 2014; Schomburg et al., 2014). Current source density analysis and independent component analysis indicate that the pyramidal cell layer, stratum radiatum and stratum lacunosum-moleculare, each possesses a distinct gamma oscillation. Indeed, each of these oscillations is differentially phase-amplitude coupled to theta oscillations in a task-dependent manner and the three gamma oscillators also operate at different frequencies. During waking theta activity, a medium paced gamma oscillation (60 to 120 Hz), predominantly resulting from fluctuating current sinks in stratum lacunosum-moleculare, is present on the peak of theta cycles and is coherent with layer three entorhinal cortex gamma frequency activity. This is in agreement with anatomical findings since stratum lacunosum-moleculare contains the terminal field of the projection from entorhinal cortex. On the descending theta phase, a slow gamma oscillation (30 to 80 Hz), predominantly due to fluctuating current sinks in stratum radiatum, dominates and is coherent with CA3 gamma frequency activity, again in agreement with the known structure of the hippocampus. Finally, at the theta trough, a fast gamma oscillation (above 100 Hz) is often present due to fluctuating current sources and shows coupling to CA1 pyramidal cell output. This work, along with the findings that fast gamma activity in CA3 fails to entrain CA1 neurons (Carr et al., 2012; Csicsvari et al., 2000; Sullivan et al., 2011), represents a demonstration that

coherence between gamma oscillations in an upstream region and gamma oscillations of the output of a downstream region is not the underlying basis of information transfer in the case of CA1.

Ripple LFP oscillations occur in the pyramidal cell layer and are short lasting (approximately 60 ms), high frequency (140 to 250 Hz) fluctuations that are accompanied by increased firing of pyramidal cells and many types of interneuron (Buzsáki, 1986; Buzsáki et al., 1992; Buzsáki et al., 1983; O'Keefe and Nadel, 1978). Co-occurring with the ripple oscillation is a single large negative deflection of the LFP in stratum radiatum (and a smaller amplitude positive deflection in stratum oriens) referred to as a 'sharp wave'. These two features combined give rise to the so-called sharp wave ripple (SWR) event. The sharp wave in stratum radiatum results from synchronous bursting of CA3 pyramidal cells, causing a depolarization of the apical dendrites of CA1 and CA3 pyramidal cells (Csicsvari et al., 2000; Sullivan et al., 2011). The requisite synchronous bursting activity in CA3 arises from a spread of excitatory activity in the recurrent CA3 network which, in turn, is biased by activity patterns in the dentate gyrus and entorhinal cortex (Csicsvari et al., 2000; Sullivan et al., 2011). It is also, in part, facilitated by reduced suppressive effects from subcortical inputs (Buzsáki et al., 1983; Hasselmo and Bower, 1993; Vandecasteele et al., 2014). This excitation spreads over a large volume of CA1 and CA3, thereby activating pyramidal cells and some types of GABAergic interneurons including parvalbumin expressing basket and bistratified cells (Csicsvari et al., 1999; Ellender et al., 2010; Katona et al., 2014; Klausberger et al., 2003; Lapray et al., 2012; Somogyi et al., 2013; Varga et al., 2014; Ylinen et al., 1995). Complex network interactions, including those mediated by gap junctions between the pyramidal cells and also pyramidal cell interactions with interneurons, are believed to result in the ripple oscillation (Buzsáki et al., 1992; Csicsvari et al., 2000; Draguhn et al., 1998; Klausberger et al., 2003; Schmitz et al., 2001; Traub and Bibbig, 2000; Ylinen et al., 1995). Sharp wave ripples occur most prominently during slow-wave sleep, a time when the hippocampal network does not show theta oscillatory activity (Buzsáki, 1986; O'Neill et al., 2006). Sharp wave ripples with a less pronounced sharp wave component also occur during waking. Such SWRs also occur during waking rest periods and during epochs of theta frequency activity when the animal is actively exploring (Jackson et al., 2006; O'Neill et al., 2006). The increased firing of pyramidal cells in CA1 during sharp wave ripples is not without

temporal structure. During slow-wave sleep, pyramidal cells that were active together in the same theta cycles are more likely to also be active in the same SWR event (Carr et al., 2011; O'Neill et al., 2010; Skaggs and McNaughton, 1996). Furthermore, the sequence of activation of pyramidal neurons within the SWR event reflects the sequence of activation during waking exploration, with forward and backward temporally-compressed sequences present (Davidson et al., 2009; Diba and Buzsaki, 2007; Karlsson and Frank, 2009; Lee and Wilson, 2002; O'Neill et al., 2006; Skaggs and McNaughton, 1996). Because waking firing relationships of hippocampal neurons reflect waking events and environmental representations, this activity during sleep is thought important for memory consolidation through the strengthening of the relevant synaptic connections within the hippocampus (Buzsáki, 1989; Carr et al., 2011; O'Neill et al., 2010). Sharp wave ripple activity is also proposed to play a role in the creation and strengthening of neocortical memory representations, a concept supported by the fact that SWR events show a correlation to cortical spindle oscillations and cortical activity (Chrobak and Buzsáki, 1996; Chrobak and Buzsáki, 1998; Clemens et al., 2007; Clemens et al., 2011; Isomura et al., 2006; Siapas et al., 2005). Electrical stimulation triggered on SWR events during sleep reduces memory performance (Ego-Stengel and Wilson, 2010; Girardeau et al., 2009), and SWR activity can predict memory performance (Dupret et al., 2010). Furthermore, the role of SWR firing patterns in memory function is not limited to sleep with forward and reverse replay occurring during waking SWR (Diba and Buzsaki, 2007; Foster and Wilson, 2006). Waking SWR activity may aid the formation of initial associations between cells facilitating later sleep reactivation (Dupret et al., 2010; O'Neill et al., 2006). It may also contribute to the establishment of higher-order associations in episodic memory (Diba and Buzsaki, 2007; Wikenheiser and Redish, 2013).

1.7 Interneurons and single cell electrophysiology of the hippocampus

Due to the extremely close proximity of large numbers of cells in the hippocampal pyramidal cell layer, isolating action potentials from individual cells proved challenging for early studies, although a certain level of separation was possible based on spike shape and amplitude, combined with careful movement of the electrode (Ranck Jr, 1973). This problem was largely overcome in later studies through the use of electrodes with multiple recording sites in close

proximity such as stereotrode or tetrodes (Gray et al., 1995; McNaughton et al., 1983). Detection of clusters in principal component space of the resulting multi-channel spike recordings allowed improved isolation on the basis that different cells produced differing spike shapes across the multiple recording sites (Abeles and Goldstein, 1977; Csicsvari et al., 1999; Gray et al., 1995; Harris et al., 2000; McNaughton et al., 1983). Such recordings from the hippocampal pyramidal cell layer have revealed many cells with moderate mean firing rates (in the range 0.1 Hz to 5 Hz) that often fire complex spike bursts interspersed with a number of cells showing higher mean firing rates and more regular firing patterns (Ranck Jr, 1973). Complex spike cells are the glutamatergic cells of the pyramidal cell layer and are often place cells (O'Keefe, 1976). They can be readily identified from recordings since the bursting property of the complex spikes results in a characteristically shaped auto-correlogram (Lapray et al., 2012).

The non-complex spike cells with higher firing rates (typically greater than 10 Hz), found with cell bodies in the pyramidal cell layer and distributed throughout the various layers of the hippocampus proper, can be classified as putative GABAergic interneurons (Ranck Jr, 1973). Hippocampal interneurons are a diverse population comprised of numerous distinct cell types providing a variety of functions including modulation and coordination of pyramidal cell firing (Bezaire and Soltesz, 2013; Klausberger and Somogyi, 2008; Lovett-Barron et al., 2012; Royer et al., 2012; Somogyi et al., 2013). They also have a role in coupling information to and from other brain areas through the formation of long projecting axons or receiving synaptic input from incoming projection axons (Ferraguti et al., 2005; Freund and Antal, 1988; Jinno et al., 2007; Léránth and Frotscher, 1987). Interneurons migrate into the hippocampus from the medial and caudal ganglionic eminences at various time points during development (Kepecs and Fishell, 2014; Tricoire et al., 2011). Over twenty types of interneuron have been identified in CA1 to date based on experiments using extracellular single cell recording and juxtacellular labelling (Bezaire and Soltesz, 2013; Klausberger and Somogyi, 2008; Somogyi et al., 2013). In such experiments, the firing activity of a single cell is recorded using a neurobiotin filled glass pipette positioned near the cell body. During recording the pipette performs as a high impedance electrode (15 - 20 MΩ). At the end of recording, current flow is induced in the pipette forcing a tracer substance (typically neurobiotin) out of the pipette and across the

plasma cell membrane of the same neuron, filling its cytosol with neurobiotin (Pinault, 1996). The neurobiotin labelled cell can then be identified in subsequent histochemical analyses. The different hippocampal interneuron types identified in CA1 to date on the basis of a combination of differing expression of molecular markers, differing cell structure and specificity of synapse formation, and differing firing properties across brain states in relation to the local field potential, are schematised in Figure 1.2.

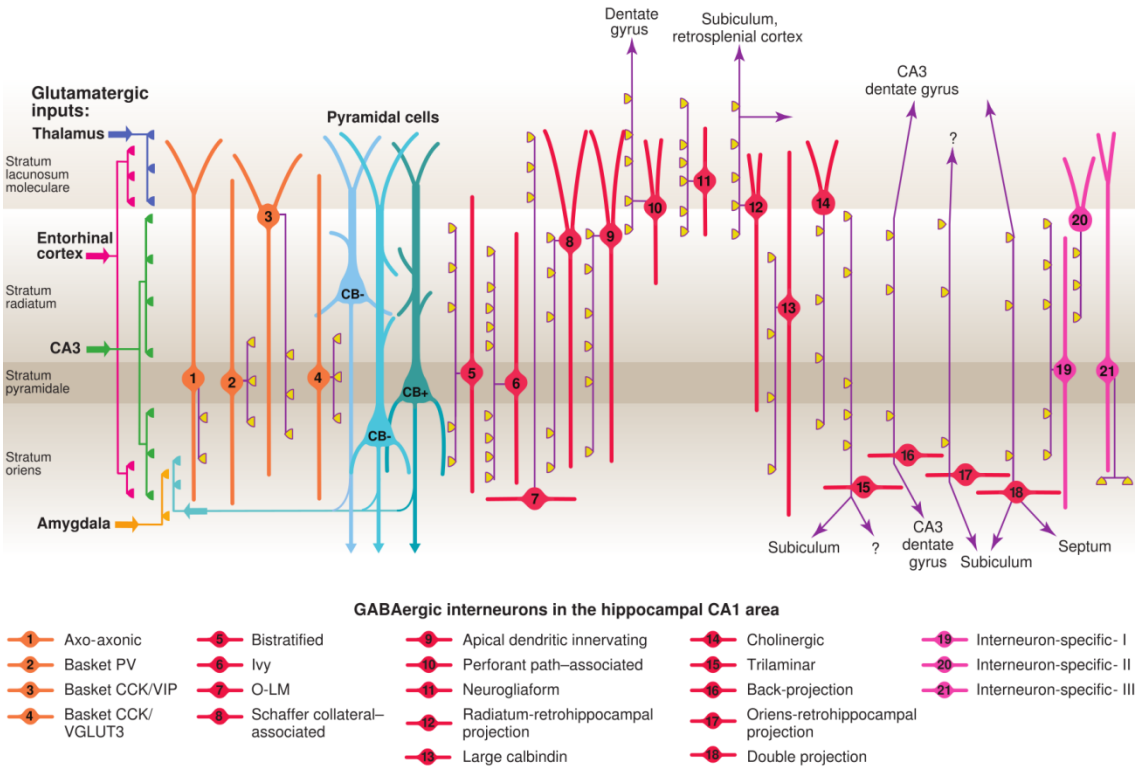

Figure 1.2 *Schematic depicting the various classes of CA1 interneuron*
Schematic depicting the various classes of interneuron in the hippocampal CA1 area reproduced from (Klausberger and Somogyi, 2008). The axon of each interneuron class is shown in purple, with the main synaptic terminations in relation to the laminar structure of the CA1 subfield depicted by the yellow triangles. The typical cell body location and position of the dendritic tree are shown in orange for interneuron classes which target the axon initial segment, soma and perisomatic regions of pyramidal neurons (blue). Interneuron classes which mainly target other interneurons are shown in pink and the remaining classes are shown in red. The main termination fields of five glutamatergic inputs are shown to the left. Note the association of the output synapses of different interneuron types with the perisomatic region (left) and either the Schaffer collateral/commissural or the entorhinal pathway termination zones (right). VIP, vasoactive intestinal polypeptide; VGLUT, vesicular glutamate transporter; O-LM, oriens-lacunosum moleculare.

The various interneuron types provide targeted inhibition to specific locations along the pyramidal cells, potentially allowing differing influence on the information processing functions of the network and the coordination of pyramidal cell input and output. Axo-axonic cells give rise to axons forming synapses exclusively with the axon initial segment of pyramidal cells, potentially allowing the most direct control over pyramidal cell output (Klausberger et al., 2003; Somogyi et al., 1983; Varga et al., 2014; Viney et al., 2013). Basket cells innervate pyramidal cell somata and proximal dendrites and thus, are well placed to also have a relatively direct influence on pyramidal cell output (Cajal, 1893; Klausberger et al., 2003; Klausberger et al., 2005; Lapray et al., 2012; Varga et al., 2012; Varga et al., 2014). Other types of interneuron, such as ivy cells, bistratified cells and Schaffer collateral-associated cells target the basal and oblique dendrites and, as such, are aligned with the glutamatergic input from CA3, while other types, such as oriens-lacunosum moleculare (O-LM) cells and neurogliaform cells, target the apical dendritic tuft in lacunosum-moleculare where glutamatergic input arrives from entorhinal cortex (Fuentealba et al., 2008; Katona et al., 2014; Klausberger et al., 2004; Klausberger et al., 2005; Lapray et al., 2012; Price et al., 2005; Varga et al., 2012; Varga et al., 2014). Additionally, there are numerous interneuron types that, in addition to forming local synapses in CA1, produce long-range projecting axons with some types projecting back to CA3 and the dentate gyrus, while other types project forward to subiculum and beyond to other structures (Ferraguti et al., 2005; Jinno et al., 2007; Sik et al., 1995). Projection GABAergic cells may be involved in the coordination of information flow between input and output structures. Finally, there is a population of interneurons that predominantly form synapses with other interneurons (Acsády et al., 1996; Gulyás et al., 1996; Gulyás et al., 2003). Beyond the diversity seen in the specificity of axonal targets, interneuron types with similar targets can differ due to the positioning of their dendritic tree and cell body thus drawing input information from different regions of the network. For example, O-LM cells and neurogliaform cells both innervate the pyramidal cell apical dendrites in stratum lacunosum-moleculare; however, O-LM cells are positioned in stratum oriens and receive a facilitating input from local CA1 pyramidal neurons, whereas neurogliaform cells are located in stratum lacunosum-moleculare predominantly receiving glutamatergic input from entorhinal cortex (Ali and Thomson, 1998; Price et al., 2005). Furthermore, interneuron types differ in their ability to

release neuropeptides, such as somatostatin, neuropeptide y (NPY), cholecystokinin (CCK) and vasoactive intestinal polypeptide (VIP), allowing yet another means for the different types of interneuron to differentially influence network activity (Boehm and Betz, 1997; Colmers et al., 1985; Katona et al., 2014; Tallent and Siggins, 1997; van den Pol, 2012).

Large scale extracellular recordings, as well as recordings of identified cells, show that the firing of many types of interneuron is strongly locked to particular phases of theta band oscillations (Csicsvari et al., 1999; Katona et al., 2014; Lapray et al., 2012; Somogyi et al., 2013; Varga et al., 2012; Viney et al., 2013). The different interneuron types provide differentially timed influence to specific domains of the CA1 network providing both spatially and temporally aligned influence on different aspects of network input, output and function (Lovett-Barron et al., 2012; Royer et al., 2012; Somogyi et al., 2013). Different interneuron classes also participate in other brain states and network events such as sharp wave ripples (Csicsvari et al., 1999; Somogyi et al., 2013). It has also been demonstrated that individual interneurons can associate with a representation of a specific environment, and such interneurons play a role in coordinating network activity associated with competing environmental representations (Dupret et al., 2013).

1.8 Overview of midbrain dopaminergic cell groups

Dopaminergic neurons and the action of the neurotransmitter dopamine has been the subject of intense study since the 1960s for a number of reasons. Evidence implicating dopamine as a neurotransmitter emerged in the late 1950s (Carlsson et al., 1958; Carlsson et al., 1957; Montagu, 1957). It soon after became apparent that dopamine signalling was involved in motor function, and that dysfunction of the dopamine system underlined the cardinal (motor) symptoms of Parkinson's disease including shaking (tremor at rest), slowness of movement, rigidity and difficulty initiating movement (Bertler and Rosengren, 1959; Carlsson, 1959; Ehringer and Hornykiewicz, 1960). This observation was followed by the development of a treatment for Parkinson's disease through the oral administration of L-DOPA (a precursor for the synthesis of dopamine) representing one of the major success stories in neuroscience (Björklund and Dunnett, 2007b; Cotzias et al., 1967). Another factor enabling the study of dopaminergic neurons at this time was the development of a histofluorescence method (prior

to the advent of versatile immunohistochemical methods) allowing visualisation of catecholamines (including noradrenaline and dopamine) and serotonin (Carlsson et al., 1962; Falck et al., 1962). This method was used to provide a detailed account of the anatomical organisation of dopaminergic neurons (along with other catecholamine containing neurons) in the rat brain and their grouping into a number of nuclei numbered A1-12 (Dahlstroem and Fuxe, 1964). Additional nuclei (A13 to A17) were subsequently added along with three adrenaline-containing cell groups (C1 to C3) and this naming convention has been widely adopted across species, proving convenient because the precise location of the nuclei varies across vertebrates and cells of a single nucleus can be distributed across anatomical boundaries (Hökfelt et al., 1984; Smeets and González, 2000). With the generation of antibodies raised against tyrosine hydroxylase (TH) and other enzymes involved in dopamine/catecholamine synthesis, it was possible to distinguish between the different catecholamines more accurately, thereby confirming ten major dopaminergic cell groups in the midbrain and forebrain (A8 to A17). In the Murinae brain, the meso-diencephalic tegmental groups located at the base of the midbrain are separated in three groups and are located in the retrorubral field (A8), the substantia nigra pars compacta (A9) and the ventral tegmental area (A10). The other groups are the caudal diencephalic periaqueductal gray groups (A11), the hypothalamic groups (A12, A14 and A15), the zona incerta cell group in the ventral thalamus (A13), the periglomerular cells in the olfactory bulb (A16) and the interplexiform cells in the retina (A17). A schematic of the location of the various nuclei and their general projections in the developing and adult rodent brain is shown in Figure 1.3 (Björklund and Dunnett, 2007a; Hökfelt et al., 1984). The A8 to A17 nomenclature refers only to the clusters of the cell bodies of dopaminergic neurons themselves in contrast to the brain structure names which refer to the entire anatomical structure in which the cluster is predominantly contained e.g. ventral tegmental area in the case of the A10 dopaminergic cell group.

Though united by their common use of dopamine as a neurotransmitter, the dopaminergic neuron groupings have distinct functions and differing molecular profiles. The meso-diencephalic dopaminergic neurons (groups A8 , A9 and A10) form a single constellation in the base of the midbrain uniquely expressing the gene Pitx3 (Smidt et al., 1997). These cells are the main focus in this thesis and are referred to throughout as midbrain dopaminergic

neurons. They project to the striatum, cortex and limbic regions via the mesostriatal, mesocortical and mesolimbic pathways, respectively, and provide the main dopaminergic innervation of the forebrain (Bentivoglio and Morelli, 2005). While they are broadly divided into three sub groups (A8, A9 and A10) there is ever increasing evidence for further divisions within these groups (Fu et al., 2012; Roeper, 2013).

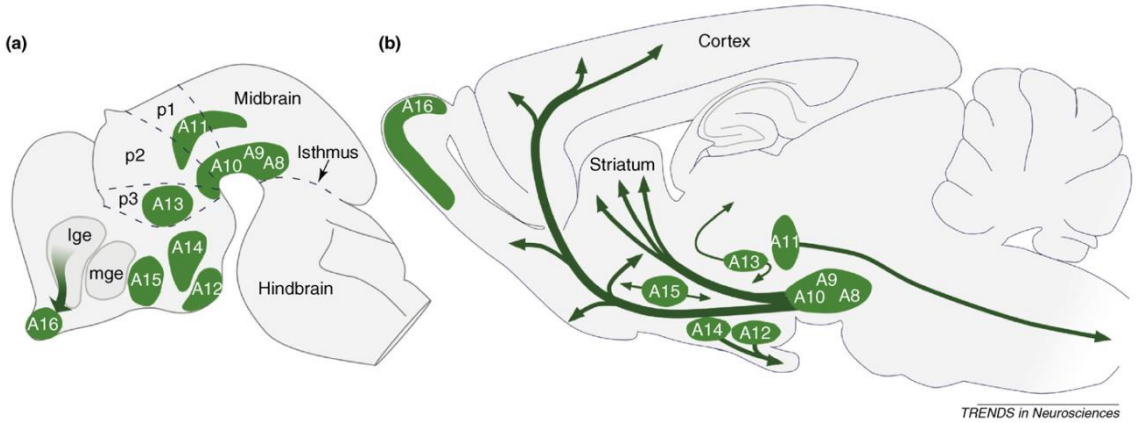

Figure 1.3 *Schematic of dopaminergic neuron cell groups*
Schematic depicting the distribution of dopaminergic (DA) neuron cell groups in the developing and adult rodent brain reproduced from (Björklund and Dunnett, 2007a). Nine cell groups are shown in this schematic sagittal view of, ***(a)*** *the developing and,* ***(b)*** *the adult rat brain. The numbering of the cell groups, from A8 to A16, was introduced in the classic study of (Dahlstroem and Fuxe, 1964). The drawing in (a) is modified from (Marín et al., 2005). The principal projections of the DA cell groups are illustrated by arrows in (b). LGE, lateral ganglionic eminence; MGE, medial ganglionic eminence; p1-p3, prosomeres 1-3.*

The majority of A9 dopaminergic cells are located in the substantia nigra pars compacta (SNc) and are the predominant source of the mesostriatal projection, also referred to as the nigrostriatal pathway in reference both to the connection itself and the fibre bundle through which it travels. This bundle assembles at the rostral medial aspect of the substantia nigra and runs along the medial aspect of the internal capsule terminating in the striatum (Hökfelt et al., 1984). Additionally, A9 dopaminergic neurons are more vulnerable to dysfunction and degeneration in Parkinson's disease (Ma et al., 1995; Pakkenberg et al., 1991), and related to their selective projections to the striatum, are better associated with the motor functions associated with midbrain dopaminergic neurons.

The A10 dopaminergic cells are located in the ventral tegmental area (VTA). The A10 groups are sometimes referred to as the A10 complex reflecting the fact that they are perhaps the most heterogeneous of the Dahlström and Fuxe groupings consisting of a number of cell groups. When considered as a homologous group, it is often reasonable to also include the A8 dopaminergic cells that are located in the adjacent retrorubral field (RRF; not to be confused with the retrorubral nucleus, a nearby independent non-dopaminergic cell group in the rostral hindbrain). The A8/A10 groups are the predominant source of the mesocortical and mesolimbic pathways projecting through the medial forebrain bundle (Yetnikoff et al., 2014) and as such, are frequently associated with the value and error prediction coding properties of midbrain dopaminergic neurons outlined in the next section. It is also important to note at this point that this early view represents a simplification, and there is much overlap in the source of these projections, with A9 cells giving rise to mesocortical/mesolimbic projections and A8/A10 cells giving rise to mesostriatal projections. Further detail on this is provided in section 1.11.

1.9 Dopamine, value and error prediction

In addition to their central role in motor output networks, midbrain dopaminergic neurons show transient or 'phasic' responses locked to rewarding events or cues predicting rewards (Schultz, 2007; Schultz et al., 1997). Phasic responses are most frequently measured over many repeated trials in terms of an increase in the firing of a cell at a particular fixed time point relative to an event such as the onset of a reward predicting cue. The increase can be quantified compared to the mean background activity of the cell and, while phasic responses can be produced by bursting activity, it is also possible for responses to be quantified as phasic due to an increased probability of single spikes at the time point of interest. Such reward predicting responses are present independent of the sensory modality through which the event is perceived providing a highly abstract value signal which is relayed widely throughout the brain. Extensive recordings of midbrain dopaminergic neurons in primates first revealed responses to encountering unpredicted rewards independent of movement initiation (Romo and Schultz, 1990). It subsequently became apparent that on learning a cue to predict the rewarding event, such as a tone or a door opening (conditioned stimulus, CS), the response shifts to the time of the predicting cue and is no longer present at reward delivery (Ljungberg

et al., 1992; Mirenowicz and Schultz, 1994). Additionally, once an animal has learned such a contingency and the reward is then omitted after CS presentation there is a drop in dopaminergic neuron firing at the expected time of reward delivery (effectively a response to the omitted reward). Raster plots showing recordings from a primate midbrain dopaminergic neuron with such response properties can be seen in Figure 1.4 adapted from Schultz et al. (1997). These response properties of midbrain dopaminergic neurons are often referred to as coding a reward prediction error. Dopaminergic neurons thus code the mismatch in value between expected and actual outcome, a signal at the heart of many formal theories of animal learning such as the Rescorla-Wagner learning rule and temporal difference learning (Montague et al., 1995; Schultz et al., 1997; Sutton and Barto, 1998).

Furthermore, the firing of midbrain dopaminergic neurons has been shown to mimic a previously established observation, often used in support of such learning theories, to claim that learning is informed by error prediction rather than the simple pairing of events. Referred to as blocking, this is the observation that an animal fails to learn the reward contingency of a cue which is predictive of reward if, during the opportunity to learn the contingency, the reward is also predicted by another previously learned cue. Dopaminergic neurons fail to show a phasic response to such a blocked cue, instead responding to the reward delivery, thus matching the observed failure of the animal to learn and strengthening the evidence that the dopamine response itself instructs learning (Waelti et al., 2001).

The sophistication of expectation coding by midbrain dopaminergic neurons extends to anticipation of reward omission predicted by a 'conditioned inhibitor' cue. Here, an animal first learns that a cue (the conditioned inhibitor) is not followed by reward. Then, when a well learned reward predicting cue is presented along with the conditioned inhibitor cue, the phasic response of midbrain dopaminergic neurons which would ordinarily occur in response to the rewarding cue is supressed (Tobler et al., 2003). Also, if a reward is delivered after presentation of a learned conditioned inhibitor a strong phasic response occurs (strong positive prediction error).

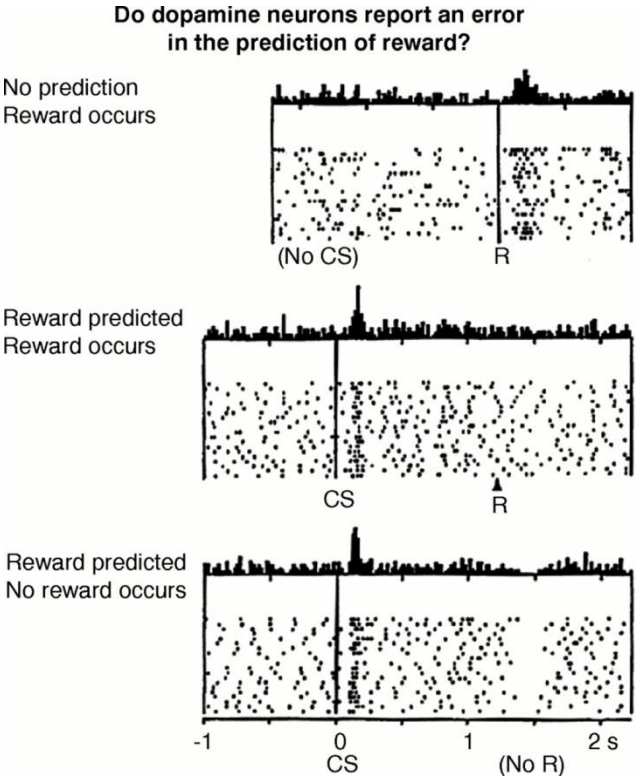

Figure 1.4 *Phasic responses of a putative dopaminergic neuron*
Raster plots showing phasic responses of a putative dopaminergic neuron recorded in a monkey receiving rewards over repeated trials reproduced from (Schultz et al., 1997). The cell fires after receipt of an unpredicted reward (R) consisting of a drop of juice (top). After learning, the conditioned stimulus (CS) predicts reward, and the reward occurs according to the prediction. The dopaminergic neuron is activated by the reward-predicting stimulus and there is no longer a response after reward delivery (middle). After learning, the conditioned stimulus predicts a reward, but the reward fails to occur because of a mistake in the behavioural response of the monkey. The activity of the dopaminergic neuron is depressed exactly at the time when the reward would have occurred (bottom).

Finally, the link between dopamine error prediction responses and actual choice behaviour was strengthened further by two recent studies. The first showed that the error prediction responses of midbrain dopaminergic neurons integrate value across multiple subjectively related reward associated variables such as amount, risk and reward type, producing subjective value responses exactly matching the extent these variables influenced the actual choices of the monkey. That is, the combined economic value across the subjectively related variables reduced to a common value scale based on the choices of the monkey was reflected in the prediction error responses of midbrain dopaminergic neurons, such that a particular reward dimension influenced dopaminergic activity only to the extent that it influenced choice

(Lak et al., 2014). Secondly, dopamine error prediction responses reflect 'risk seeking' behaviour. Monkeys and humans show nonlinear risk taking that is dependent on the size of the reward, such that they are risk seeking for low rewards and risk adverse for larger rewards, and this too is seen in the responses of midbrain dopaminergic neurons (Stauffer et al., 2014).

While much of the correlative evidence implicating dopamine as an error prediction signal which informs learning was generated in primate experiments, other studies in rodents were required to obtain causal evidence. Early studies using pharmacological manipulations provided some evidence but lacked the temporal resolution required to fully demonstrate causality in learning (Iordanova et al., 2006; O'Tuathaigh et al., 2003; Takahashi et al., 2009). However this was no longer a problem with the advent of optogenetic manipulations. Fifty hertz phasic activation (25 pulses at 50 Hz optical stimulation delivered every minute) of midbrain dopaminergic neurons was sufficient to produce conditioned place preference (CPP) for one chamber over another, even when the alternative chamber was stimulated with the same pulse parameters at the reduced frequency of one hertz (Tsai et al., 2009). More direct evidence for the error prediction properties of the dopamine signal as causal in learning was provided by Steinberg and colleagues (2013) who trained rats in a blocking paradigm. Consistent with previous studies, when the reward delivery was already predicted (or 'blocked') by a previously learned cue, animals fail to learn the association between a new cue and reward. It is hypothesised that dopamine signalling underlies this behaviour since there is no dopamine response (no error prediction) at the time of reward reflecting the fact that the reward is predicted by the previously learned cue (Waelti et al., 2001). However, Steinberg and colleagues activated midbrain dopaminergic neurons during reward delivery in the blocking paradigm providing an artificial error prediction. This was sufficient for animals to learn the blocked cue and show conditioned behaviour in response to its presentation thus providing a key piece of causal evidence demonstrating dopamine error prediction signalling as informative for learning.

Another study of importance in rodents is that of Cohen and colleagues (2012) who performed extracellular tetrode recordings. The mice learned odour cues to be predictive of a reward and the recorded cells were classified based on their spiking activity in bins spanning cue presentation and reward delivery. Classification was performed using principal component

analysis followed by unsupervised, hierarchical clustering and yielded three clusters. Type I neurons (52%) showed phasic responses to cue presentation with many showing an additional smaller phasic response to reward delivery; type II neurons (31%) showed sustained excitation to the reward predicting cue and type III neurons (18%) showed sustained inhibition. Furthermore, the light activated ion channel channelrhodopsin-2 was expressed in dopaminergic neurons in some of these animals while channelrhodopsin-2 was expressed in GABAergic neurons of the other animals. A number of the cells could be matched by waveform shape as responding to laser stimulation. All dopaminergic neurons which responded to laser stimulation were type I neurons and all GABAergic neurons which responded to laser light were type II.

While the majority of dopaminergic neurons show phasic inhibition to aversive stimuli such as an airpuff (Cohen et al., 2012; Lak et al., 2014; Schultz et al., 1997), there are also some reports of a smaller proportion of dopaminergic neurons showing excitatory responses to aversive stimuli (Cohen et al., 2012; Matsumoto and Hikosaka, 2009). This still needs to be treated with some caution since most of the evidence suggesting this has relied on identification of dopaminergic neurons based on the characteristics from electrophysiological recordings, a method prone to false identification (Ungless and Grace, 2012), and experiments using extracellular single cell recording and juxtacellular labelling (which allow immunohistochemical identification of the cells) to date have not reported such cells (Ungless et al., 2004). It is suggested that in the monkey these cells are located more dorsolaterally in the substantia nigra pars compacta (Matsumoto and Hikosaka, 2009). Given the wide range of projection targets for dopaminergic neurons (introduced in section 1.11) and the diversity among dopaminergic neurons (introduced in section 1.10), it seems plausible that diversity in response characteristics is also present. Neurons excited by appetitive stimuli and inhibited by aversive stimuli can send a value signal to many brain targets, neurons excited by appetitive stimuli and aversive stimuli may signal motivational saliency in a similar fashion (Matsumoto and Hikosaka, 2009).

1.10 Cell diversity in midbrain dopaminergic nuclei

The meso-diencephalic dopaminergic (mdDA) neurons (groups A8 , A9 and A10) and the brain structures in which they are contained, the retrorubral field (RRF), the substantia nigra pars compacta (SNc) and the ventral tegmental area (VTA) respectively, are often thought of as being relatively homogenous. However, it is becoming increasingly apparent that a highly intricate diversity is present (Lammel et al., 2014; Morales and Root, 2014; Roeper, 2013; Yetnikoff et al., 2014). In the VTA of the rat brain, approximately 64% of neurons are dopaminergic, approximately 34% are GABAergic and 2-3% are glutamatergic, but these proportions are not uniform throughout the subfields that make up the VTA (Nair-Roberts et al., 2008; Yetnikoff et al., 2014). Furthermore, the proportion of GABAergic cells is slightly less in the SNc than in the VTA and is much higher (58%) in the RRF (Nair-Roberts et al., 2008). The glutamatergic cells of the VTA are mainly located in the rostro-medial portion of the VTA (Nair-Roberts et al., 2008; Yamaguchi et al., 2007). Nair-Roberts and colleagues (2008) using non-radioactive *in situ* hybridisation reported few if any VGluT2 immunopositive cells in the SNc and the RRF of the rat brain. However, Yamaguchi and colleagues (2013) subsequently reported the presence of TH immunonegative VGluT2 mRNA containing cells in the SNc and the RRF using radioactive *in situ* hybridisation.

The view of midbrain dopamine regions consisting of distinct neuronal populations based on distinct neurotransmitter release has been complicated in recent years by a number of studies showing the functional release of GABA and/or glutamate from the axon terminals of midbrain dopaminergic neurons (Alsiö et al., 2011; Chuhma et al., 2009; Chuhma et al., 2004; Fortin et al., 2012; Hnasko et al., 2010; Hnasko et al., 2012; Joyce and Rayport, 2000; Rayport, 2001; Stamatakis et al., 2013; Stuber et al., 2010; Tritsch et al., 2012). Further investigation is required to ascertain the fine detail of how the dual neurotransmitter release from these cells arises, given that the previously mentioned studies which used a combination of immunohistochemistry and *in situ* hybridization to detect standard markers associated with such neurotransmitters, did not report abundant cells with markers for more than one neurotransmitter. A subpopulation of VGluT2 mRNA containing cells in the VTA (but not the SNc and RRF) has been shown to express TH but these cells are fewer in number than 'VGluT2 only' or 'TH only' cells (Yamaguchi et al., 2011) and are even less abundant in the mouse

(Yamaguchi et al., 2015). Other points of note which may prove important in explaining this apparent discrepancy include evidence that glutamate co-transmission may have a greater role during the growth and development of dopaminergic neurons, becoming less prevalent in the adult brain (Fortin et al., 2012; Mendez et al., 2008), while there is also evidence that GABA release can be facilitated by the vesicular transporter for dopamine (vesicular monoamine transporter, VMAT2) independent from the vesicular GABA transporter VGAT (Tritsch et al., 2012). Additional investigation of which cells give rise to axons capable of the dual transmitter release may provide additional means to delineate subpopulations of midbrain dopaminergic neurons.

While many postulate that further delineation of midbrain dopaminergic nuclei may soon become apparent based on projection targets, expression of molecular markers and functional differences (Lammel et al., 2014; Morales and Root, 2014; Roeper, 2013; Yetnikoff et al., 2014), there are nevertheless five long standing anatomical defined subfields of the VTA which have proven useful over the last thirty five years of research. They are the paranigral nucleus (PN), the interfascicular nucleus (IF), the parabrachial pigmented nucleus (PBP), the caudal linear nucleus (CLi), and the rostral linear nucleus (RLi) (Fu et al., 2012; Halliday and Törk, 1986; Phillipson, 1979a, b). Additionally, the rostrodorsal VTA region is often separated as an additional subfield abbreviated VTAR and the rostroventral part of the PBP often separated as the parainterfascicular nucleus (PIF) (Franklin and Paxinos, 2008; Fu et al., 2012; Nair-Roberts et al., 2008). These subfields can be partially differentiated by cytoarchitectonic differences and partially by the presence of differing cellular markers. However, these areas thus far have not been associated with distinct functional roles or as having distinct projection targets, with such attributes instead generally being reported in terms of gradients across the structures.

Finally, independent of the initially established anatomical delineations outlined so far, in what perhaps represents the most relevant means of subdivision; midbrain dopaminergic neurons can be broken into a ‘dorsal tier’ and a ‘ventral tier’, based in part on the expression of the calcium binding protein calbindin (Bentivoglio and Morelli, 2005; Björklund and Dunnett, 2007a; Fu et al., 2012; Iversen et al., 2009; McRitchie et al., 1996). Dorsal tier dopaminergic neurons express calbindin, tend to be more round in shape and are located in the dorsal aspects of the VTA, SN and RRF. Conversely, ventral tier dopaminergic neurons are calbindin

negative and more angular in shape. They are more densely packed and located in the more ventral aspects of the VTA and SNc. However, there is not a discrete border between the two populations with the regions occupied by dorsal and ventral tier neurons overlapping. Ventral tier dopaminergic neurons appear to be more susceptible to degradation in Parkinson's disease, prompting much research into the factors differentiating them from dorsal tier neurons (Double et al., 2010). Increased expression of the G protein-coupled inward rectifying potassium channel GIRK-2 in ventral tier neurons has been reported by some (Björklund and Dunnett, 2007a; Chung et al., 2005; Mendez et al., 2005; Schein et al., 1998; Thompson et al., 2005), however also see (Reyes et al., 2012). Other potentially relevant differences are reviewed by Double et al. (2010) and include among many possibilities increased expression of D2 dopamine autoreceptors and increased expression of dopamine transporter protein DAT.

1.11 Projection targets of midbrain dopaminergic neurons

Midbrain dopaminergic neurons project to multiple forebrain targets including many cortical, limbic and basal ganglia brain areas via the mesocortical, mesolimbic and mesostriatal pathways. The mesocortical and mesolimbic projections both project through the medial forebrain bundle and are often best considered as a single mesolimbocortical projection distinct from mesostriatal fibres which exit the dorsolateral medial forebrain bundle and run along the medial aspect of the internal capsule terminating in the striatum (Bentivoglio and Morelli, 2005; Björklund and Lindvall, 1984; Hökfelt et al., 1984). While it can be a convenient heuristic to consider mesostriatal fibres as predominantly originating from A9, SNc, ventral tier, calbindin-negative type dopaminergic neurons and mesolimbocortical fibres as originating from A10, VTA, dorsal tier, calbindin-positive type dopaminergic neurons this represents a simplification on a number of levels. The first simplification lies in assuming synonymy of the classifying terms (A10 vs. VTA vs. dorsal tier), the differences between which are outlined in the previous sections. The second simplification lies in the fact that, no matter the classification scheme chosen, each projection contains fibres originating from dopaminergic neurons in the population not typically associated with that projection. For example, in addition to neurons projecting to the striatum, the SNc also contains neurons which project to cortical and limbic areas. The heuristic does however represent a truth in that the respective projections do receive a greater contribution from their associated groupings of dopaminergic

neurons (Bentivoglio and Morelli, 2005; Björklund and Dunnett, 2007a; Fallon and Moore, 1978; Swanson, 1982; Yetnikoff et al., 2014). This can also be thought of in terms of projection targets forming a gradient across the midbrain dopaminergic nuclei. However, tracer studies indicate that while the cell bodies of these two projections are intermixed, dopaminergic neurons sending collaterals to more than one brain area are rare thus allowing for potential functional separation of the projections to the various targets (Fallon and Loughlin, 1982; Loughlin and Fallon, 1984; Matsuda et al., 2009; Swanson, 1982; Takada and Hattori, 1987), although this is still a source of debate particularly in the case of a portion of SNc neurons (Yetnikoff et al., 2014). Furthermore, beyond the evidence for approximate spatial organisation of midbrain dopaminergic cells to the two main projection pathways, there is evidence for further approximate topographical organisation based on finer resolution discrimination of projection targets (Bentivoglio and Morelli, 2005; Björklund and Dunnett, 2007a; Swanson, 1982).

The forebrain structure most densely and extensively innervated by midbrain dopaminergic fibres is the striatum (Bentivoglio and Morelli, 2005; Björklund and Dunnett, 2007a; Björklund and Lindvall, 1984; Fallon and Moore, 1978; Iversen et al., 2009; Loughlin and Fallon, 1984; Matsuda et al., 2009; Swanson, 1982). Based on neurochemical and neuroanatomical properties, the striatum is composed of two compartments arranged as a mosaic, the patches/striasomes and the matrix; ventral tier dopaminergic neurons project heavily to the patch compartment and dorsal tier neurons project to the matrix. Additionally, there is a gradient present; dopaminergic projections to the matrix compartment of the dorsal striatum more frequently originate from cells located at the more dorsolateral-caudal extent of the midbrain dopaminergic nuclei, whereas the innervation of the ventral striatum originates in greater numbers from cells towards the more ventromedial-rostral extent of the midbrain dopaminergic cells. This produces a greater projection from the SNc to the dorsal striatum (caudate putamen) and a greater projection from the VTA to the central nucleus of the amygdala and ventral striatum including the nucleus accumbens. Dopaminergic innervation of the basal ganglia is by no means limited to the striatum; most basal ganglia structures including the external and internal segments of the globus pallidus (entopeduncular nucleus in rodents), parts of the ventral pallidum and the subthalamic nucleus, receive a significant

dopaminergic innervation from midbrain dopaminergic nuclei (Björklund and Dunnett, 2007a; Fallon and Moore, 1978; Fuchs and Hauber, 2004; Gauthier et al., 1999; Hassani et al., 1997; Klitenick et al., 1992; Lindvall and Björklund, 1979). This high level of dopaminergic connectivity implicates dopaminergic signalling as a central component at all levels of basal ganglia networks.

Beyond the projections to basal ganglia networks many forebrain areas receive innervation from midbrain dopaminergic neurons including the olfactory tubercle, amygdala, lateral habenula, lateral septum (Lindvall, 1975), subventricular zone, thalamus (García-Cabezas et al., 2009) and, of key relevance for the work in this thesis, the hippocampus. Additionally midbrain dopaminergic neurons project widely through the neocortex especially to cingulate, prefrontal and perirhinal cortex (Lindvall et al., 1978). The projections to the thalamus and neocortex are more extensive in primates than rodents (Berger et al., 1991; García-Cabezas et al., 2009; Yetnikoff et al., 2014). While there is evidence that the projections to the olfactory tubercle, amygdala and septum originate preferentially from subgroups of the midbrain dopaminergic nuclei, no such organisation in the origin of the projections to neocortex is reported to date (Björklund and Dunnett, 2007a).

1.12 Dopamine and the hippocampus

There are a number of lines of evidence for the action of dopamine as playing a role in memory related processes in the hippocampus. Anatomical studies availing of biochemical and tracer methods indicate a projection of midbrain dopaminergic cells to the hippocampus (Gasbarri et al., 1994a; Gasbarri et al., 1996; Gasbarri et al., 1994b; Ishikawa et al., 1982; Samson et al., 1990; Scatton et al., 1980; Swanson, 1982; Verney et al., 1985). However, details in relation to this projection remain unclear and I will address this topic in greater detail in Chapter 3. Beyond the anatomical evidence, a number of studies using D1/D5 receptor agonists (e.g. SKF38393) or antagonists (e.g. SCH23390) have shown evidence linking the action of the neurotransmitter dopamine to various stages of memory formation in the hippocampus. Brief exposure to a novel environment lowers the threshold for long term potentiation (LTP) induction at CA1 synapses. This is prevented by application of D1/D5 receptor antagonist. Conversely, D1/D5 agonist is sufficient to induce LTP at the lower

threshold without exploration of the novel environment (Li et al., 2003). This suggests that D1/D5 receptor activation can directly modulate hippocampal mechanisms of LTP. Intra-hippocampal infusion of D1/D5 receptor antagonist has also been shown to reduce the stabilisation of new memories if applied before encoding (i.e. initial learning trial) but not if applied immediately after encoding (Bethus et al., 2010; O'Carroll et al., 2006). Of note here is that performance was impaired when assessed 6 and 24 hours after encoding but not 20 and 30 min after implying a role for dopamine in the longer term stabilisation of the memory. Furthermore, novel experience thirty minutes after encoding of a weak memory resulted in increased 24 hour persistence of this weak memory and novel experience 1 hour before weak memory encoding rescued the persistence of a memory ordinarily lost by the infusion of D1/D5 antagonist (Wang et al., 2010). From this evidence, along with evidence from slice recordings (Wang et al., 2010), it has been suggested that dopamine receptor activation in the hippocampus causes a widespread 'tagging' which initiates second messenger systems. This, in turn, produces longer lasting potentiation of synapses that are potentiated while the second messenger systems are active, explaining the extension of dopamine action to events which occur, not at the time of, but around the time of dopamine receptor activation (Redondo and Morris, 2011; Takeuchi et al., 2014; Wang et al., 2010). A separate study suggests that dopamine action in the hippocampus later in the memory consolidation process can have an effect. It found that formation of fear memories could be disrupted by intra-hippocampal infusion of D1/D5 antagonist 12 hours, but not immediately or 9 hours after encoding, while infusion of D1/D5 agonist at the 12 hour time point increased the persistence of the fear memory (Rossato et al., 2009). Finally, the long term (6 hour) stability of place maps was enhanced by systemic injection of a D1/D5 receptor agonist and reduced by a D1/D5 receptor antagonist (Kentros et al., 2004). Injection occurred in the middle of exploration of an already familiar environment. Taken together, these experiments suggest dopamine action within the hippocampus, at or around the time of encoding, activates processes which increase the persistence of the encoded memory through both the lowering of the threshold for LTP induction and increasing secondary mechanisms involved in the maintenance of the newly strengthened synapses.

1.13 Aims

In order to be retained as memories, representations created in the brain during experience must be preserved in a manner that allows future recall. However, not all details that are perceived during experience, or indeed not even all experiences, are retained in such a fashion. The processes underlying how some information is preserved as memories while other information is not, and what processes influence which information is retained, is central to the understanding of memory function in the brain. Given the evidence outlined in the previous section implicating dopamine action in the hippocampus as increasing memory retention, the aims of this thesis were to establish (1) what changes in hippocampal network activity occur to support such increased memory retention, (2) whether the required dopamine arises from midbrain dopaminergic neurons and (3) what midbrain activity produces such a dopamine-mediated signal.

In order to address these aims, I performed large scale extracellular recordings using tetrodes from the pyramidal layer in the CA1 subfield of the hippocampus and from the ventral tegmental area (VTA) in the midbrain. This was combined with selective (optogenetic) activation of midbrain dopaminergic neurons through the genetically targeted expression of the light activated ion channel channelrhodopsin-2. Since studies implicating dopamine action within the hippocampus as facilitating increased memory function have also demonstrated that this effect can be mimicked by exposure to a novel environment (Kentros et al., 2004; Li et al., 2003; Wang et al., 2010), I performed recordings in both familiar and novel open fields. I also performed recordings during sleep before and after the exploration sessions to capture any potential effects on sleep reactivation, a process thought important for the retention of new memories (Buzsáki, 1989; Carr et al., 2011; O'Neill et al., 2010; Skaggs and McNaughton, 1996). Additionally, I present results from the activation of dopaminergic projections during a learning task.

The experimental procedures and methods of analysis used throughout this thesis are presented in the next chapter. The results are broken into four chapters. I first present anatomical evidence for the projection of midbrain dopaminergic neurons to the dorsal hippocampal formation (Chapter 3). I then present data from midbrain recordings investigating

the effect of spatial novelty on the spiking activity of midbrain neurons (Chapter 4). In Chapter 5, I investigate the effect on hippocampal network dynamics of activating midbrain dopaminergic neurons during exploration of an open field. In Chapter 6, I present data on the effect of activating midbrain dopaminergic neurons during a spatial learning task. Finally, I conclude this thesis with a chapter discussing the implications of the findings. Many of the results presented in this thesis are also published in McNamara et al. (2014).

Chapter 2 Experimental procedures and methods of analysis

2.1 Subjects

Experiments involving animals were conducted according to the UK Animals (Scientific Procedures) Act 1986 under personal and project licenses issued by the Home Office following ethical review. Data from a total of eighteen DAT-IRES-Cre$^{+/-}$ mice and five PV-IRES-Cre$^{+/+}$ mice are reported in this thesis. Four DAT-IRES-Cre mice were used to report anatomical evidence for the projection of midbrain dopaminergic neurons to the dorsal hippocampus in chapter three. Ten DAT-IRES-Cre mice were used in the open field experiments reported in chapters four and five. The final four DAT-IRES-Cre mice were recorded performing the crossword maze experiments and five PV-IRES-Cre mice were used to establish the hippocampal dependency of the crossword maze task, both reported in chapter six. All DAT-IRES-Cre animals used were male adult transgenic heterozygote mice (3-8 month-old) and bred from homozygotes for the DAT-internal ribosome entry site (IRES)-Cre transgene (Jackson Laboratories, B6.SJL-Slc6a3$^{tm1.1(cre)Bkmn}$/J, stock number 006660) and hence expressed Cre recombinase in dopaminergic neurons (Bäckman et al., 2006). All PV-IRES-Cre mice were adult male homozygotes for the Parvalbumin-IRES-Cre transgene (Jackson Laboratories, B6;129P2-Pvalb$^{tm1(cre)Arbr}$/J, stock number 008069) and thus expressed Cre recombinase in parvalbumin expressing interneurons. Animals were housed with their littermates until used in the procedure with free access to food and water in a dedicated housing room with a 12/12h light/dark cycle. Experiments were performed during the light cycle.

2.2 Viral vectors

In order to generate expression of the light activated ion channel channelrhodopsin-2 in cells expressing Cre recombinase, I injected a viral vector into the required brain area. The viral vector was adeno-associated virus serotype two (AAV_2) containing a plasmid with the

elongation factor 1-alpha promoter (EF1a) followed by LoxP sites flanking the inverted sequence for channelrhodopsin-2 with H134R mutation fused to enhanced yellow fluorescent protein (ChR2-eYFP) followed by the woodchuck hepatitis post-transcriptional regulatory element (WPRE), and was ordered from Virus Vector Core, Chapel Hill, NC ($pAAV_2$-EF1a-DIO-hChR2(H134R)-eYFP-WPRE, $2.5x10^{12}$ molecules/µl). The virus is capable of transfecting all cells, however, only in the presence of Cre recombinase is the sequence flanked by the LoxP sites inverted thus returning the ChR2-eYFP sequence to the correct order allowing expression of ChR2-eYFP protein driven from the EF1a promoter. Two of the DAT-IRES-Cre mice which were used as control animals were injected with a similar viral vector without the channelrhodopsin-2 sequence resulting in the expression of eYFP alone ($pAAV_2$-EF1a-DIO-eYFP, $2.5x10^{12}$ molecules/µl, Virus Vector Core, Chapel Hill, NC).

2.3 Anaesthesia and surgical procedures

During surgical procedures, mice were induced in a chamber with isoflurane (5%) and oxygen (2 l/min). The surgical area was shaved and the animal was moved to a stereotaxic frame, where it was maintained under deep anaesthesia using isoflurane (0.5-2%) and oxygen (2 l/min) delivered through a mask. Analgesia was also provided (buprenorphine, 0.1 mg/kg) and the animal's body temperature was maintained using a heat pad. After thoroughly disinfecting the area, an incision was performed above the skull and craniotomies were performed above the implantation/injection sites before the *dura mater* was cut and removed. For the initial subjects the viral vector was delivered in the same procedures as the implant, whereas these were performed in separate procedures for later subjects reducing the time the animal spent with the implant present.

2.4 Delivery of viral vectors

Viral vectors were injected into the brain through a glass micropipette (Cetin et al., 2007). Micropipettes were pulled from 5 µl glass micropipettes (BRAND GMBH, Wertheim, Germany; Cat. No. 708707) and the tip was broken with a forceps such that the break was straight and the internal diameter was 18-22µm. A 5 ml syringe was attached via rubber tubing to the back end of the pipette. This allowed negative pressure to be applied within the pipette allowing the virus to be drawn up into the pipette from a droplet placed on a piece of parafilm. Once

the pipette was in position in the brain, positive pressure could then be applied allowing the virus to disperse into the brain. In DAT-IRES-Cre animals, injections were delivered to the ventral tegmental area (VTA) either to the right hemisphere or bilaterally using stereotaxic coordinates 3.25 mm posterior, ±0.5 mm lateral from bregma and 3.8 to 4 mm ventral from the brain surface. For PV-IRES-Cre animals, the viral vector was delivered bilaterally to the CA1 subfields of the dorsal hippocampi using stereotaxic coordinates 2.00 mm posterior, ±1.6 mm lateral from bregma and 1.2 mm ventral from the brain surface. For each injection site, the loaded pipette was first slowly positioned at the appropriate coordinates using the stereotaxic frame and allowed to settle for three minutes. Then positive pressure was applied using the syringe and 1 µl of viral vector ($2.5x10^{12}$ molecules/µl) was delivered at a rate of less than 0.1 µl/minute, guided by graduations marked on the pipette. Finally, the pressure was equalised by removing and reattaching the syringe from the rubber tubing, and a further three minutes was allowed to pass before slowly withdrawing the pipette from the brain.

2.5 Implantation of optic fibres and tetrodes

Surgical implants were prepared before the surgical procedure. Tetrodes were twisted and cut from four individual 12 µm diameter insulated tungsten wires providing four independent recording sites at the tip of the tetrode (H-Formvar insulation with Butyral bond coat, California Fine Wire, Grover Beach CA). To enable their independent movement, each tetrode was mounted in a cannula and attached to a screw via a nylon shuttle. Implants consisted of eight or ten independently movable tetrodes and one or two optic fibres assembled with connectors in a nylon casing. The casing enclosed the optic fibre preventing escaped light from illuminating the environment. The implant was prepared to provide the relative three dimensional positioning required of the tetrodes and optic fibres to reach their targets within the brain. Tetrodes targeting the same area as the optic fibre were typically positioned around the optic fibre within a distance of 0.5 mm. They were positioned level or slightly above the tip of the optic fibre allowing them to be moved gradually into the light field and target brain area post recovery.

During the implantation surgery, prior to performing the craniotomy, stainless-steel screws were inserted into the skull and covered in dental cement serving as an anchor to which the

implant could later be secured. Two screws above the cerebellum served as ground electrodes and all signals were measured with reference to the potential at these screws. After performing the craniotomy and duratomy, the implant was aligned using the stereotaxic frame and lowered into the brain. Paraffin wax was applied to the exposed portion of the electrodes and optic fibers. Finally, the implantation was secured to the anchor screws using dental cement; this also enclosed the paraffin wax. Optic fibers targeted at dCA1 were positioned 2 mm posterior and 1.6 mm lateral from bregma and lowered into the brain a distance of 0.9 to 1 mm. For simultaneous midbrain and hippocampal recordings with VTA targeted optic fiber, the implant was positioned at a 40 degree angle from the antero-posterior axis on the horizontal plane and then at an angle of 10 degrees from the dorso-ventral axis. The optic fiber was positioned at 2.7 mm posterior and 1 mm lateral from bregma and lowered into the brain at the angle described a distance of 3.9 to 4.2 mm.

2.6 Photostimulation

Photostimulation was generated using a 473 nm diode pumped solid state laser (Laser 2000, Ringstead, UK) and delivered to the brain through two lengths of optic fibre (with black plastic jackets to prevent illumination of the environment) and a rotary joint with splitter in the case of bilaterally implanted animals (Doric Lenses, Québec, Canada). The final optic fibres (on the animal end) were coupled to the implanted fibre using an M3 connector. The output intensity delivered to the implanted fibre was approximately 20 mW. In the open field, DAT-IRES-Cre mice received either burst mode photostimulation (trains of 20 light pulses 10 ms in duration with pulses at 50 ms intervals and a burst train delivered every 40 seconds) or tonic mode photostimulation (single light pulses 10 ms in duration delivered every 2 seconds). For the crossword maze experiments, additional DAT-IRES-Cre mice received burst mode photostimulation with pulse duration of 20 ms and burst trains delivered every 20 seconds. For experiments aimed at disrupting hippocampal network activity by local stimulation of PV expressing interneurons, PV-IRES-Cre mice received 473 nm photostimulation applied randomly during 80% of the learning trials, using trains of 10 ms pulses every 16 ms. The laser was off during the inter-trial intervals. In all crossword maze experiments, each mouse alternated between days with photostimulation off and days with photostimulation on.

2.7 Data acquisition

Each signal was buffered on the head of the animal, using an operational amplifier in a non-inverting unity gain configuration (Axona Ltd, www.axona.com), and transmitted over a single strand of litz wire to a dual stage amplifier and band pass filter (gain 1000, pass band 0.1 Hz to 5 kHz, Sensorium Inc., Charlotte, VT). The amplified and filtered signals, along with a synchronization signal from the position tracking system and the activation signal for the laser, were digitized at a rate of 20 kHz and saved to disk by a PC with 16 bit analogue to digital converter cards (United Electronics Industries, Canton, MA). In order to track the location of the animal, three LEDs (red, green and blue) were attached to the electrode casing above the head of the animal and captured at 25 frames per second by an overhead colour camera (Sony). The camera was attached to a PC which extracted the position data in real time.

2.8 Post-recovery and familiarisation with the recording apparatus

After initial recovery from implantation and before recording commenced, each mouse was connected to the recording apparatus and familiarized (through spontaneous exploration) with the familiar open field environment or crossword maze (without barriers) as applicable. This typically lasted one to two hours a day for at least a week. During these training days, if the animal stopped exploring for an extended period in the familiar open field, I introduced my hand above the centre of the open field and this tended to cause the mouse to start moving again. This was to prevent the animal from developing such a habit, thus ensuring good coverage of the environment during recordings aiding the calculation of measures related to the spatial firing of neurons. During this time, tetrodes were gradually lowered over days, through the short distance remaining to reach the required brain area. All mice used in recordings were also familiarized with a 12x12 cm high walled box containing home cage bedding which was used for rest recordings (sleep and long periods of awake immobility). Mice were not used in any other experiments and an animal was either used for open field recordings or crossword maze recordings but never both.

2.9 General recording procedure

At the start of each recording day, hippocampal tetrodes were lowered into stratum pyramidale and midbrain ones were moved slightly in search of action potentials. The animal was then left in the home cage for at least one hour before recording started. At the end of each recording day, hippocampal tetrodes were raised slightly to minimize mechanical damage caused to the stratum pyramidale by tetrodes left within this layer over night, in order to maximize the cell yield and number of recording days per mouse. No further recording days were performed once the number of cells decreased below the number of cells obtained in the initial days. Stratum pyramidale was located using the profile of sharp wave ripple events and presence of multiunit spiking activity. Recordings were always performed in the same room under dim lighting with the recording arena surrounded by a black circular curtain.

2.10 Open field experiments

Open field recording arenas consisted of various boxes of different shapes (polygons with some curved edges surrounded by walls, approximate area generally near 0.25 m^2) constructed from plastic or wood (sometimes lined with brown paper). Open field exploration recording sessions were approximately 30 minutes in duration during which mice spontaneously explored the open field in the absence of any food rewards. Several open field conditions were used. They were as follows: exploration in a familiar open field, i.e. one which the animal has been previously exposed to, ('familiar'); exploration in a novel open field, i.e. one which the animal has never before experienced, ('novel'); exploration in a novel open field with burst mode photostimulation delivered to the VTA ('novel VTA-ON burst'); exploration in a novel open field with burst mode photostimulation delivered to the dorsal CA1 ('novel dCA1-ON burst'); novel dCA1-ON burst in animals which did not receive the ChR2-eYFP viral construct but were instead injected with a viral construct coding for eYFP only ('novel dCA1-ON burst eYFP ctrl.'); novel dCA1-ON burst in animals injected with SCH23390, a selective and potent antagonist of D1/D5 dopaminergic receptors (Sigma, #D054; 0.1mg/kg in 0.9% saline, i.p.), 30 minutes prior to the exploration of a novel environment ('novel dCA1-ON burst SCH23390'); exploration in a novel open field with tonic mode photostimulation delivered to the dorsal CA1 ('novel dCA1-ON tonic'); and finally; exploration in a familiar open field with burst mode photostimulation delivered to the dorsal CA1 ('familiar dCA1-ON burst'). Each day

up to four conditions were recorded. In between each condition and before and after all conditions, rest recordings were taken. During rest recordings, mice were placed in a 12x12 cm high walled box containing home cage bedding to which they had previously been familiarised. Each rest recording was approximately 30 minutes in duration.

2.11 Crossword maze experiments

The crossword-like maze (Figure 2.1) consisted of four start boxes and eight intersecting open tracks forming fourteen intersections inspired by a layout used previously by Tolman (1948). The width of each track was 5 cm with a 1.5 cm high rim along the edges. The entire maze measured 95 cm square excluding start boxes. The maze was painted black and suspended 5 cm above a black table. Distal cue cards were placed on the curtain surrounding the maze and some cue objects were placed on the supporting table dispersed throughout the maze. In order to promote allocentric spatial navigation by distal cues, the maze was randomly rotated relative to the cues at the beginning of each day. Mice performing the crossword maze task were maintained at 85% of their post-operative body weight. The recording protocol used consisted of the following ordered stages: rest, pre-learning, rest, learning, rest and probe (Figure 6.1). During the pre-learning stage the animal explored the maze with the start boxes closed and in the absence of barriers and rewards for approximately 20 minutes.

For the learning stage two start boxes and one food reward location (at the end of one of the five tracks protruding from the maze) were selected as in use for that day and the maze was configured with a new arrangement of up to seven barriers (10 cm in height) such that there was only one path from each start-box to the reward (Figure 2.1). Mice were given up to twenty trials (mean = 18.7; median = 19.0; quartile range = 18.0-20.0) to learn to find the reward with the start point randomly switching between the two start boxes. The per trial reward was 4 µl of condensed milk diluted 30% in water and was placed on a plastic cap at the goal location. A similar plastic cap (without reward) was placed in each of the other four tracks protruding from the maze. A glass vial (with perforated lid) containing an aliquot of the reward yet non accessible was placed inside the two start boxes to signal the onset of the learning phase to the animal. The board was cleaned after each learning trial to discourage the use of an odour guided search strategy.

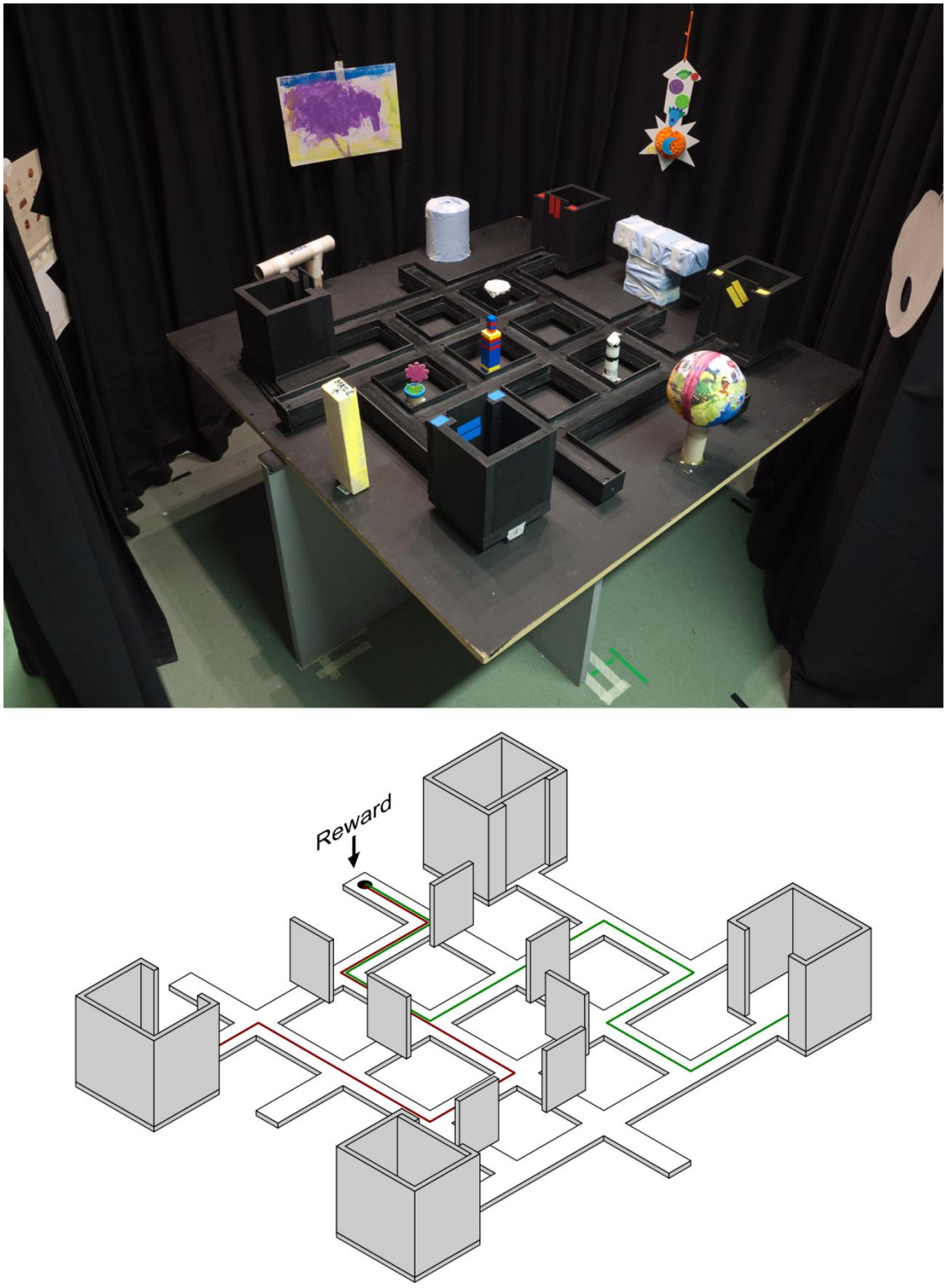

Figure 2.1 *The crossword maze*
Top, photograph of the crossword maze without barriers showing the cue objects and the distal cue cards on the curtain surrounding the maze. Bottom, isometric projection of the crossword maze showing an example configuration of barriers and reward location. On any given recording day, only two of the start boxes were used. The shortest paths from the in-use start boxes to the reward location are shown in red and green.

For the probe stage (conducted 1 hour after the learning stage ended), the maze was maintained in the same layout as the learning stage but no reward was present. Mice were released from one of the in-use start boxes and allowed to explore the maze for 3 minutes. Mice were released a further 3 times during the probe stage in order to ensure good coverage of the maze to calculate spatial rate maps (3 minutes each release; 12 minutes total probe duration). The path length to first reaching of the reward location was used to evaluate memory performance. When combining across maze configurations, path lengths were normalized by the relevant shortest possible path (Figure 2.1).

As with the open field experiments, during rest recordings, mice were placed in a 12x12 cm high walled box containing home cage bedding to which they had previously been familiarised and rest recordings were approximately 30 minutes in duration. The number of crossword maze recording days included in this thesis is 12 days without photostimulation and 13 days with photostimulation for experiments involving the DAT-IRES-Cre mice; 13 days (12 probe tests) without photostimulation and 9 days with photostimulation for experiments involving the PV-IRES-Cre mice.

2.12 Spike detection and unit isolation

The recorded signals were digitally band pass filtered (800 Hz to 5 kHz) offline for spike detection and unit isolation. Spikes were detected using a threshold in the root mean square (RMS) power (0.2 ms sliding window) of the filtered signal. Unit isolation was performed on the first three or four principal components calculated for each channel recorded by the tetrode in question. This was achieved by automatic over-clustering (KlustaKwik, klusta-team.github.com) followed by graphically-based manual recombination and further isolation informed by cloud shape in principal component space, cross-channel spike waveforms, auto-correlation histograms and cross-correlation histograms (Csicsvari et al., 1999; Harris et al., 2000). To analyse changes in the firing patterns of pyramidal ensembles over time, and reliably monitor cell pairs across recording sessions, it was necessary to ensure that the sample of cells was taken from clusters with stable firing. Therefore, all the sessions recorded on a given day were clustered together. Only well-isolated and stable units over the entire recording day were used for further analysis; namely units that showed a clear refractory period in their auto-

correlations and well-defined cluster boundaries across all recording sessions of the day. Units were deemed independent from each other by (1) their distinct spike waveform, (2) the absence of refractory period in their cross-correlations and (3) separable principal component boundaries using a measure based on the Mahalanobis distance (Csicsvari et al., 1999; Harris et al., 2001). Hippocampal pyramidal cells were identified by their auto-correlogram and firing rate as previously described (Csicsvari et al., 1999). Only pyramidal cells with average firing rate greater than 0.1 Hz (0.2 Hz for crossword maze experiments) were included in reactivation and place field based analysis to ensure a misleading result was not produced by correlations between cells which fired very little spikes in the epochs of interest.

2.13 Detection of theta oscillations, SWR events and behavioural states

Theta oscillations and SWR events were detected off-line using digital band pass filter methods as previously described (Csicsvari et al., 1999; Dupret et al., 2010; O'Neill et al., 2008). First, the theta/delta power ratio was measured in 1600 ms segments (800 ms steps between measurement windows), using Thomson's multi-taper method (Csicsvari et al., 1999; Mitra and Pesaran, 1999; Thomson, 1982). The theta/delta power ratio was used to mark periods of theta activity and individual theta oscillatory waves were identified within these periods by first applying a conservative band-pass filter (5-28 Hz) to the wideband signal. This allowed precise detection of the trough of individual waves from the filtered trace without over-smoothing the signal. Next, phase alignment was performed to these minima and theta windows were demarcated spanning from peak-to-peak. Windows with a corresponding theta frequency of 5-12 Hz were used in further analysis. Sharp wave ripple (SWR) event detection was performed in rest epochs when the instantaneous speed of the animal was less than 2 cm/s and the theta/delta ratio was less than 2. Recorded signals were band-pass filtered (135-250 Hz), and the signal from a ripple-free reference electrode was subtracted to eliminate common-mode noise (such as muscle artefacts). Next the RMS power of the processed signal was calculated for each electrode and summed across CA1 pyramidal cell layer electrodes to reduce variability. The threshold for SWR event detection was set to 7 SD above the background mean power. The proportion of pyramidal cells active in SWR events was calculated for recordings with at least 5 pyramidal cells. The SWR firing rate histograms of

pyramidal cells were calculated using 20 ms bins in reference to the SWR peak (i.e., peak of ripple-band power).

2.14 Measures of burst firing

In the raster plots of Figure 4.4 individual spikes are coloured grey and spikes occurring within bursts coloured black. Bursts were classified as trains of at least two spikes with inter spike intervals (ISI) of less than 50 ms. This conservative intra-burst spike interval threshold of 50 ms (intra-burst frequency of 20 Hz) was chosen over the often used criteria for dopaminergic cells of less than 80 ms (12.5 Hz) for start of burst and greater than 160 ms (6.25 Hz) for end of burst established in anaesthetized rats (Grace and Bunney, 1984a; Ungless and Grace, 2012), in order to allow sufficient clearance between the burst interval threshold frequency and some of the higher mean rates (11 Hz) seen in the light identified units from behaving mice reported here. Note that use of a 80 ms cut-off produced similar findings.

The burst firing of midbrain cells is quantified here using three measures. Burst ratio, coefficient of variation (CV) and an alternative of CV called CV2 (Holt et al., 1996). Burst ratio was calculated as the total number of burst spikes divided by the total number of single spikes. This allowed longer bursts with many spikes to have a more representative contribution to the ratio than spike doublets or triplets compared to measures which count all bursts equally irrespective of length. It also has the added advantage of not requiring a 160 ms end of burst criteria which was originally included by Grace and Bunney (1984a) to allow for the observation that there is often a missed spike within a burst that isolates the later spikes from the first spikes of the same burst since the burst ratio measure used here takes into account all burst spikes. Coefficient of variation (CV) is the ratio of the standard deviation of the ISI to the mean ISI and provides a dimensionless measure for the level of dispersion of the distribution of ISI, with a high value indicative of burst-like firing, and a low value indicative of regularly paced firing. The alternative measure CV2 provides a similar estimate; however, it limits the comparison of variation to adjacent ISI removing sensitivity to slow, non-burst related variations in mean rate. It was calculated as the mean value across the spike train of two times the absolute value of the difference over the sum of adjacent ISI and has a value of one for a Poisson process (Holt et al., 1996).

2.15 Reactivation

Reactivation strength was measured as the Pearson correlation coefficient between the tendencies of hippocampal pyramidal cell pairs to fire together (co-fire) across theta cycles during exploration (theta co-firing) with their tendency to co-fire in SWR events during rest (SWR co-firing) (Dupret et al., 2010; O'Neill et al., 2008). To measure theta co-firing during exploration, I first established for each pyramidal cell its instantaneous firing rate counts (IFRC) in windows spanning from peak-to-peak of detected theta cycles and then calculated the correlation coefficient between the IFRCs for each cell pair. Likewise, SWR co-firing values were calculated as the correlation coefficients between IFRCs of pyramidal cell pairs taken from 100 ms windows centred on the peak power of SWR events. The reactivation strength was then calculated as the Pearson correlation coefficient between the theta bin co-firing values and the SWR bin co-firing values. Detected theta windows corresponded to periods of active exploration and SWR events were restricted to times of behavioural immobility. Only simultaneously recorded cells were paired.

2.16 Spatial rate maps

To calculate spatial rate maps, the horizontal plane of the recording arena was divided into bins of approximately 2x2 cm^2. Spike count maps, the number of spikes fired in each bin, were calculated for each unit. An occupancy map for each exploration session was also calculated as the time spent by the animal in each bin. All maps were then smoothed by convolution with a Gaussian kernel having standard deviation equal to one bin width. Finally, spatial rate maps were generated by normalizing (dividing) the smoothed spike count maps by the corresponding smoothed occupancy map.

2.17 Population map similarity

The population map similarity measure, as applied previously (Dupret et al., 2010; O'Neill et al., 2008), was used to compare the degree to which the relative locations of the preferred firing fields of cells was maintained between two periods of exploration. This was done by comparing all the spatial rate maps from two different time periods, in a pairwise fashion, in the same manner as the co-firing analysis used for reactivation does for cell firing patterns across LFP events but performing binning over space rather than time. This provides a measure

of the degree to which cells which fired in similar regions of space (i.e., overlapping place fields) still fire in similar regions of space later. It is calculated by first computing the place field similarity (PFS) value for each cell pair during the first time period as the Pearson correlation coefficient from the direct bin-wise comparisons between the spatial rate maps of the two cells limited to valid bins (occupancy greater than zero). This is repeated for the second time period and the population map similarity between the two time periods is then calculated as the Pearson correlation coefficient between the PFS values from each of the time periods. Hippocampal place cells screened for their spatial tuning using a sparsity value of no more than 0.3 (Dupret et al., 2010) were included in this analysis.

2.18 Spatial tuning measures

Coherence and sparsity were calculated from the unsmoothed place rate maps as reported before (Muller and Kubie, 1989; Skaggs et al., 1996). Coherence reflects the similarity of the firing rate in adjacent bins, and is the *z* transform of the Pearson correlation (across all bins) between the rate in a bin and the average rate of its eight nearest neighbours (Muller and Kubie, 1989). Sparsity corresponds with the proportion of the environment in which a cell fires, corrected for dwell time, and is defined as $(\Sigma P_i R_i)^2/\Sigma P_i R_i^2$, where P_i is the probability of the mouse occupying bin *i* and R_i is the firing rate in bin *i* (Skaggs et al., 1996).

2.19 Error intervals, statistical tests and software

All error intervals quoted are ± standard error of the mean or standard error of the correlation coefficient calculated as the square root of $(1-r^2)/(n-2)$ where *r* is the Pearson correlation coefficient and *n* the number of cell pairs (Zar, 1999). All tests performed were two-sided. All P values for the comparison of Pearson correlation coefficients were calculated using Z statistics after application of Fisher's *r* to *z* transform. Other tests, wherever appropriate, are mentioned along with the value. Recorded data was analysed on a Linux PC (fedora; getfedora.org) using C programs, BASH scripts and the ipython (Perez and Granger, 2007) interactive Scientific Computing environment (ipython.org) with the NumPy (numpy.org), SciPy (scipy.org) and Pandas (pandas.pydata.org) packages. Statistical analyses were performed using SciPy and R (r-project.org). Sample sizes in this study are similar to those generally employed in the field and

were not pre-determined by a sample size calculation. Data distributions for parametric tests were assumed to be normal but this was not formally tested.

2.20 Tissue processing and immunocytochemistry

To produce anatomical data presented in Chapter 3, mice were deeply anesthetized with isoflurane/pentobarbital and transcardially perfused with phosphate buffer saline (PBS) followed by fixative (paraformaldehyde dissolved in PBS, 4% wt/vol), brains were extracted and sectioned into 70 µm thick coronal sections. Sections were washed three times in PBS between each of the following steps. Cell membranes were made permeable and non-specific protein binding was blocked by incubation for 1 hour in PBS-triton (0.3%) and normal donkey serum (NDS, 10%). Next, sections were incubated for 48 hours at 4 °C in a solution of primary antibodies against green fluorescent protein (GFP, used to recognize ChR2-eYFP) and tyrosine hydroxylase (TH, for the DAT-IRES-Cre brain sections) or parvalbumin (PV, for the PV-IRES-Cre brain sections), washed and then further incubated in a solution with corresponding secondary antibodies (raised in donkey) conjugated with DyLight488 or Alexa488 and Cy3 (Table 2.1). Both antibody solutions were diluted in PBS-triton (0.3%) and NDS (1%). Finally, sections were counterstained with DAPI (diluted 1:10000) for 20 minutes and mounted on glass slides using VectaShield (Vector Laboratories).

Table 2.1 *Antibody information*

Molecule	Host species	Dilution	Source and code	Antibody specificity information	Used in combination with
green fluorescent protein (GFP)	chicken	1:500	Aves Labs, Tigard, Oregon, USA (www.aveslabs.com) GFP-1020	Western blot and immunohistochemistry tests (Aves Labs, product data sheet)	donkey anti-chicken DyLight488 (1:500) Jackson, 703-485-155; donkey anti-chicken Alexa488 (1:500) Jackson, 703-545-155
green fluorescent protein (GFP)	rat	1:500	Nacalai Tesque, Kyoto, Japan (www.nacalai.com) GF090R/04404-84	Western blot[1]	donkey anti-rat Alexa488 (1:500) Invitrogen, A21208
tyrosine hydroxylase (TH)	rabbit	1:500	EMD Millipore Corporation, Billerica, MA, USA (www.millipore.com) AB152	Western blot[2] (and Millipore product page)	donkey anti-rabbit Cy3 (1:500) Jackson, 711-165-152
tyrosine hydroxylase (TH)	chicken	1:500	Abcam, Cambridge, UK (www.abcam.com) ab76442	Western blot[3]	donkey anti-chicken Cy3 (1:500) Jackson, 703-165-155
parvalbumin (PV)	mouse	1:4000	EMD Millipore Corporation, Billerica, MA, USA (www.millipore.com) MAB1572	Western blot and immunohistochemistry tests (Millipore product page)	donkey anti-mouse Cy3 (1:1000) Jackson, 715-165-150

1. Tomiyoshi, G., Nakanishi, A., Takenaka, K., Yoshida, K. & Miki, Y. *Cancer Sci.* **99**, 747-754 (2008).
2. Yamamoto, K., Ruuskanen, J.O., Wullimann, M.F. & Vernier, P. *Mol. Cell. Neurosci.* **43**, 394-402 (2010).
3. Samaco, R.C., *et al. Proc. Natl. Acad. Sci. USA* **106**, 21966-21971 (2009).

2.21 Microscopic analyses and 3D reconstruction

Specificity of virus transfection was quantified from both hemispheres of four bilaterally injected brains. Three consecutive sections centred on the injection coordinate (bregma -3.25) were selected (Franklin and Paxinos, 2008). An exhaustive tiled grid of 20 µm thick (0.8 µm step) z-stacks to span the VTA was acquired from the top of each section using an epifluorescence microscope (Imager.M2 with filter set 38 and a Plan-Neofluar 40x/1.3 objective, Zeiss). Only grid tiles which were deemed to be within the VTA regions (A10 cell groups) (Fu et al., 2012) were included in the counting. Greater than 900 cells were counted per brain. Three-dimensional reconstruction of transfected dCA1 axons was completed using the same microscope and Neurolucida software (MBF Bioscience). Images included in this thesis were acquired using a confocal microscope (Imager.Z1 with LSM 710 scan head and Plan-Neofluar 5x/0.16, Plan-Apochromat 40x/1.3, 63x/1.4 or 100x/1.46 objective, Zeiss) in sequential scanning mode with the following excitation laser and emission filter wavelengths. DAPI: 405 nm, 409-499 nm; eYFP/DyLight488: 488 nm, 493-571 nm; Cy3: 543 nm, 566-729 nm. Acquisition and analysis were completed using ZEN 2008, v5.0 (Zeiss) and ImageJ (rsb.info.nih.gov) software. Z-stacks were flattened using maximum intensity projection.

Chapter 3 Anatomical evidence for the projection of midbrain dopaminergic neurons to the dorsal hippocampus

3.1 Introduction

A number of studies have presented evidence for the projection of midbrain dopaminergic neurons to the hippocampus proper in rats (Gasbarri et al., 1994a; Gasbarri et al., 1996; Gasbarri et al., 1994b; Ishikawa et al., 1982; Samson et al., 1990; Scatton et al., 1980; Swanson, 1982; Verney et al., 1985). One of the more convincing early reports was by Scatton and colleagues (1980) who reported reduced dihydroxyphenylacetic acid (DOPAC; a metabolite of dopamine) levels in the rat hippocampus after electrolytic or chemical lesion of the ventral tegmental area (A10) or substantia nigra (A9). Morphological evidence followed a few years later, when Verney and colleagues (1985) performed tyrosine-hydroxylase (TH) immunocytochemistry in the hippocampus of noradrenaline-depleted rats. They reported the presence of immunoreactive axons in fimbria, alveus and innervating the deep layers (stratum oriens) of CA1, subiculum and prosubiculum, particularly in the ventral part of the hippocampus. Another group of studies reported the presence of connections from the ventral tegmental area (VTA) to the hippocampus by first using anterograde tracing with phaseolus vulgaris-leucoagglutinin (PHA-L) injected in the VTA and retrograde fluorescent tracers injected in the HPC (Gasbarri et al., 1994a). They followed this with a combined retrograde tracing and immunohistochemical study to determine if the projection was dopaminergic, reporting that 15-18% of the retrogradely labelled VTA and substantia nigra (SN) cells showed anti-TH (tyrosine-hydroxylase) immunoreactivity (Gasbarri et al., 1994b). The same group subsequently reported a similar finding for a projection from the RRF/A8 dopaminergic cell group (Gasbarri et al., 1996). Across all these rat studies, the dopaminergic innervation of the hippocampus is described as less dense than that seen in other brain areas previously reported

to receive sizable dopaminergic innervation, such as the striatum and amygdala (Björklund and Lindvall, 1984). Most reports also indicate a greater projection to the ventral than dorsal hippocampus. Additionally, midbrain dopaminergic cells have been found to project to the subgranular zone of the dentate gyrus where dopamine signalling has been implicated in the proliferation of precursor cells during adult neurogenesis, in both mice and rats (Höglinger et al., 2014; Hoglinger et al., 2004; Mu et al., 2011).

Investigations in primates have also found evidence for a projection from the VTA to the hippocampus (Amaral and Cowan, 1980; Lewis and Sesack, 1997; Samson et al., 1990). It is suggested that the dopaminergic innervation of the hippocampus found in primates is more dense than that seen in rodents (Lewis and Sesack, 1997; Samson et al., 1990). This is primarily based on a study by Samson and colleagues (1990) who used antibodies to dopamine-beta-hydroxylase (DBH) and TH in the hippocampus and attributed the DBH immunopositive fibres as noradrenergic fibres and the TH immunopositive fibres as dopaminergic. As acknowledged by the authors, this may not be a fully reliable assumption and should be treated with some caution since TH immunoreactivity could be labelling dopaminergic, noradrenergic or both fibres. This is because DA is a precursor of noradrenaline. However, in this particular preparation from cynomolgus monkeys with the particular antibodies used, the two antibodies appear to label separate populations of fibres and, therefore, the assumption that TH immunoreactivity reflects the dopaminergic fibres may be reasonable. The density of innervation could be even higher in humans. Studies investigating this question partially suggest the opposite, however results are somewhat discrepant and potential difficulties with fixation, post-mortem interval and antibodies in human studies mean this is still an open question (Lewis and Sesack, 1997).

A final piece of evidence suggestive of a functional dopaminergic projection to the hippocampus, or at least for dopamine as a functional neurotransmitter in the hippocampus, is the presence of both D1-type and D2-type dopamine receptors. To date, results from experiments using antibodies raised against dopamine receptors have proven somewhat difficult to interpret clearly due to technical difficulties, but such studies have provided some evidence for the presence of dopamine receptors in the hippocampus (Ciliax et al., 2000; Levey et al., 1993; Smith and Greene, 2012). Additional evidence comes from studies using reporters

of the relevant mRNA, transgenic lines driving expression of a reporter such as a fluorescent protein under the relevant promoter, or the selective binding of radio-ligands. All three methods indicate both D1-type (particularly D5 receptors) and D2-type receptors are present in the hippocampus (Bentivoglio and Morelli, 2005; Fremeau et al., 1991; Gangarossa et al., 2012; Laurier et al., 1994; Meador-Woodruff et al., 1992; Savasta et al., 1986; van der Weide et al., 1987). Taken together, results from across all four methods provide a strong indication of the presence of dopamine receptors in the hippocampus, both dorsal and ventral.

Much of the reports in relation to dopaminergic innervation of the hippocampus indicate the presence of dopaminergic fibres in the ventral hippocampus, however, much of the literature focusing on the memory functions are from recordings in the dorsal hippocampus. Also, at the time of starting my DPhil studies, there was no information on dopaminergic innervation of the hippocampus in mice. In this chapter, I focus my investigation of dopaminergic innervation to the dorsal hippocampus, since I wished to perform recordings in the dorsal portion of the hippocampus with the aim of relating the midbrain dopaminergic system and the memory functions of the hippocampus.

3.2 Experimental outline

Advances in transgenic mouse lines and viral vector based techniques presented a chance to investigate further the nature of midbrain derived dopaminergic innervation of the hippocampus and overcome some of the technical difficulties faced by the early tracer studies. Here I investigated if transfected axons were present in the dorsal hippocampus after injection of a Cre activated viral vector in the ventral tegmental area (VTA) of *DAT-IRES-Cre*$^{+/-}$ mice. To this end, I performed bilateral injections delivering 1 µl of viral vector per hemisphere to the VTA of four *DAT-IRES-Cre*$^{+/-}$ mice. Mice were anaesthetized and transcardially perfused with phosphate buffer saline (PBS) followed by fixative (see section 2.20). The brains were then sectioned and antibodies to tyrosine-hydroxylase (TH) and eYFP were applied allowing visualisation of protein expression (see section 2.20). Sections were also counterstained with DAPI. During cutting, the order of sections was maintained to allow 3D reconstruction (see section 2.21). Investigations reported in this chapter were completed with the assistance of visiting student Caroline Etienne.

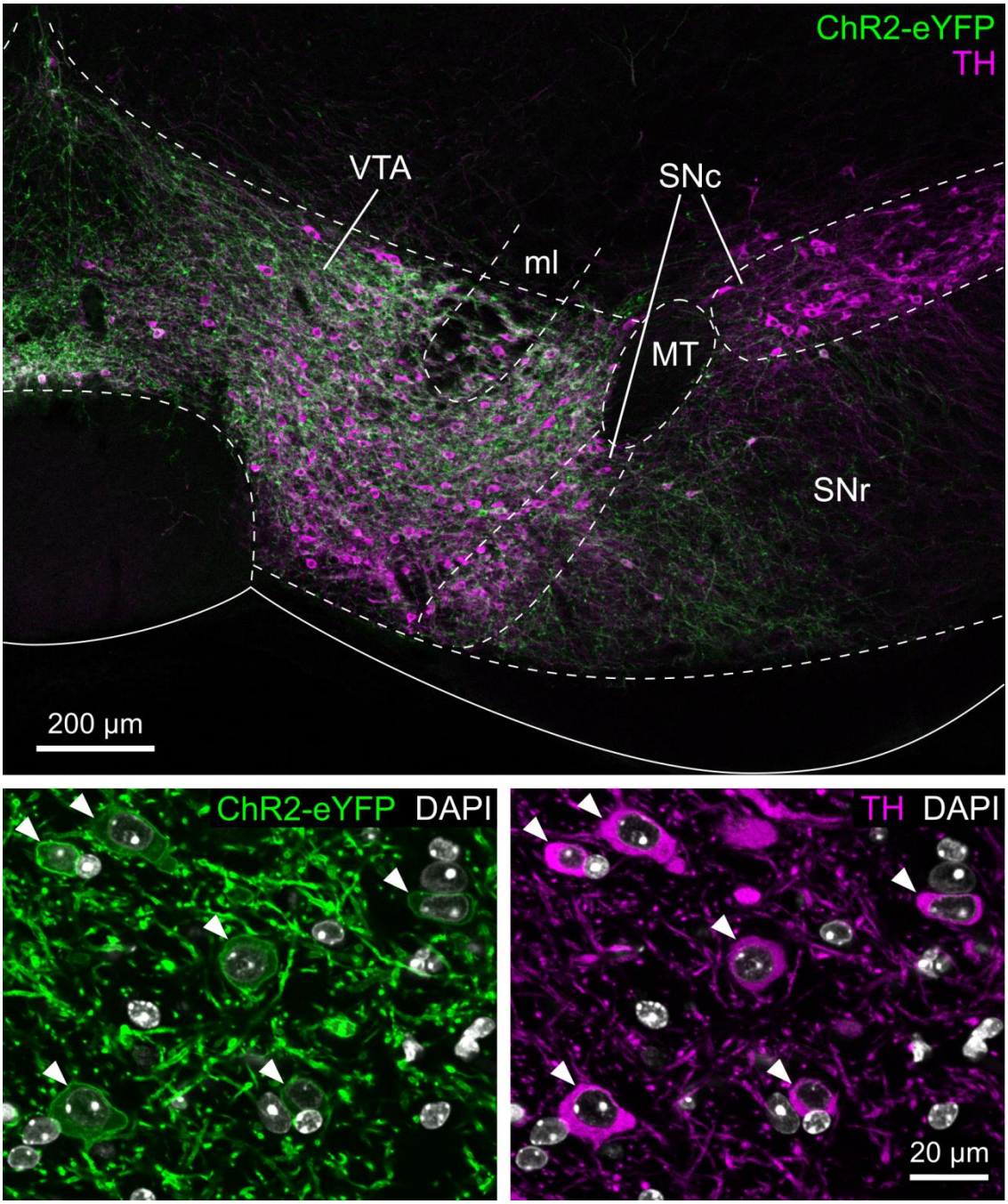

Figure 3.1 *Expression of ChR2-eYFP in the VTA*

Top, low magnification confocal image from a coronal section located at bregma -3.25 mm showing ChR2-eYFP expression (green) at the injection site in the VTA and minimal expression in the SNc. Anti-TH immunofluorescence is shown in magenta identifying dopaminergic cells. Bottom, split panel higher magnification image from the same section showing Chr2-eYFP expression (left), co-localising with anti-TH immunofluorescence (right). Cell nuclei are shown through counterstaining with DAPI (white). Cell bodies immunopositive for TH are marked with the white arrows. VTA, ventral tegmental area; SNc, substantia nigra pars compacta; SNr, substantia nigra pars reticulata; ml, medial lemniscus; MT, medial terminal nucleus.

3.3 Expression of ChR2-eYFP in dopaminergic neurons after viral transfection in the midbrain

The stereotaxic coordinates used for injection of the viral vector were located in the centre of the VTA. This produced greater ChR2-eYFP expression in the VTA than in the substantia nigra pars compacta (SNc), as can be seen in the top panel of Figure 3.1. Expression of ChR2-eYFP at the injection site was quantified by, first, identifying the section at bregma -3.25 mm as the section with the location of the medial lemniscus (ml) and the medial terminal nucleus (MT) in relation to anti-TH immunofluorescence, matching that seen in Figure 3.1. This section and the sections on either side of it were then used for quantification, giving a total of 12 sections (3 from each animal). Cell counting was performed in both hemispheres within the region marked VTA on Figure 3.1. Expression of ChR2-eYFP was nearly exclusively in dopaminergic neurons with 98.6 ± 0.4% (n = 4 mice) of ChR2-eYFP expressing VTA neurons co-expressing tyrosine hydroxylase (TH). The efficiency of virus transfection near the injection site was also high with 76 ± 7% of TH immunopositive neurons co-expressing ChR2-eYFP.

3.4 Transfected dopaminergic axonal segments were present in the hippocampal formation

Axons expressing ChR2-eYFP were present in the dorsal hippocampus of all four animals. The axons were also immunopositive for tyrosine hydroxylase (TH). Co-expression of the two markers indicated the axons originated from midbrain dopaminergic neurons and were not resulting from non-specific expression of the viral construct. Four axonal segments in the dorsal CA1 co-expressing ChR2-eYFP and TH are shown in Figure 3.2. Axons expressing ChR2-eYFP were present in the fornix and continued caudally entering the septal pole of the hippocampus, entering stratum oriens and beyond as well as continuing in the white matter tracts of the dorsal fornix, fimbria and alveus towards the ventral hippocampus, occasionally descending from alveolus into stratum oriens and onwards to more superficial hippocampal layers.

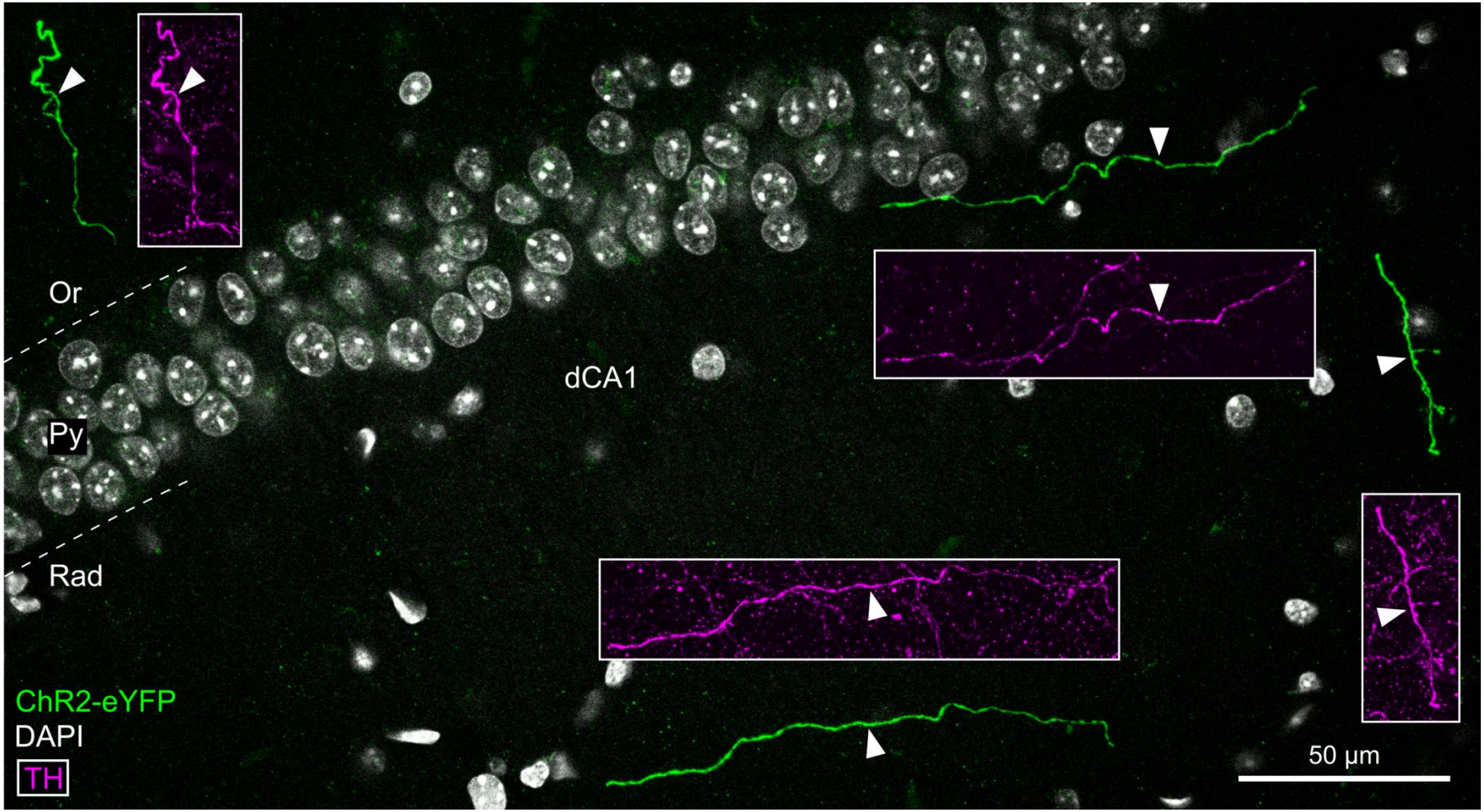
Or
Py
Rad
dCA1
ChR2-eYFP
DAPI
TH
50 µm

Figure 3.2 *Transfected axonal segments present in dorsal CA1*
Transfected axonal segments present in dorsal CA1 after viral injection in the VTA. Maximum intensity projection through a dorsal CA1 (dCA1) 70 µm coronal section (approximately bregma -1.6 mm with picture centred 0.6 mm from the midline), showing four transfected axonal segments expressing ChR2-eYFP in green (florescence was amplified through the application of antibodies to ChR2-eYFP). Cell nuclei from a single 1 µm thick confocal plane through the middle of the section are shown through counterstaining with DAPI (white). Insets show maximum intensity projections of anti-TH immunofluorescence in the same axonal segments (magenta). Or, stratum oriens; Py, stratum pyramidale; Rad, stratum radiatum.

The locations of these fibres within the hippocampus were traced in three dimensions through successive coronal sections from approximately bregma -1 mm to -2.5 mm in two animals. Coronal, sagittal and horizontal projections of the traced axons in animal one and two are shown in Figure 3.3 and Figure 3.6 respectively. The spreading out of the fibres from the septal pole extending along the rostral caudal axis is evident in these figures. The location of the fibres with respect to the layers of the hippocampus can be seen in the coronal views of the individual slice tracings in Figure 3.4 and Figure 3.7. Antibodies to TH were applied to a number of the sections, and axonal segments verified as co-expressing TH are coloured magenta in the tracings. Finally, axonal segments matched as continuing from one section to the next, were spliced together and coloured accordingly. This is shown in Figure 3.5 and Figure 3.8, along with the reconstructed surface formed by alveus to stratum oriens border. Two oblique projections provide a view of axons within the surface created by the alveus to stratum oriens border, while a coronal projection allows visualisation of the axons running in the alveus and white matter around the outside of the hippocampus.

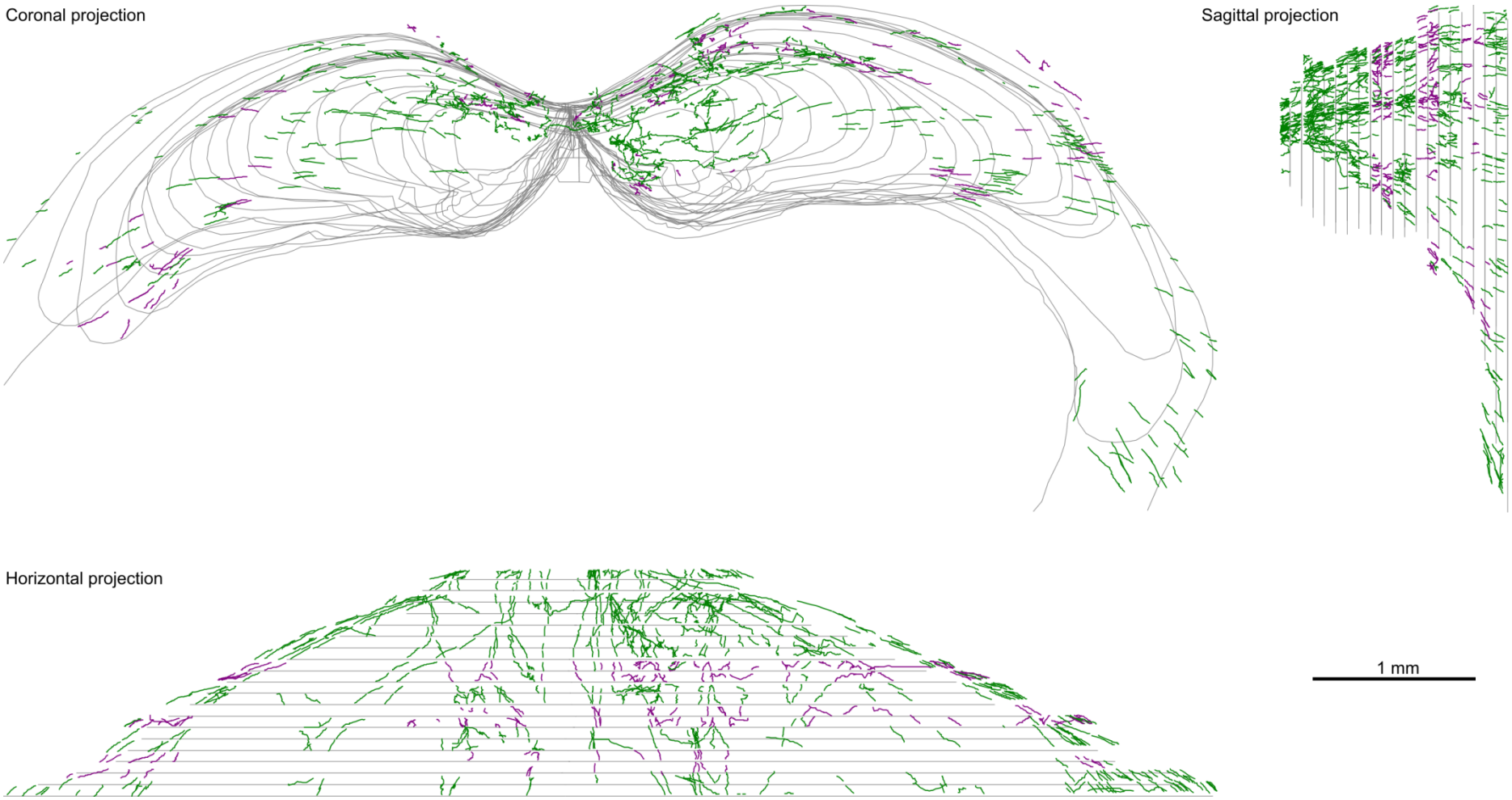
Coronal projection
Sagittal projection
Horizontal projection
1 mm

Figure 3.3 *ChR2-eYFP expressing dCA1 axonal segments (orthographic projection animal 1)*
Orthographic projection of ChR2-eYFP expressing axonal segments traced in dorsal CA1 of animal one. Tracings of axonal segments are shown in green. The alveus to stratum oriens border is traced in grey. Antibodies against tyrosine hydroxylase (TH) were applied to six of the sections and axonal segments verified as co-expressing TH are shown in magenta.

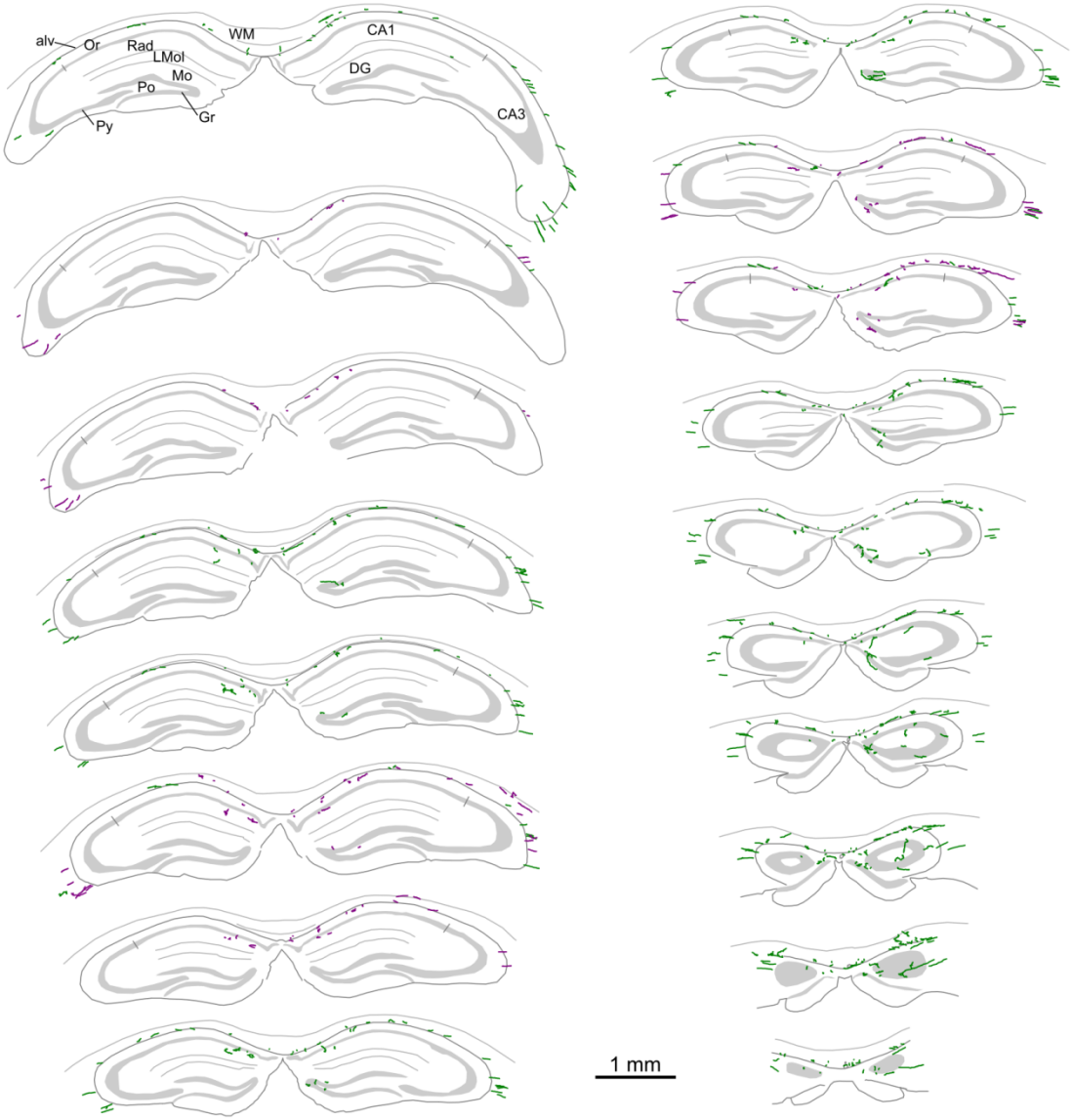

Figure 3.4 *ChR2-eYFP expressing dCA1 axonal segments (slice tracings animal 1)*
Individual slice tracings of ChR2-eYFP expressing axonal segments traced in dorsal CA1 of animal one. Tracings of axonal segments are shown in green. The outline of structures including alveus (alv) and overlying white matter (WM); stratum oriens (Or); stratum pyramidale (Py); stratum radiatum (Rad); stratum lacunosum moleculare (LMol); and the molecular (Mo), granule (Gr) and polymorphic (Po) layers of the dentate gyrus (DG) were also traced (grey). Antibodies against tyrosine hydroxylase (TH) were applied to six of the sections and axonal segments verified as co-expressing TH are shown in magenta.

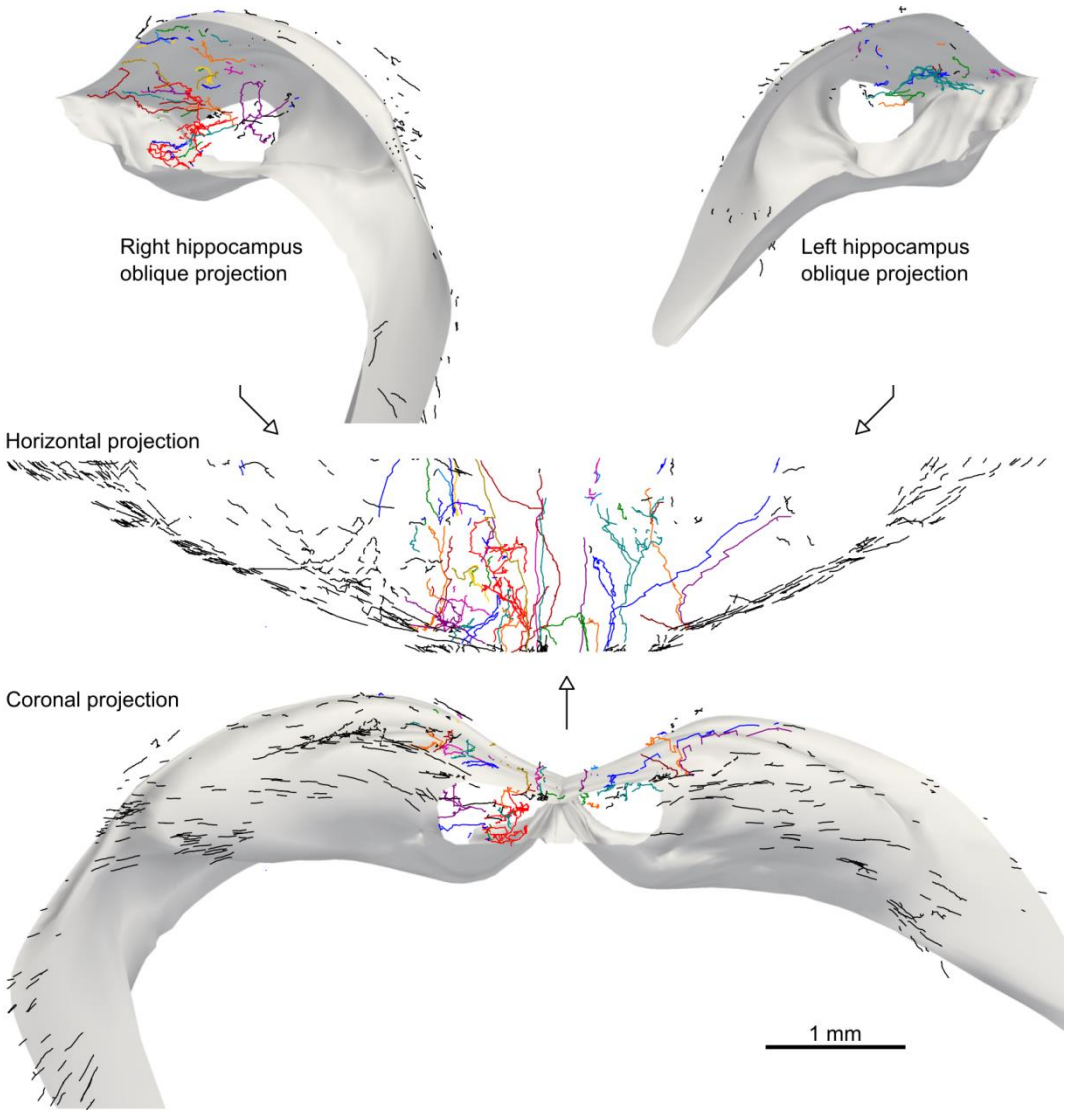

Figure 3.5 *ChR2-eYFP expressing dCA1 axonal segments (spliced reconstruction animal 1)*
Spliced reconstructions of ChR2-eYFP expressing axonal segments traced in dCA1 of animal one. Axons matched as continuing from one section to the other were spliced together. Different colours are used to show the different groupings. Axonal segments extending through alveus and some segments in the overlying white matter which were not spliced together are shown in black. The reconstructed surface is the alveus to stratum oriens border with smoothing applied. The arrows show the angle of the three vertical views with respect to the horizontal view. In the oblique projections only the near hippocampus is shown.

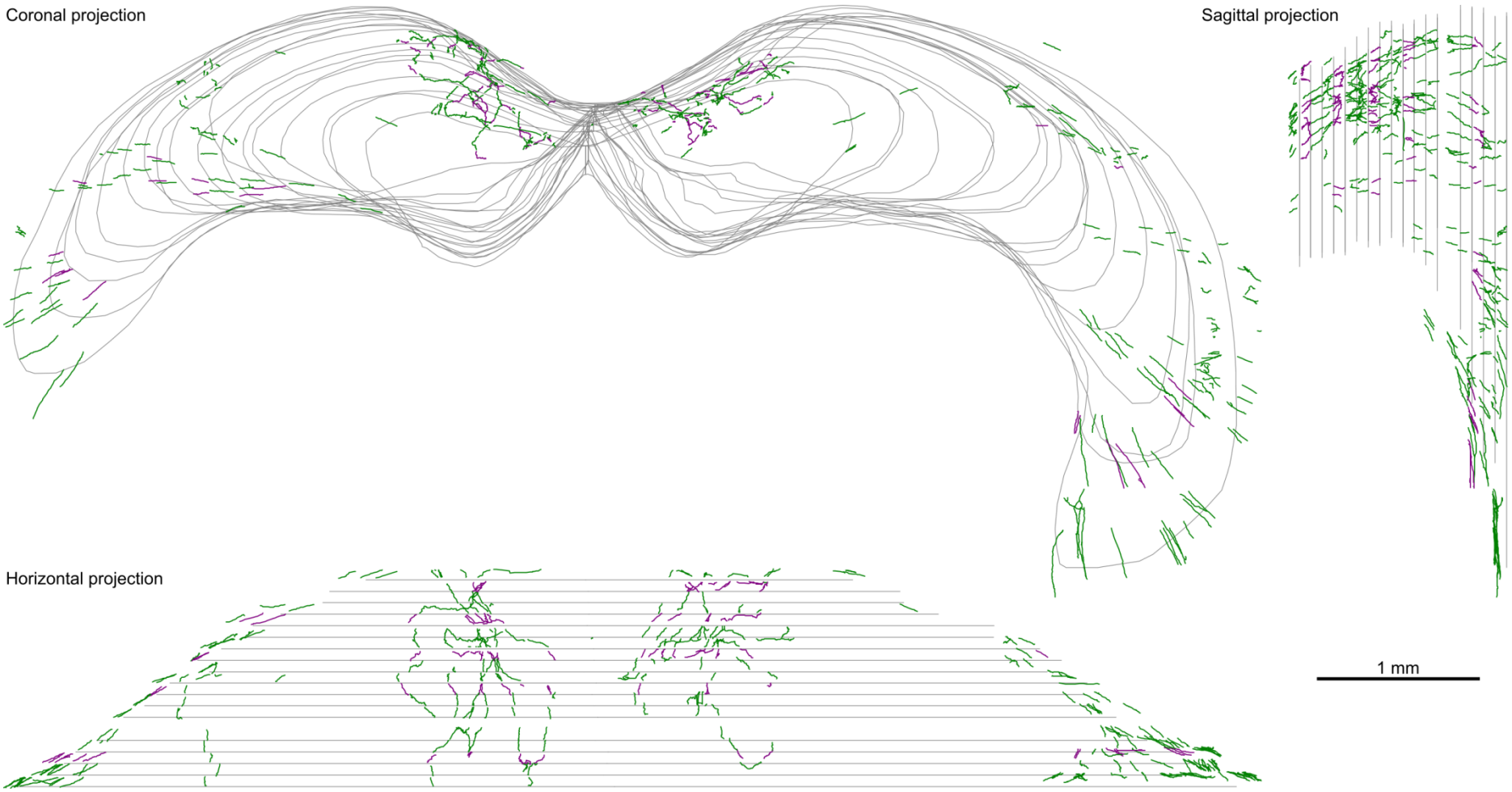
Coronal projection
Sagittal projection
Horizontal projection
1 mm

Figure 3.6 *ChR2-eYFP expressing dCA1 axonal segments (orthographic projection animal 2)*
Orthographic projection of ChR2-eYFP expressing axonal segments traced in dorsal CA1 of animal two. Tracings of axonal segments are shown in green. The alveus to stratum oriens border is traced in grey. Antibodies against tyrosine hydroxylase (TH) were applied to five of the sections and axonal segments verified as co-expressing TH are shown in magenta.

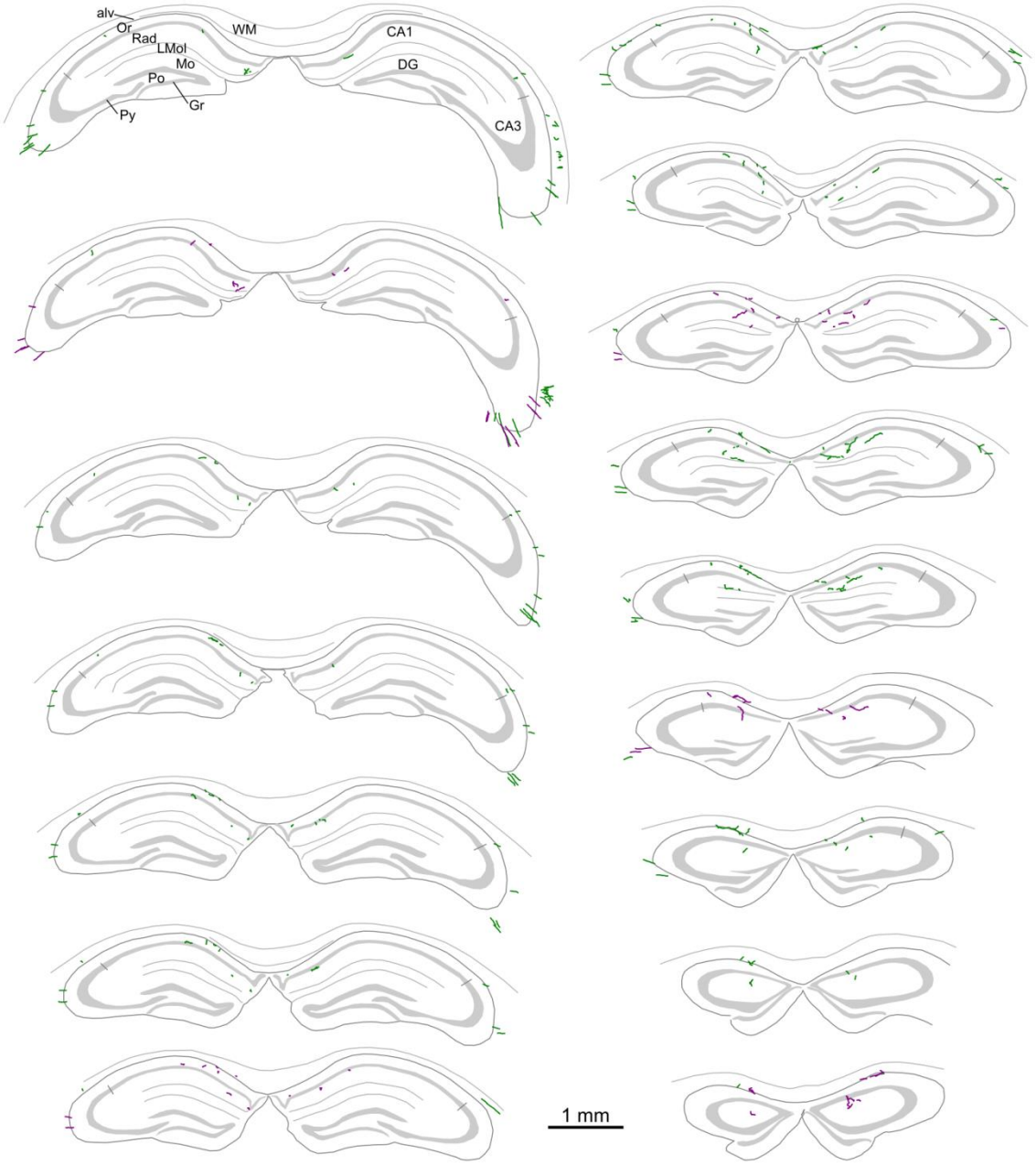

Figure 3.7 *ChR2-eYFP expressing dCA1 axonal segments (slice tracings animal 2)*
Tracings of axonal segments are shown in green. The outline of structures including alveus (alv) and overlying white matter (WM); stratum oriens (Or); stratum pyramidale (Py); stratum radiatum (Rad); stratum lacunosum moleculare (LMol); and the molecular (Mo), granule (Gr) and polymorphic (Po) layers of the dentate gyrus (DG) were also traced (grey). Antibodies against tyrosine hydroxylase (TH) were applied to five of the sections and axonal segments verified as co-expressing TH are shown in magenta.

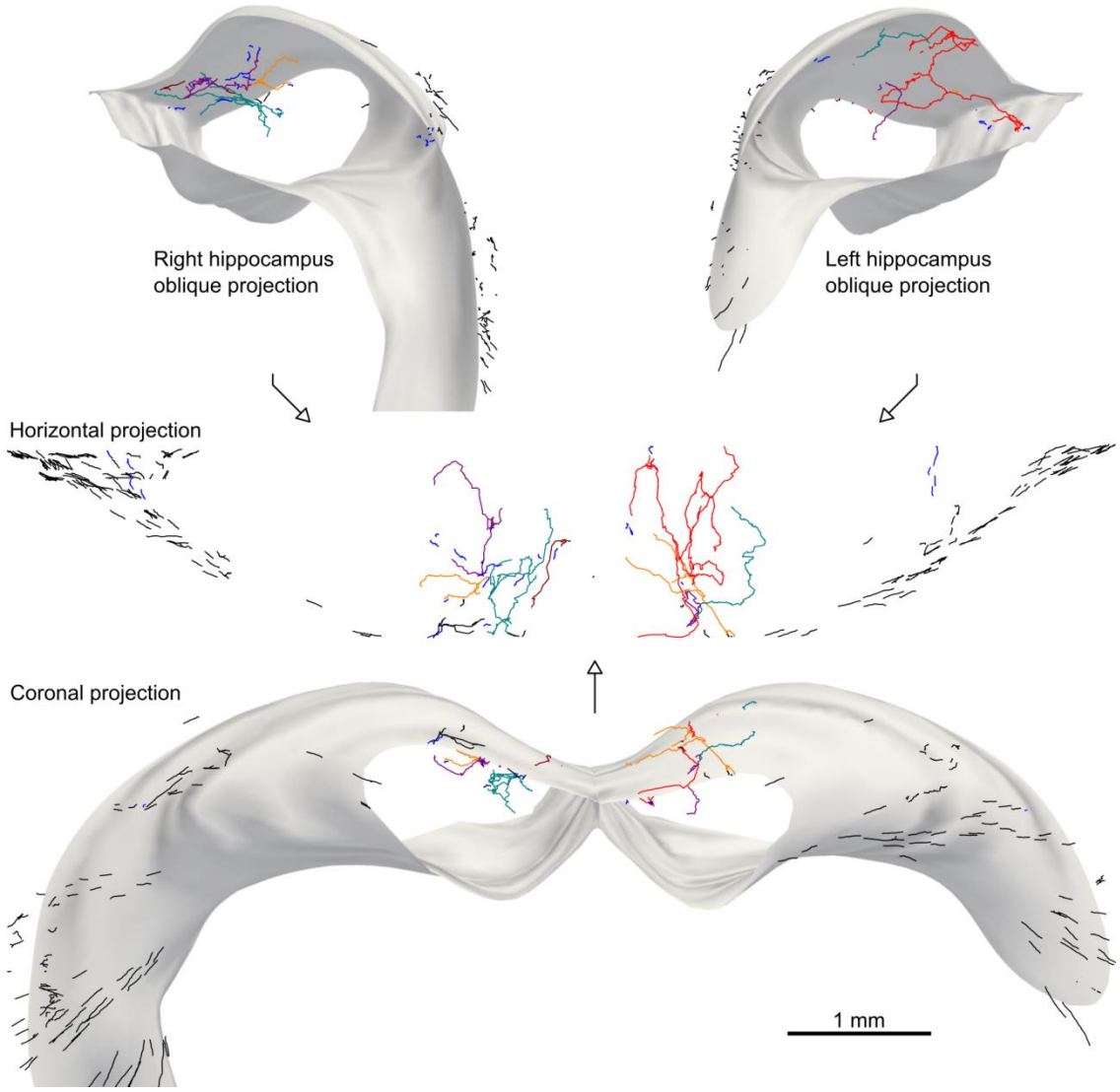

Figure 3.8 *ChR2-eYFP expressing dCA1 axonal segments (spliced reconstruction animal 2)*
Spliced reconstructions of ChR2-eYFP expressing axonal segments traced in dCA1 of animal two. Axons matched as continuing from one section to the other were spliced together. Different colours are used to show the different groupings. Axonal segments extending through alveus and some segments in the overlying white matter which were not spliced together are shown in black. The reconstructed surface is the alveus to stratum oriens border with smoothing applied. The arrows show the angle of the three vertical views with respect to the horizontal view. In the oblique projections only the near hippocampus is shown.

Axons entering stratum oriens of the CA3 subfield at the septal pole of the hippocampus continued through CA2 into CA1 while other fibres directly entered CA1 from the alveus. In relation to the superficial-deep axis, axons extended from stratum oriens through stratum pyramidale to stratum radiatum. No ChR2-eYFP expressing axon was clearly present in stratum lacunosum moleculare of the sections featured in the figures provided here; however, in one of the other animals such an axon was present. Axons expressing ChR2-eYFP were also found extending from the septal pole of the hippocampus innervating the molecular, granule and polymorphic layers of the dentate gyrus. It is worth noting that the axon coloured red in Figure 3.5, on entering the hippocampus via the septal pole, branches ventrally and innervates the molecular, granule and polymorphic layers of the dentate gyrus, as well as, branching dorsally and innervating strata oriens, pyramidale and radiatum of the hippocampus proper.

3.5 Discussion

Data presented here demonstrate that, in *DAT-IRES-Cre*$^{+/-}$ mice, there is a dopaminergic projection to the dorsal hippocampus including the CA1 subfield. The density of innervation was low suggesting that aspects of its mechanism of action, or that of its postsynaptic targets, are perhaps different to that in densely innervated areas, such as the striatum. The distance of projection suggests it would be less likely to be evolutionarily preserved across species without some functional relevance. Further support for the functional relevance of this projection is the presence of dopamine receptors in the hippocampus. That D5 receptors are the more prevalent D1-type receptor in the hippocampus, whereas D1 receptors are the prevalent D1-type receptor in the striatum, is also suggestive of differing aspects in the mechanisms of action and specialisation of dopamine function between the two brain areas (Ciliax et al., 2000; Laurier et al., 1994).

There are a number of potential means by which a sparse innervation of a brain area can provide a large functional impact. The projection fibres could target a specific population of local interneurons, which could in turn project extensively throughout the network enabling the projection to exert a greater influence on the hippocampal network. In support of this idea, other projections have been shown to target interneurons e.g. it has been demonstrated that GABAergic neurons in the septum selectively project to parvalbumin and calbindin

expressing interneurons in the hippocampus (Freund and Antal, 1988). Alternatively, reduced innervation by dopaminergic fibres could also bring reduced dopamine uptake. If the dopamine signal to the hippocampus is a less time locked, slow transient signal compared to the striatal dopamine signal, then non-synaptic volume transmission with reduced enzymatic degradation, reduced recapture, and abundant, highly-sensitive, G-protein-coupled receptors, may be ideal for such a sustained signal.

Further work is still required to establish additional anatomical facts about the midbrain derived innervation of the hippocampus. The sparse nature of the innervation means that it could be derived from a relatively small number of dopaminergic neurons. Given increasing evidence for diversity among midbrain dopaminergic neurons (Lammel et al., 2014; Morales and Root, 2014; Roeper, 2013; Yetnikoff et al., 2014), improved retrograde tracers should be used to investigate the precise origin within the midbrain dopaminergic nuclei of the projection to the hippocampus. It is possible that these neurons are located away from the centre of the VTA and I did not achieve complete transfection of this population in these experiments. This may explain the slight variation in the quantity of innervation seen in the tracings reported here, and it is possible that the innervation is greater than that shown in the tracings provided here.

The investigations reported in this chapter represent important verification of a number of items as present and working correctly within my experimental setup allowing me to proceed with combined extracellular recording and optogenetic activation of the dopaminergic projection to the dorsal hippocampus. Firstly, virus transfection was effective; secondly, ChR2-eYFP expression was specific to dopaminergic neurons; and thirdly, ChR2-eYFP expressing axons were present in the dorsal hippocampus including in the CA1 subfield.

Chapter 4 Midbrain dopaminergic nuclei and spatial novelty

4.1 Introduction

As described in more detail in section 1.9, midbrain dopaminergic neurons show transient responses to rewarding events or cues predicting rewards often referred to as 'phasic' responses (Schultz, 2007; Schultz et al., 1997). This response is considered to code a reward prediction error since, as an animal learns the relationship between a reward predicting cue and reward delivery, the phasic excitatory response shifts from the time of reward delivery to the time of the reward predicting cue (Schultz, 2007; Schultz et al., 1997). Furthermore, if the reward is omitted a phasic drop in activity occurs. There is also accumulating evidence that a small subset of midbrain dopaminergic neurons show excitatory responses to aversive stimuli, with some of these neurons also showing excitatory responses to rewarding stimuli, suggesting they may signal motivational saliency (Cohen et al., 2012; Matsumoto and Hikosaka, 2009). It is important to note that bursts of action potentials are not required to produce a phasic response. Phasic responses are most frequently measured in the firing of a cell over many repeated trials, and a phasic response can be produced by an increased probability of single spikes at the time point of interest. While the phasic responses of midbrain dopaminergic neurons to discrete rewarding and aversive events have been the focus of many studies, much less is reported on the sustained responses of midbrain dopaminergic neurons to less temporally discreet events, such as free exploration in a novel environment versus a familiar environment. Motivated by the idea that dopaminergic neurons may be able to show more sustained responses capable of coding for less discrete events, in this chapter I investigate the activity in midbrain dopaminergic nuclei across exploration in a familiar and a novel environment.

Two modes of *in vivo* firing have been associated with midbrain dopaminergic neurons; lower frequency, pacemaker-like 'regular firing', consisting of single action potentials often occurring with a regular inter spike interval (0.2-1 seconds), and 'burst mode firing', featuring transient bursts of action potentials, consisting of up to as much as ten spikes occurring at short (less than 80 ms) inter spike intervals (Grace and Bunney, 1984a, b; Overton and Clark, 1997; Roeper, 2013). The burst firing of dopaminergic cells is thought to support transient release of dopamine in target structures and contribute to the phasic responses often seen in response to reward (Roeper, 2013; Zweifel et al., 2009). However, the simultaneous activation of a number of dopaminergic neurons (as opposed to the burst firing of a single cell) seems to be required to produce a dopamine transient measurable with voltammetry in the striatum (Marinelli and McCutcheon, 2014).

Any potential change in the firing patterns and burst activity of midbrain dopaminergic cells, associated with sustained exploration in familiar compared to novel environments, will be investigated in this chapter. A number of measures are prevalent in the reporting of burst mode activity of midbrain dopaminergic neurons. The most straight forward is using a fixed threshold in the inter spike interval (ISI) to assign spikes as being within bursts or single isolated spikes (Grace and Bunney, 1984a). The ratio of burst to single spikes (burst ratio) can then give an indication of the level of burst mode firing of the cell. However, this measure does not account for different mean firing rates between cells. While a typically used threshold of 80 ms may work well for midbrain dopaminergic cells firing at lower (< 5 Hz) mean rates, for faster firing rates up to 12 Hz the threshold value is already close to the mean ISI such that a perfectly regular firing rhythmic cell firing at 13 Hz would have all its spikes classified as within a burst. The coefficient of variation (CV) is a standard dimensionless statistical measure for the level of dispersion of a distribution, and is defined as the ratio of the standard deviation to the mean. A CV value near zero indicates highly regular firing; whereas, higher CV values indicate greater dispersion of the distribution of inter spike intervals, suggestive of greater burst mode firing. One problem associated with CV is that the variation measure is applied to the entire time interval over which it is applied and gradual changes in mean firing rate are reported as increased variation. The alternative measure CV2 removes this sensitivity by performing the comparison of variation on adjacent spike intervals (Holt et al., 1996). It also has the added

advantage of being normalised, such that, a perfectly rhythmic cell has a CV2 of zero and a Poisson process has a CV2 of one. In addition to these measures to quantify the propensity of the cell to fire bursts, there are a number of methods to detect individual bursts within a spike train such as Poisson Surprise (Legendy and Salcman, 1985), Robust Gaussian Surprise (Ko et al., 2012) or hidden semi-Markov point process models (Tokdar et al., 2010).

4.2 Experimental outline

I performed extracellular recordings using tetrodes in two DAT-IRES-Cre mice (Bäckman et al., 2006). Mice were first injected in the ventral tegmental area (VTA) with a Cre inducible viral vector coding for a chimeric protein formed of the light activated ion channel channelrhodopsin-2 and enhanced yellow florescent protein (see section 2.2). The mice subsequently received an implant containing four tetrodes and an optic fibre targeted at the VTA (see section 2.5). These mice also received four tetrodes located in the dorsal CA1. The CA1 data is presented in Chapter 5. During recordings, mice were allowed to freely explore familiar and novel open fields in the absence of rewards or laser activation. Photoactivation of midbrain dopaminergic neurons was enabled during a separate exploration session each day. Units were identified through the identification of clusters in the combined recordings across all the recordings taken on a given day, allowing the same cells to be followed across exploration in the different environments and conditions.

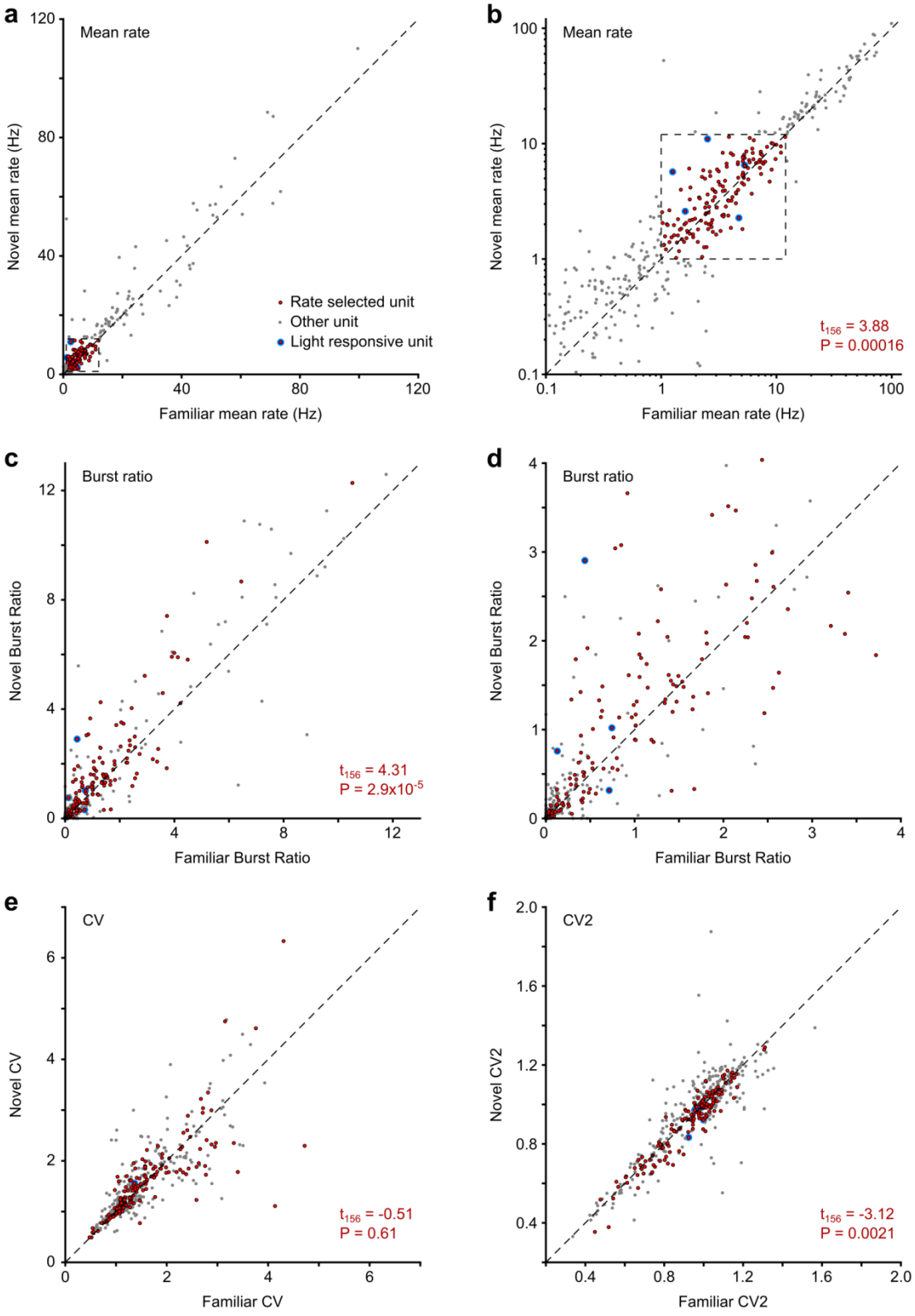
a
Mean rate
Novel mean rate (Hz)
Familiar mean rate (Hz)
Rate selected unit
Other unit
Light responsive unit
b
Mean rate
Novel mean rate (Hz)
Familiar mean rate (Hz)
t156 = 3.88
P = 0.00016
c
Burst ratio
Novel Burst Ratio
Familiar Burst Ratio
t156 = 4.31
P = 2.9x10-5
d
Burst ratio
Novel Burst Ratio
Familiar Burst Ratio
e
CV
Novel CV
Familiar CV
t156 = -0.51
P = 0.61
f
CV2
Novel CV2
Familiar CV2
t156 = -3.12
P = 0.0021

Figure 4.1 *Midbrain firing activity in familiar versus novel environments*
Scatter plots of firing activity during exploration of familiar versus novel environments. Dashed lines show the locus of activity in the novel environment equalling that in the familiar environment. Cells with a mean firing rate between 1 and 12 Hz, enclosed in the dashed square, are highlighted in red and were used for the statistics reported on the plots. Cells which could be matched as responding to light in a subsequent recording are highlighted with a blue surround. ***(a)*** *Comparison of mean firing rate of each cell plotted with a linear scale.* ***(b)*** *Comparison of mean firing rate of each cell plotted with a logarithmic scale.* ***(c)*** *Comparison of the proportion of spikes occurring within low latency bursts (< 50 ms inter spike interval) to single spikes.* ***(d)*** *Enlarged lower section of (c).* ***(e)*** *Comparison of coefficient of variation (CV).* ***(f)*** *Comparison of CV2 measure (Holt et al., 1996).*

4.3 Firing activity in midbrain dopaminergic nuclei changes in novel versus familiar environments

After unit isolation, a total of 416 cells were isolated from recordings on midbrain tetrodes. The scatter plots of Figure 4.1a,b show the mean firing rate of each unit over the first 10 minutes exploration in the familiar (x-axis) and novel (y-axis) environment plotted on a linear (Figure 4.1a) and a logarithmic scale (Figure 4.1b). The dotted line indicates the line of equal mean rate between the familiar and novel environments. Note how more of the points are located above the line than below in Figure 4.1b, signifying that more cells had a higher mean firing rate in the novel environment compared to the mean rate in the familiar environment. Points contained within the square on each plot represent cells which had a mean firing rate of above 1 Hz and below 12 Hz in both the familiar and novel environments, a firing rate range typical of the expected mean firing rate of dopaminergic neurons (Cohen et al., 2012). A total of 157 cells fell into this category and analysis in this chapter was performed on these cells. The mean firing rate increased in the novel environment compared to the familiar environment (novelty-induced rate change = 0.56 ± 0.14 Hz, t_{156} = 3.88, P = 0.00016, paired t-test). Analysis was performed on data from the first 10 minutes of exploration in each environment.

The ratio of single spikes to spikes occurring in low latency bursts (inter spike interval less than 50 ms) was higher during exploration of the novel environment than the familiar environment (novelty-induced change in burst ratio = 0.31 ± 0.07, t_{156} = 4.31, P = 2.9×10^{-5}, paired t-test). This is shown in the scatter plots of Figure 4.1c,d. However, measures of the extent of variability of

the inter spike interval independent of the mean rate did not show indication of an increased propensity to fire action potentials in bursts beyond that capable of being explained due to an increase in mean firing rate. Pairwise comparison of the coefficient of variation (CV) was not significantly different between the two conditions (novelty-induced change in CV = -0.021 ± 0.04, t_{156} = -0.51, P = 0.61, paired t-test). The alternative measure CV2 (which is not sensitive to slow variations in mean rate) showed a slight decrease from exploration in the familiar to exploration in the novel environment (novelty-induced change in CV2 = -0.013 ± 0.0041, t_{156} = -3.12, P = 0.0021, paired t-test).

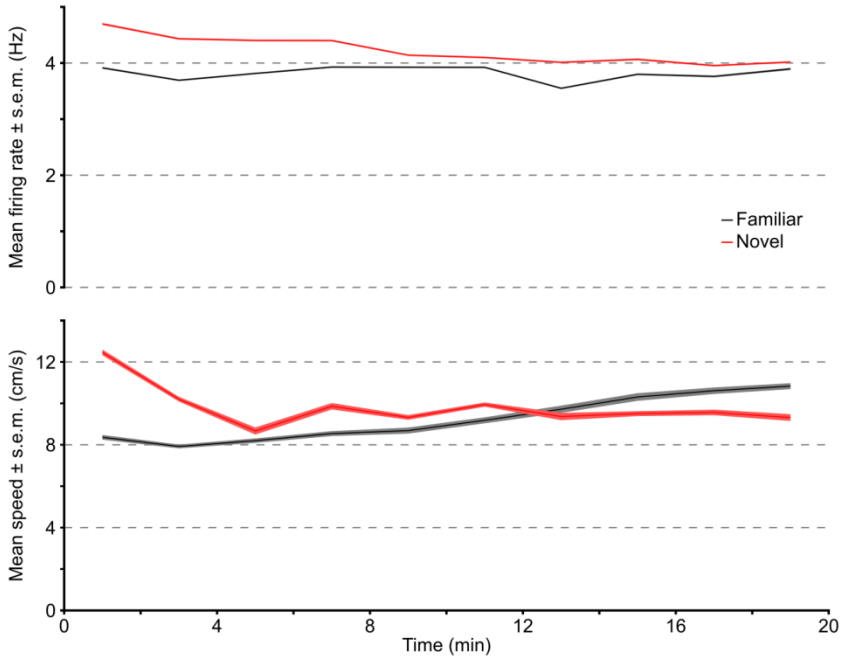

Figure 4.2 *Progression of mean firing rate and mean animal speed over time*
(a) *Time progression of mean firing rate across animals and days during exploration of the familiar and novel environments.* ***(b)*** *Time progression of mean animal speed across animals and days during exploration of the familiar and novel environments.*

The progression of mean firing rate and mean animal speed over the first 20 minutes exploration in each environment is shown in Figure 4.2. The mean firing rate starts slightly higher in the novel environment and drops proportional to the time spent in the environment, whereas, the mean firing rate in the familiar environment remained constant across time (linear regression on mean rate values across 2 minute time bins, novel: time zero value = 4.56 Hz, slope = -0.0374 Hz/minute, r = -0.077, P = 0.002; familiar: time zero value = 3.84 Hz, slope =

-0.0027 Hz/minute, r = -0.0060, P = 0.813). The mean speed of the animals was slightly elevated for the first moments of exploration of the novel environment and remained steady thereafter (Figure 4.2, elevated by approximately 3 cm/s for approximately 3-4 minutes). In contrast, the mean speed grew slightly as a function of time in the familiar environment (Figure 4.2). Over 20 minutes exploration, the mean speed was not significantly different in the two environments (t_{11} = 1.56, P = 0.15, paired t-test).

The distribution of change in mean firing rate from familiar to novel environments is shown in Figure 4.3. Note how a larger number of cells increase in rate by more than 2 Hz from familiar to novel (positive axis) compared to the number which increase by more than 2 Hz from novel to familiar (negative axis).

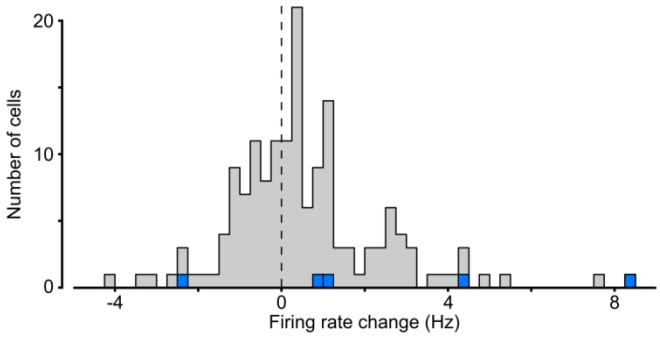

Figure 4.3 *Distribution of firing rate changes between familiar and novel environments*
Cells which could be matched as responding to light in a subsequent recording are highlighted in blue.

4.4 Light responsive units

Pulses of blue laser light were delivered to the VTA via an optic fibre in a separate exploration, after the exploration of the familiar and novel environments. Of the units isolated from the combined recordings across all the conditions, five showed an increased probability of firing action potentials with low latency (less than 3 ms) to the onset of the laser pulses. These units are detailed in Figure 4.4. The low latency increased firing probability can be seen in the cross-correlation with light pulse onset (panel a). Panel b shows spikes recorded during the earlier exploration alongside those occurring with low latency to laser pulse onset, allowing visualisation of the level of matching between spontaneous and light induced spikes. Many of the other recordings in the wider data set showed spikes occurring at low latency to light pulse

onset, indicating that many more dopaminergic cells are present in the data set beyond those highlighted in Figure 4.4. Such spikes were often of larger amplitude and had a higher probability of light induced discharge, suggesting such tetrodes were located closer to the light source; however, it was not possible to accurately match the light induced spike shape to one of the multiple units isolated from the same tetrode across all four channels of the tetrode. This was most likely due to the light induced spike reflecting the simultaneous activation of more than one transfected cell within the recording range of the tetrode.

The five cells identified as dopaminergic through response to light pulse onset are highlighted in blue on the scatter plots of Figure 4.1 and in the distribution of Figure 4.3. Four of the cells showed an increase in firing rate from familiar to novel exploration, with two showing a large increase (> 3 Hz), while only one cell showed a decrease. When firing at higher rates, these cells had more action potentials occurring in bursts, with an inter spike interval of less than 50 ms, and this can be seen in the raster plots showing the first 10 minutes of exploration in each environment where burst spikes are coloured black and single spikes grey (Figure 4.4 panel d). The firing of both burst spikes and single spikes was well distributed throughout the environment. The location of firing of each identified cell superimposed on the path taken by the animal is shown in panel c of Figure 4.4.

Interestingly, the firing patterns of these units very closely matched that of a Poisson process having similar mean rate. Histograms of the inter spike intervals (ISI) for each cell overlaid with that expected of a Poisson process of the same rate are shown in Figure 4.5a. For each cell, the ISI histogram scales with the rate difference seen between the novel and familiar environment. Furthermore, the shape of each ISI distribution, in relation to that expected of a rate-matched Poisson process, is maintained. The cumulative ISI histograms of Figure 4.5b, expressed as a proportion of total intervals and normalised in time by the mean firing rate, show near perfect alignment between the familiar and novel environment, and are aligned to that expected of a rate-matched Poisson process. Cell 1 shows a slight deviation from this, and is slightly more likely to fire action potentials at lower latencies than a rate-matched Poisson process. The dotted lines on each plot mark an ISI of 50 ms illustrating that, with the firing pattern maintained, an increase in rate produces both a greater proportion and a greater number of low latency spikes.

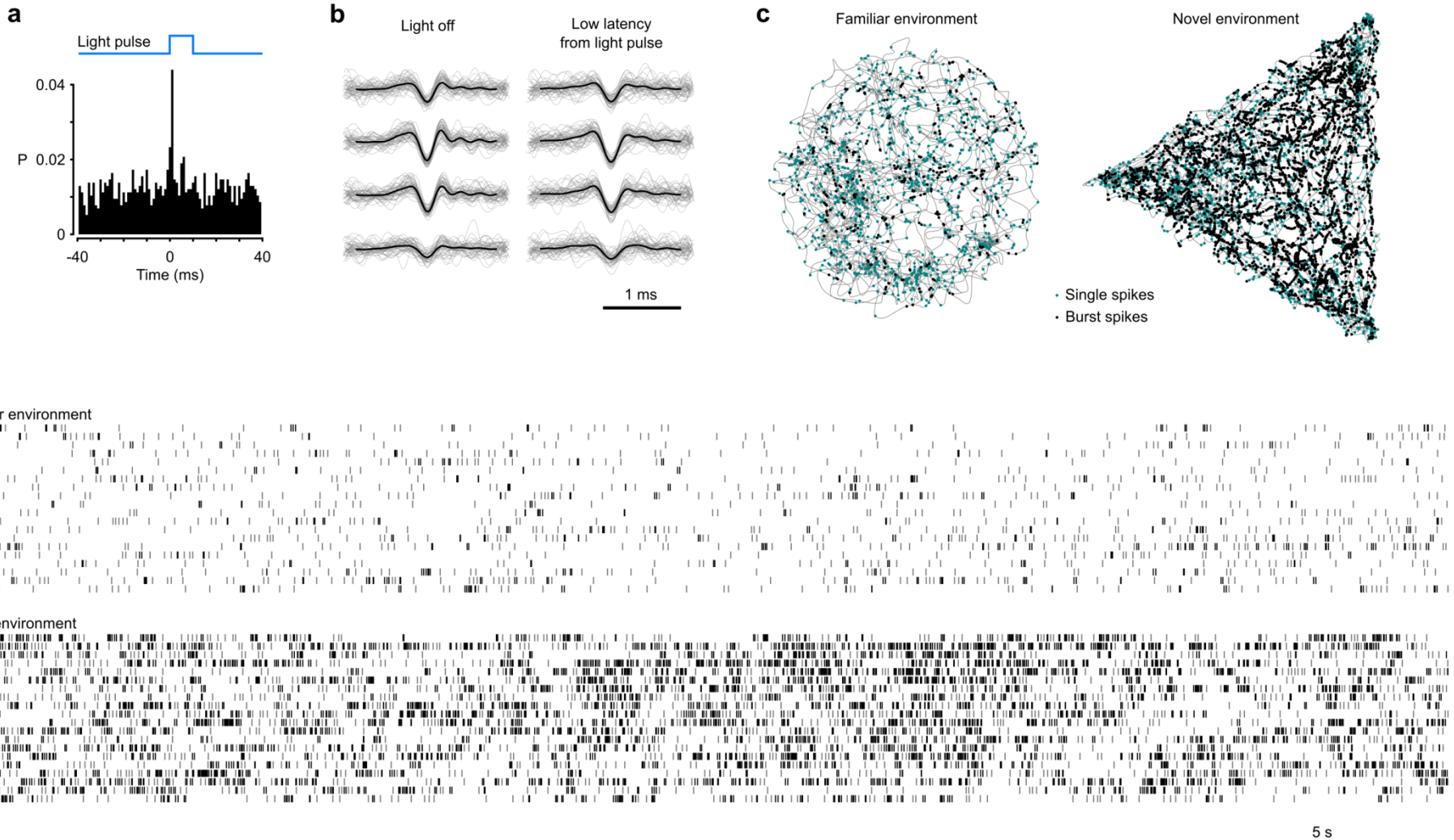

Raster plots from the same cell over 10 minutes in each environment (each line 30 seconds)

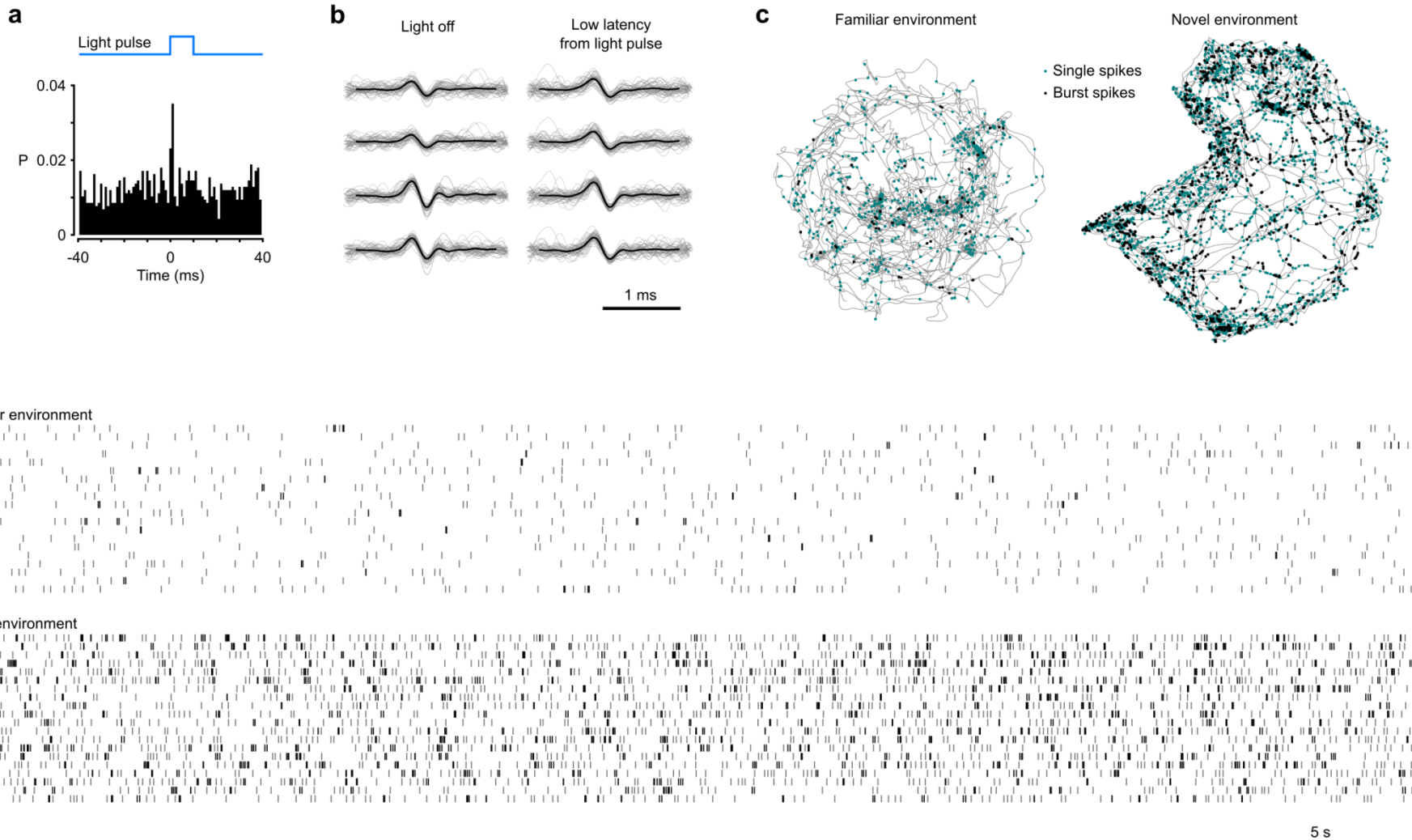

Raster plots from the same cell over 10 minutes in each environment (each line 30 seconds)

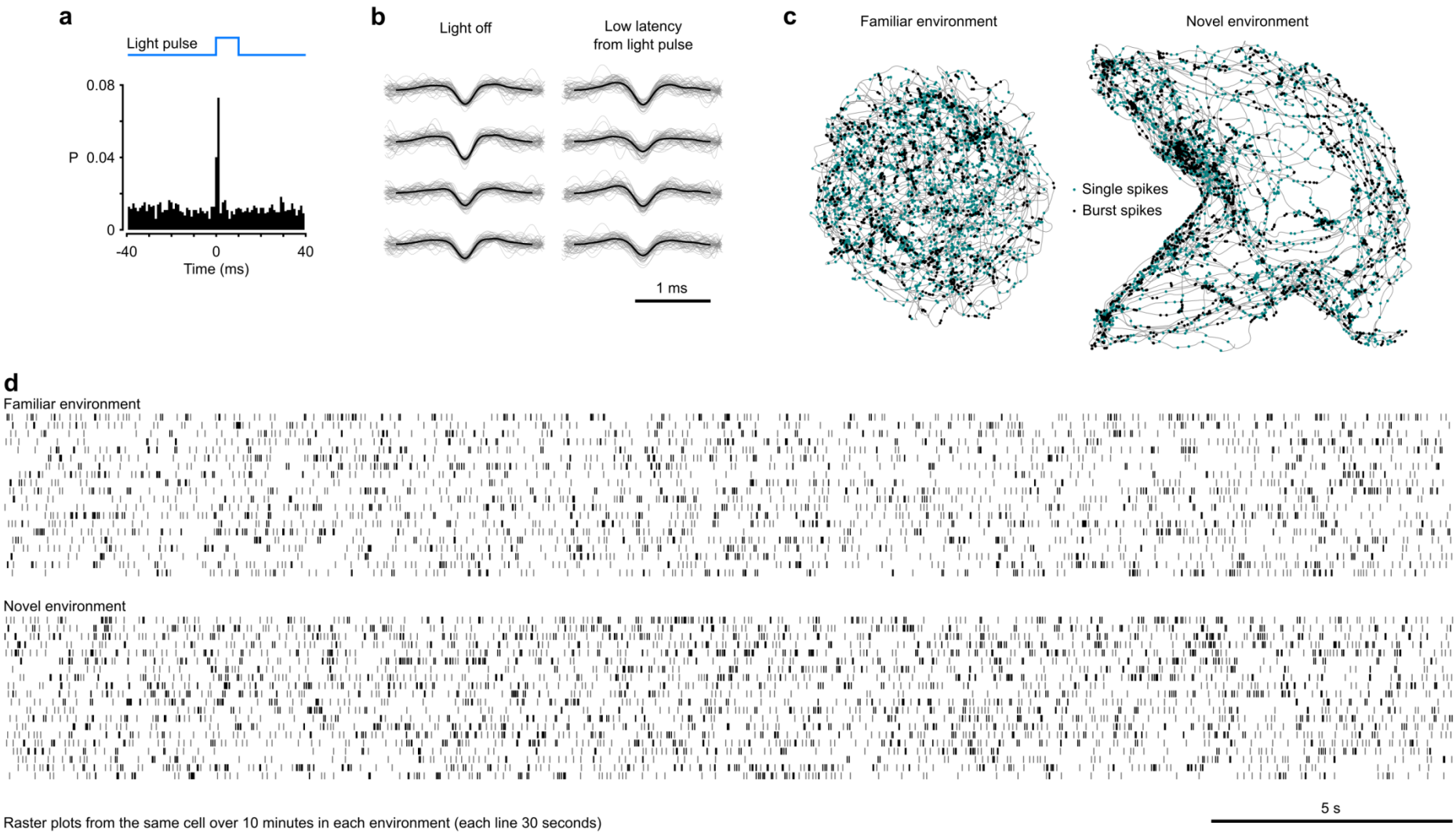

Raster plots from the same cell over 10 minutes in each environment (each line 30 seconds)

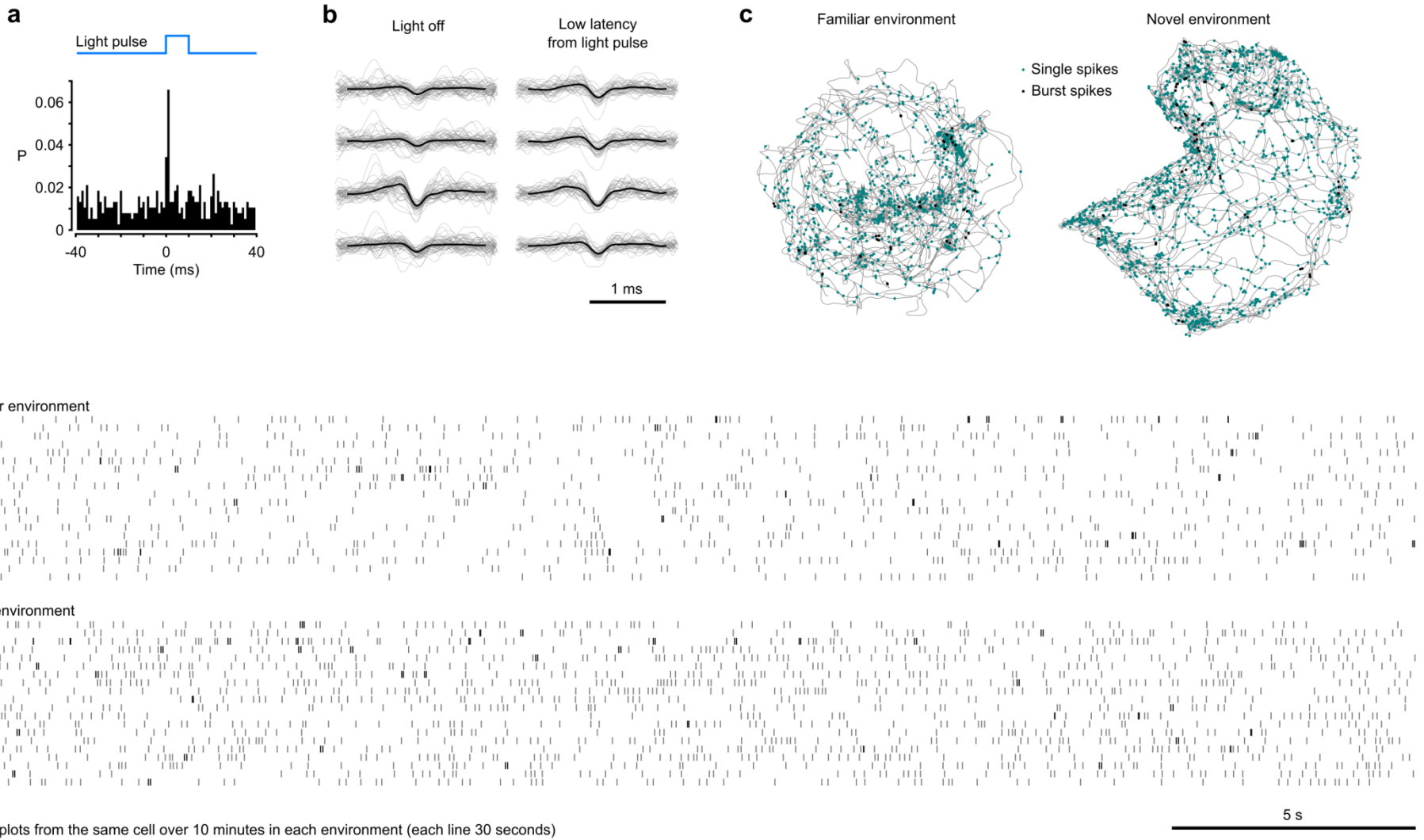

Raster plots from the same cell over 10 minutes in each environment (each line 30 seconds)

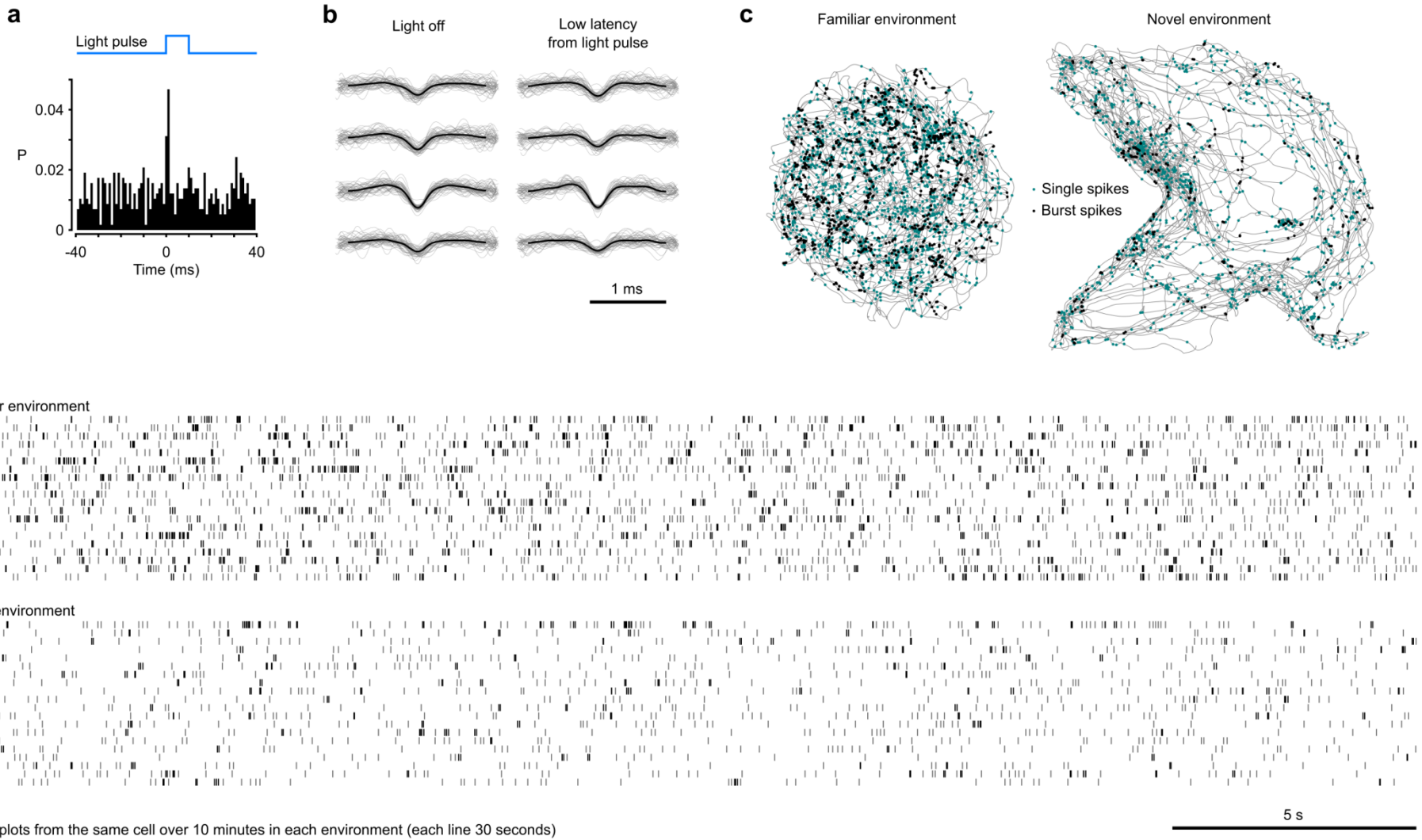

Raster plots from the same cell over 10 minutes in each environment (each line 30 seconds)

Figure 4.4 *Firing of light responsive cells 1-5*

One cell is shown per page. ***(a)*** *Cross correlation with light pulse onset recorded after exploration of the familiar and novel environments.* ***(b)*** *Spike shape across the four channels of the tetrode for spikes recorded during exploration of the familiar environment in the absence of photostimulation (left), and spikes recorded at low latency (< 3 ms) to the onset of the laser pulse (right), corresponding to the peak in the cross-correlogram in (a).* ***(c)*** *Path of the animal over the first 10 minutes of exploration in the familiar (left) and novel (right) environments, with the location of the animal at each spike occurrence superimposed.* ***(d)*** *Raster plots of the cell for the entire first 10 minutes during exploration in the familiar (top) and novel (bottom) environments. Note each row represents consecutive 30 second recordings from the same cell.*

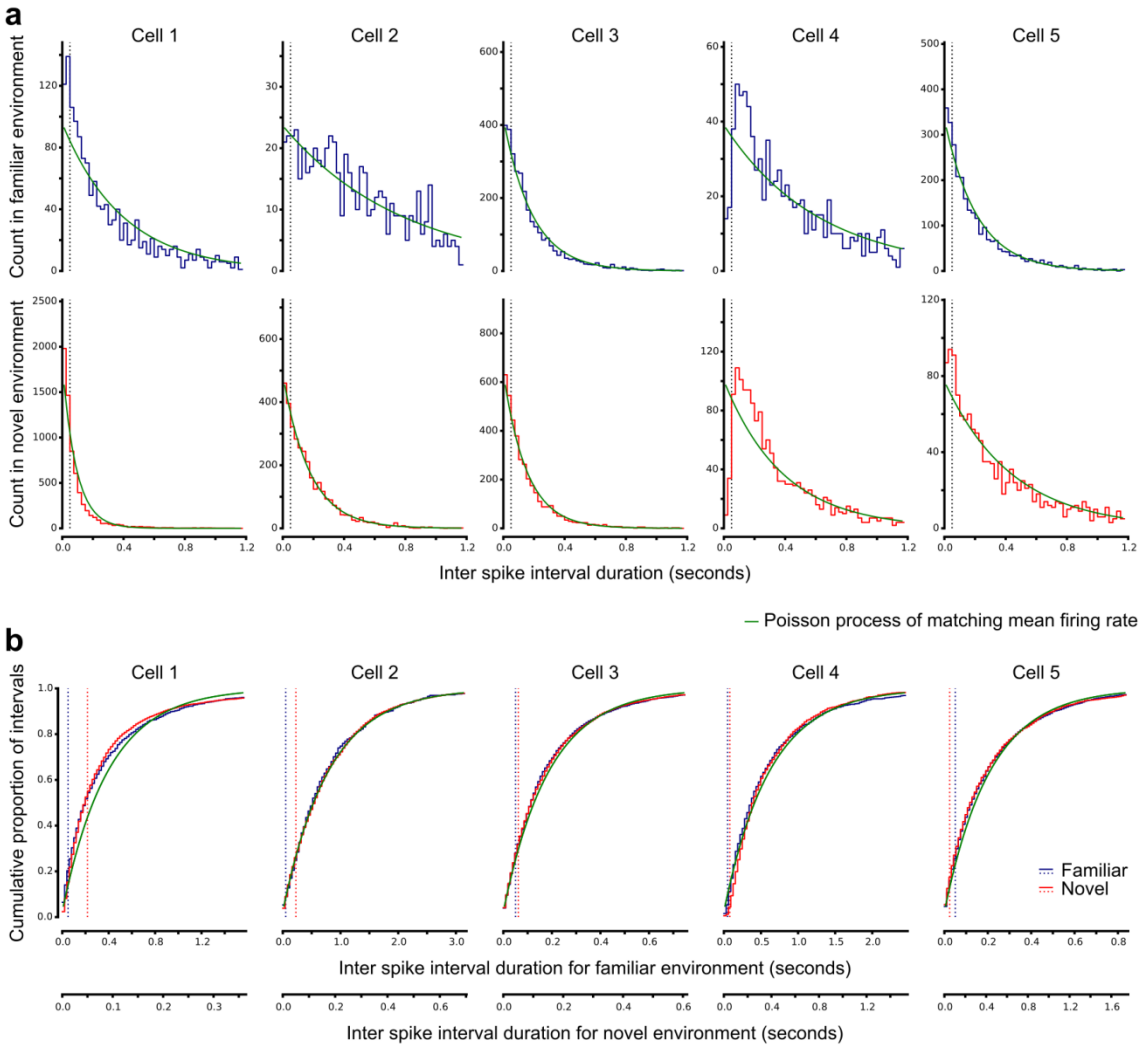

Figure 4.5 *Inter spike interval histograms of light responsive cells*

(a) *Inter spike interval histograms (ISI) for each cell compiled from the first 10 minutes of exploration in the familiar (top) and novel (bottom) environments. The distribution expected of a Poisson process of the same rate is shown on each plot in green.* ***(b)*** *Normalised cumulative ISI histograms plotted with the time axis scaled by the mean rate. The x-axis duration on each plot equals four times the mean ISI. An ISI of 0.5 is shown by the dotted lines.*

4.5 Discussion

Data presented in this chapter indicate that the sustained activity of midbrain dopaminergic neurons can change in relation to temporally extended events, in this case, exposure to a novel as opposed to a familiar environment. This finding extends the coding potential and signalling capability of midbrain dopaminergic neurons, complementing the previously reported phasic changes in activity levels coding for discrete-in-time events, such as rewarding, aversive and salient stimuli. I have chosen to use the phrase changes in 'sustained activity' as opposed to 'tonic activity' since in many publications tonic activity is used to refer to pacemaker-like regular firing around a fixed ISI whereas many of the cells recorded here had firing patterns very close to that expected of a Poisson process. This is true of the light identified units and also evident in the scatter plot of CV2 values for the larger data set in Figure 4.1f. Many of the CV2 values are clustered around a value of one and also extending up towards 1.2 indicating a greater than Poisson propensity to fire bursts. While many of the recorded cells showed Poisson like firing, the data did also contain cells with regular firing and others with burst mode firing patterns, evident in the scatter plots of Figure 4.1e&f, and also evident in manual inspection of the raster plots of the individual cells.

Quantifying changes in the firing of midbrain dopaminergic neurons as having increase bursting activity can be viewed in two ways. Increased bursting could be interpreted to mean a change in the pattern of firing such that spikes are more likely to occur in groups than individually, and it is possible to decipher this change in the relative occurrences of spikes (i.e. the pattern of occurrence) independent of knowledge of the global time scale of the firing activity. Put differently, the difference is evident in two raster plots which are scaled in time such that they are normalised by the mean firing rate. This is perhaps the most appropriate definition, if bursting is viewed as a pattern of firing. However, depending on the context, it may be more relevant to define bursting in terms of activity occurring below a fixed temporal threshold. Consider if the downstream target of such activity responds in a nonlinear fashion, such that it produces a greater output when action potentials occur in quick succession, measured in terms of absolute time. This nonlinearity could be due to presynaptic release sites, postsynaptic receptor activation, neurotransmitter reuptake mechanisms or postsynaptic second messenger systems. In such cases, an increase in rate without a change in the pattern

of firing can produce a greater proportion of spikes occurring below a temporal threshold having an increased effect. The property that an increased rate will produce such an increase is true of many patterns of firing, including Poisson like firing. The results presented in this chapter found an increase in rate from the familiar to novel environments, and this was not accompanied by a change in the pattern of firing (CV and CV2) of many of the cells, including the light identified units. However, the pattern of firing of these cells was such that the rate increase did result in an increase in both the number and proportion (burst ratio) of action potentials occurring in bursts, when a fixed duration ISI threshold criteria was used for burst detection. This can be visualised in the rate scaled cumulative ISI histograms of Figure 4.5b, where a 50 ms threshold is marked with a dotted line. The distributions align; however, the increase in mean rate moves the location of the threshold up the cumulative distribution, causing an increase in the burst ratio. A 50 ms (20 Hz frequency equivalent) threshold was used for burst ratio calculations as a conservative choice over the often used 80 ms (12.5 Hz) start with greater than 160 ms (6.25 Hz) end of a burst criteria established in anaesthetized rats (Grace and Bunney, 1984a; Ungless and Grace, 2012), in order to allow sufficient clearance between the burst interval threshold frequency and some of the higher mean rates (11 Hz) seen in the light identified units from behaving mice (Figure 4.4). However, an 80 ms cut-off produced similar findings.

Given the growing suggestion of diversity within midbrain dopaminergic nuclei (Lammel et al., 2014; Morales and Root, 2014; Roeper, 2013; Yetnikoff et al., 2014), it is possible that a distinct subset of dopaminergic cells better show rate changes in response to environmental cues and perhaps even other temporally extended events. Note the second peak in the distribution of Figure 4.3 showing that a number of cells increased in firing rate by more than 2 Hz in the novel over the familiar environment; such a peak is not present on the negative side which would signify the converse (an increase in the familiar over the novel environment). These cells could potentially provide a suitable signal to modulate hippocampal dynamics associated with memory formation. Midbrain dopaminergic cells which show sustained responses to temporally extended events, including spatial novelty, may also have distinct projection targets, including the hippocampus, while other cells may better show phasic responses to discrete events and preferentially project to other targets.

It is also interesting to note that the stimuli invoking the sustained response seen here potentially bear some similarity to the stimuli which produce error prediction type phasic responses, since exposure to a novel environment could be classified as an unexpected or salient occurrence. Furthermore, since dopaminergic neurons can show responses from stimuli across different sensory modalities, numerous brain areas must be capable of informing midbrain dopaminergic activity either directly or indirectly, including visual and auditory areas (Schultz, 1998, 2007). Equally, environmental related novelty information present in the hippocampus could inform midbrain dopaminergic activity either directly or through projections to the nucleus accumbens and ventral pallidum to the VTA (Lisman and Grace, 2005) or via the lateral septum (Luo et al., 2011).

Chapter 5 Novelty, sleep reactivation and the effect of midbrain derived dopamine on hippocampal network dynamics in the open field

5.1 Introduction

Hippocampal reactivation of waking firing patterns during subsequent sleep is one line of evidence whereby the spatial map and memory functions of the hippocampus converge. Hippocampal reactivation is the phenomenon that the environment-specific firing associations of place cells and other firing which occur during waking experience in an environment reoccur during subsequent rest and slow wave sleep (O'Neill et al., 2006; Skaggs and McNaughton, 1996; Wilson and McNaughton, 1994). This activity is thought important for the strengthening of representations formed within the hippocampus (Buzsáki, 1989; Carr et al., 2011; O'Neill et al., 2010; O'Neill et al., 2008) as well as potentially aiding the creation and strengthening of neocortical memory representations (Chrobak and Buzsáki, 1996; Chrobak and Buzsáki, 1998; Clemens et al., 2007; Clemens et al., 2011; Isomura et al., 2006; Siapas et al., 2005). In particular, firing activity during active waking experience, when the LFP in the hippocampus is showing a prominent theta frequency oscillation, has been demonstrated to reoccur in a temporally compressed fashion during intermittent LFP events called sharp wave ripples (SWR), prominent during slow wave sleep (O'Neill et al., 2010; Skaggs and McNaughton, 1996; Wilson and McNaughton, 1994). One means to measure the strength of this reactivation is to compare the extent to which co-firing relationships between cell pairs across theta cycles correlate with co-firing relationships in subsequent SWR events (O'Neill et al., 2006; O'Neill et al., 2008). An intriguing observation in relation to SWR reactivation is that reactivation strength after exploration of a novel environment is higher than that seen after exploration of a familiar environment (O'Neill et al., 2008). Guided by this observation, the finding of

increased activity in midbrain dopaminergic neurons during exploration of novel environments (Chapter 4), and the idea that SWR reactivation increases the strength of new memories, in this chapter, I report the results of experiments investigating a potential role for midbrain derived dopamine signalling in hippocampal pyramidal neuron firing dynamics associated with memory formation. In these experiments animals explored both familiar and novel open fields.

5.2 Experimental outline

In order to determine if the midbrain dopaminergic projection to the hippocampus can modulate hippocampal electrophysiological activity associated with memory formation, I performed *in vivo* multichannel recordings combined with optogenetic activation of this projection. To achieve this, I injected DAT-IRES-Cre mice (Bäckman et al., 2006) in the VTA with a Cre inducible viral vector coding for a chimeric protein formed of the light activated ion channel channelrhodopsin-2 and enhanced yellow florescent protein (see section 2.2). This resulted in ion channel expression in dopaminergic neurons. These neurons could then be activated by application of blue light from a laser source through the chronically implanted optic fibre. Two different optic fibre implant locations were used; two animals had the optic fibre implanted directly above the VTA to activate the dopaminergic neurons at their cell bodies ('VTA-ON' configuration), whereas, for the other six animals the optic fibre was located at the top of the dorsal hippocampus ('dCA1-ON' configuration) in order to activate at the transfected dopaminergic fibres in dorsal CA1 (see section 2.5). Note in all cases the viral construct was injected in the VTA.

During recordings, the mice spontaneously explored an open field in the absence of any food rewards. Open fields of various geometries were used some of which were novel to the animal in that they had not been experienced, whereas others were familiar in that the animal had been previously exposed to the environment several times in the days before the recording. In order to assess the sleep reactivation of waking firing patterns, recordings were also taken during rest and sleep sessions before and after each exploration, during which time the mouse was placed in a small box containing home cage bedding. Photostimulation was only ever applied during the exploration sessions and never while the mouse was in the rest box. Photostimulation was delivered as 10 ms light pulses. Burst mode photostimulation consisted

of bursts of 20 light pulses (inter pulse interval of 50 ms) with bursts delivered every 40 seconds. Tonic mode photostimulation, consisting of the same number of light pulses as burst except equally spaced (one pulse delivered every two seconds), was applied in separate recording sessions. In addition, I recorded exploration sessions in the absence of photostimulation in order to provide a measure of baseline physiology and enable comparison. Finally, two control conditions were also recorded with the help of colleagues. In the first, two additional DAT-IRES-Cre mice were injected in the VTA with a Cre inducible viral construct coding for enhanced yellow florescent protein alone. Recordings were still performed across conditions, including in the presence of photostimulation. This provided a control for the illumination caused by the laser light, particularly that traveling through the brain to the back of the retina, which potentially could have had an effect on the arousal state of the animal. In the second control condition, animals expressing the light sensitive ion channels received an intraperitoneal injection of the dopamine antagonist SCH23390 prior to exploration of the open field, in the presence of burst mode photostimulation. Any effect of photoactivation of dopaminergic neurons blocked in this condition could then be better ascribed to the action of the neurotransmitter dopamine. The total number of recording sessions, the total number of CA1 pyramidal cells isolated from the recordings and the resulting total number of simultaneously recorded CA1 pyramidal cell pairs broken down per subject across the various conditions is shown in Table 5.1.

Table 5.1 *Recording sessions and cell counts*

Number of recording sessions - Number of pyramidal cells - Number of pyramidal cell pairs

	Familiar	Novel	Novel VTA-ON burst	Novel dCA1-ON burst	Novel dCA1-ON burst eYFP ctrl.	Novel dCA1-ON burst SCH23390	Novel dCA1-ON tonic	Familiar dCA1-ON burst
Per individual animal	6 - 88 - 668	6 - 89 - 684		4 - 53 - 340			2 - 34 - 297	4 - 57- 416
	6 - 132 - 1457	6 - 130 - 1404		4 - 84 - 885			2 - 47 - 535	4 - 92 - 1039
	5 - 55 - 290	6 - 64 - 346		8 - 79 - 412			4 - 42 - 252	8 - 80 - 430
	3 - 103 - 1731	3 - 113 - 2082		7 - 212 - 3324			5 - 148 - 2329	7 - 209 - 3296
	3 - 16 - 39	3 - 20 - 57	4 - 23 - 56					
	10 - 109 - 580	10 - 125 - 850	9 - 103 - 664					
	7 - 47 - 175	4 - 22 - 52		4 - 22 - 52		3 - 26 - 117		
	4 - 168 - 3973	3 - 120 - 2932		2 - 88 - 2036		5 - 205 - 4755		
	4 - 32 - 131	6 - 36 - 115			7 - 42 - 137			
	5 - 258 - 8706	5 - 266 - 9262			5 - 265 - 9294			
Total	53 - 1008 - 17750	52 - 985 - 17784	13 - 126 - 720	29 - 538 - 7049	12 - 307 - 9431	8 - 231 - 4872	13 - 271 - 3413	23 - 438 - 5181

5.3 Exploratory behaviour, CA1 network physiology and the activation of dopamine

The mice actively explored the various environments covering the entire space well. This may have been in part due to the recording protocol which consisted of periods in which the mouse rested in the relatively confined space of the sleep box interspersed with the active periods in the various open fields. This behaviour pattern was also encouraged in the training days preceding the recording days which were used to familiarise the mice with the familiar environments, sleep box and recording head-stage (see section 2.8). Figure 5.1a shows the instantaneous speed for the same mouse recorded on the same day as it explores a familiar open field, a novel open field and another novel open field with burst mode photostimulation enabled. Photostimulation did not alter exploratory behaviour. The mean speed throughout exploration recorded across animals was not different between exploration in familiar and novel environments or in the presence of photoactivation of dopaminergic neurons ($F_{3, 143}$ = 0.44, P = 0.72, one-way ANOVA, Figure 5.1b).

As an animal explores or moves through an environment the local field potential recorded from the hippocampal formation shows a prominent oscillation within the theta (5-12 Hz) frequency band (Buzsáki, 2002; Green and Arduini, 1954; Vanderwolf, 1969). The mean frequency of detected theta cycles (see section 2.13) used in the analysis here was 7.5 Hz (median 7.7 Hz with a quartile range of 6.7-8.6 Hz). Pyramidal neurons in the CA1 subfield of the hippocampus preferentially discharge action potentials near the trough of theta frequency oscillations (Csicsvari et al., 1999). The basic properties of CA1 network physiology were unaltered by photostimulation of dopaminergic neurons. The mean firing rate of hippocampal pyramidal cells was similar from familiar to novel environments and during exploration sessions where photoactivation of dopaminergic neurons was enabled ($F_{3, 2840}$ = 0.088, P = 0.97, one-way ANOVA, Figure 5.2a). Theta frequency oscillations remained present during exploration in the photostimulation enabled conditions and the mean number of theta cycles per waking session (5699.6 ± 165.5) was not different across conditions ($F_{3, 143}$ = 1.41, P = 0.24, one-way ANOVA). The distributions of instantaneous speed across theta cycles during epochs of theta activity were also similar and corresponded to periods when the animals were actively

exploring the environment (Figure 5.2b). Theta band activity was measured from the local field potential recorded in the CA1 pyramidal cell layer.

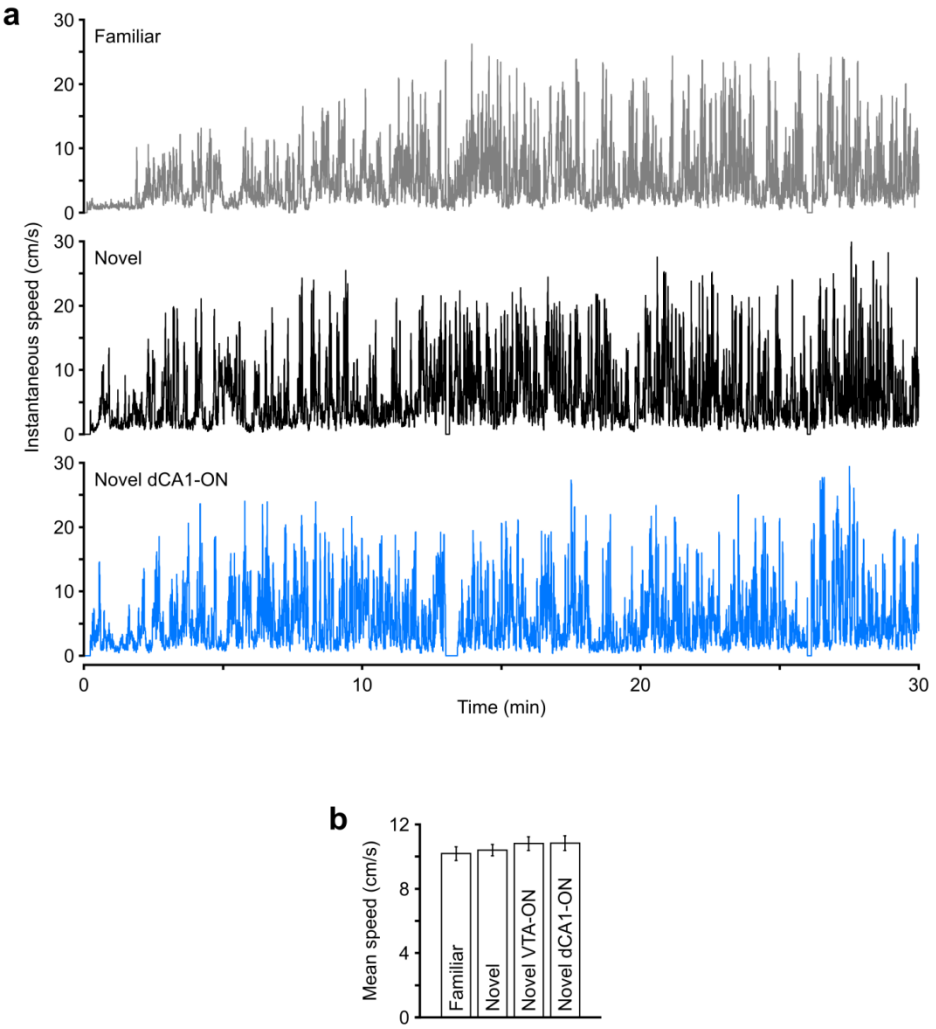

Figure 5.1 *Exploratory behaviour in open field environments*
(a) *Example instantaneous speed plots (820 ms bins) generated from exploration in the familiar open field and two novel open fields, one without photostimulation and one with photostimulation targeted at dorsal CA1 (dCA1-ON).* ***(b)*** *The mean speed across animals during exploration in the familiar, novel and novel VTA/dCA1-ON conditions (means ± s.e.m.) was not different ($F_{3, 143}$ = 0.44, P = 0.72, one-way ANOVA).*

Furthermore, the coupling of dorsal CA1 pyramidal neuron firing to the theta oscillation remained in photostimulation enabled conditions, as evidenced in the average autocorrelation histograms of dorsal CA1 pyramidal neurons. The average autocorrelation histograms for each condition show a similar level of theta modulation (Figure 5.2c). The distributions of preferred theta phase of dorsal CA1 pyramidal cells were also similar across conditions (Figure 5.2d),

showing the phase of this coupling was also unaltered in the photostimulation enabled conditions. For the preferred phase distributions, the preferred firing phase for each cell was calculated and the distribution generated with each cell providing a single preferred phase point. Finally, the presence and phase of dorsal CA1 pyramidal neuron spike coupling to the theta band oscillation can be seen in the average firing probability theta-phase histograms of Figure 5.2e. Here, the theta-phase firing probability distribution for each cell was calculated separately and the distributions were then averaged.

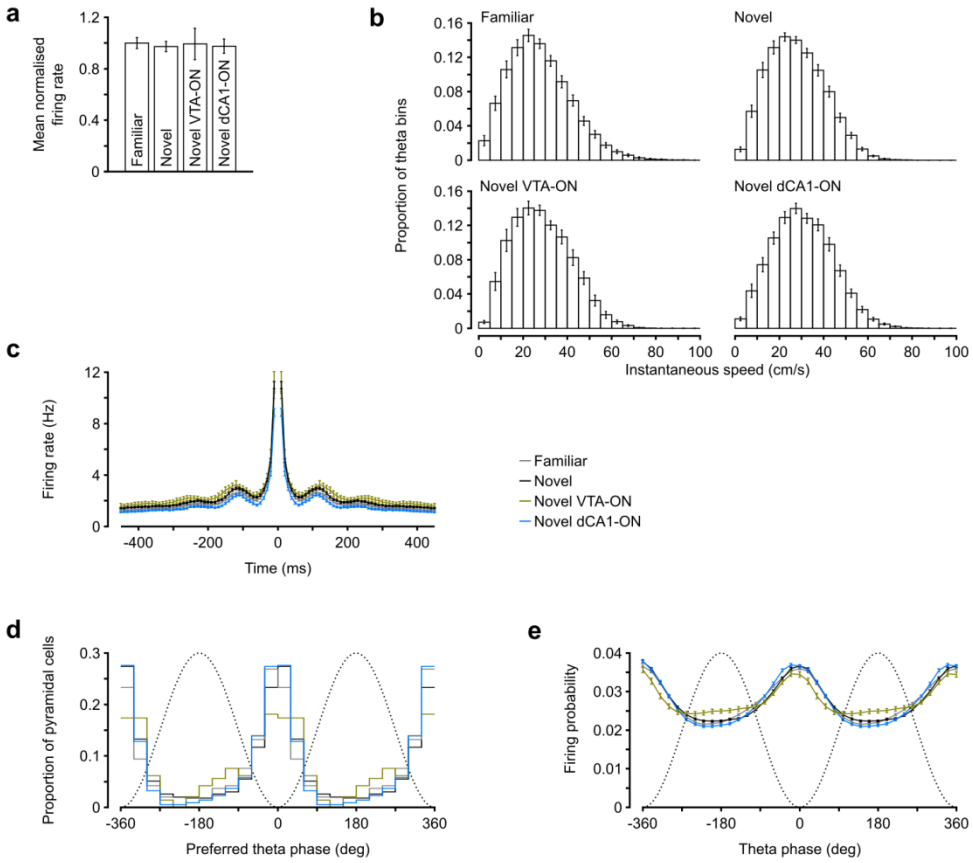

Figure 5.2 *Basic CA1 network physiology and the activation of dopamine*
(a) *The mean firing rate normalised by the mean in the familiar open field of dCA1 pyramidal cells during exploration in the familiar, novel and novel VTA/dCA1-ON conditions (means ± s.e.m.) was not different ($F_{3, 2840}$ = 0.088, P = 0.97, one-way ANOVA).* ***(b)*** *Distributions of the instantaneous speed (means ± s.e.m.) across theta cycles during epochs of theta activity during exploration in the familiar, novel and novel VTA/dCA1-ON conditions.* ***(c)*** *Average autocorrelation histograms of dCA1 pyramidal cells (10 ms bins) in the various conditions (means ± s.e.m.).* ***(d)*** *Distributions of the preferred theta phase for dCA1 pyramidal cells.* ***(e)*** *Average firing probability theta-phase histograms of dCA1 pyramidal cells (means ± s.e.m.). Dashed lines represent ideal theta waves.*

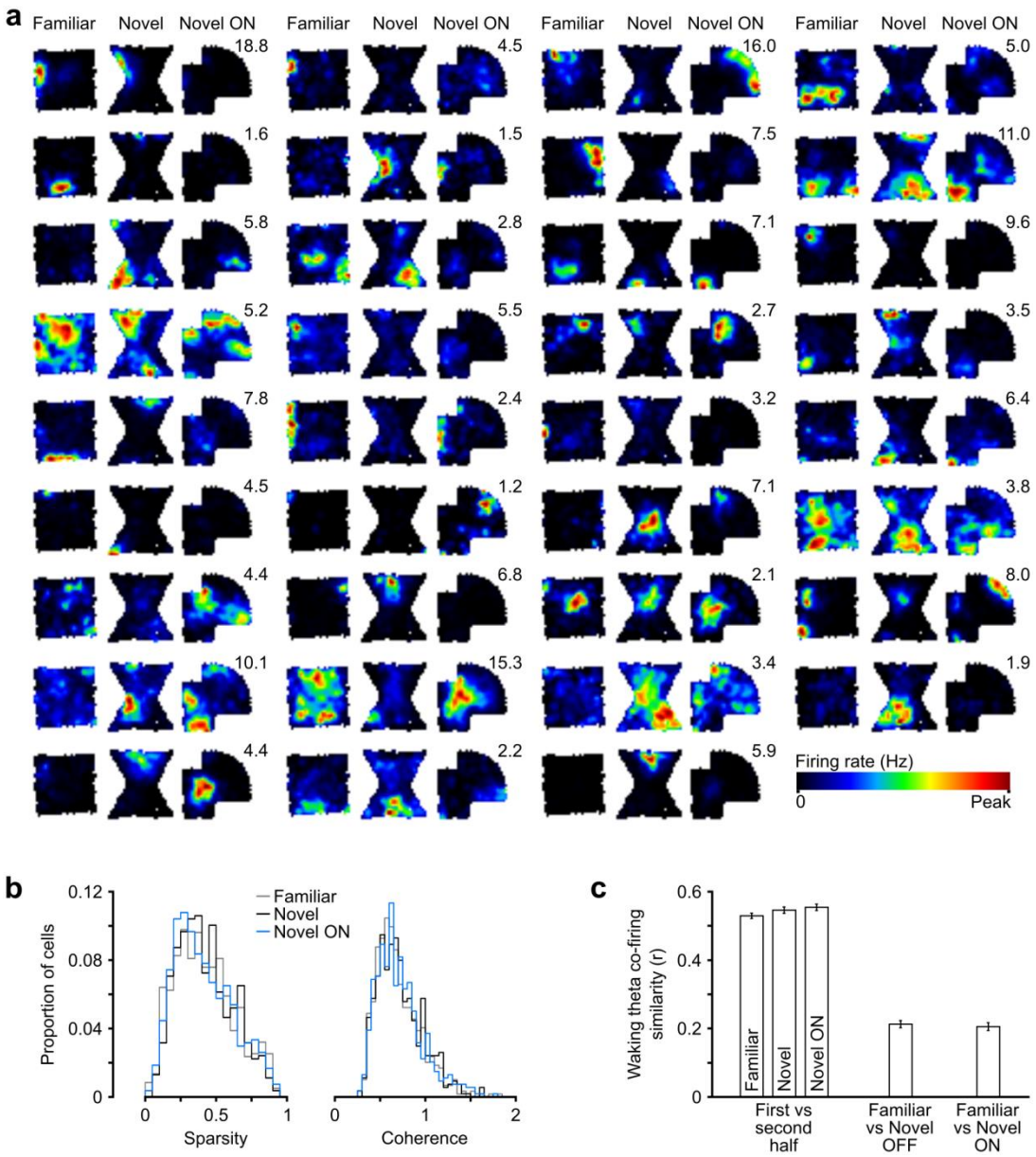

Figure 5.3 *Environmental remapping in different open fields*

(a) *Example of spatial rate maps for a set of dCA1 pyramidal cells from the same recording day followed across exploration in a familiar open field and two novel open fields, one without photostimulation and one with photostimulation targeted at dorsal CA1. The peak firing rate in Hertz is shown for each cell.* ***(b)*** *Distributions of sparsity and coherence spatial tuning measures across animals in the different conditions. The distribution of spatial tuning measures was unaltered by photostimulation (sparsity: P = 0.15, coherence: P = 0.80, Kolmogorov-Smirnov test, novel OFF versus novel ON).* ***(c)*** *Dorsal CA1 pyramidal cell co-firing correlations were similar within environments (first versus second half) and remapped (were less correlated) for between environment comparisons (all P < 0.0001, z-test, for each within environment value compared to each across environment value). The extent of remapping was unaltered by photostimulation (z = 0.46, P = 0.65, z-test, for familiar versus novel OFF compared to familiar versus novel ON).*

5.4 Spatial tuning and environmental remapping was unaltered by DA stimulation

As the mice explored the various open fields many of the dorsal CA1 pyramidal cells showed place specific increased firing within the environment, with different cells increasing their firing in different locations. Figure 5.3a shows the firing as a function of the position of the animal for a number of simultaneously recorded cells from the same animal across exploration in a familiar open field, novel open field and novel open field in the presence of dorsal CA1 targeted burst mode photostimulation. Note how some cells are more active in one environment compared to the others, and also how the locations of the firing fields varies creating differing firing relationships between the cells in the different environments. The spatial tuning of the firing can be assessed through two measures, sparsity and coherence (see section 2.18). Sparsity reflects the proportion of the environment in which the cell is active with a lower value indicating greater place specific firing (Skaggs et al., 1996). Coherence gives a measure of the 'consistency' of the map by assessing the similarity of the firing rate in adjacent spatial bins with a higher number reflecting greater consistency (Muller and Kubie, 1989). The distributions of sparsity and coherence measures across animals for exploration in a familiar open field, novel open field and novel open field in the presence of dorsal CA1 targeted burst mode photostimulation is shown in Figure 5.3b. Photostimulation did not alter the distribution of spatial tuning measures (sparsity: $P = 0.15$, coherence: $P = 0.80$, Kolmogorov-Smirnov test).

Spatial representations remapped between environments and the extent of this remapping was unaltered by photostimulation. I measured this using a correlation based co-firing measure by comparing the activity of cell pairs in theta cycle bins during exploration in one environment with that during exploration in another environment. This measure quantified the extent to which the firing relationships present in one environment were maintained in the second environment. Comparison of the first half and second half of exploration revealed that representations showed similar stability within exploration of a familiar open field, a novel open field and a novel open field in the presence of dorsal CA1 targeted burst mode photostimulation, whereas, comparison across the different environments showed reduced stability ($P < 0.0001$ for each within environment value compared to each across environment

value, z-tests, Figure 5.3c). The extent of this remapping was not different in the presence of photostimulation ($z = 0.46$, $P = 0.65$, z-test, for familiar versus novel in the absence of photostimulation compared to familiar versus novel in the presence of dorsal CA1 targeted burst mode photostimulation).

5.5 DA stimulation during waking exploration enhanced subsequent sleep reactivation

The occurrence of firing activity in hippocampal pyramidal neurons during sleep periods resembling that which occurred during the previous waking exploration is often referred to as hippocampal reactivation (O'Neill et al., 2010; Wilson and McNaughton, 1994). This reactivation of waking firing patterns occurs most prominently during high frequency local field potential (LFP) events called sharp wave ripples (SWR), and best reflects wakening firing activity which occurred at times of high theta band power in the LFP, when the animal was moving through the environment. In order to measure the strength of this reactivation, I used a correlation based co-firing measure (O'Neill et al., 2006; O'Neill et al., 2008) similar to that used for remapping in the previous section (see also section 2.15). This measure reflects the extent cells which fire together (correlated) during waking exploration still fire together in later sleep, and cells which fire separately (anti-correlated) still fire separately in later sleep. Only CA1 pyramidal cells were included in this analysis. I first calculated for each cell pair their tendency to co-fire across theta cycles during waking exploration (theta co-firing; Pearson correlation of instantaneous firing counts in theta cycle bins). I then separately calculated the tendency of the same cell pairs to co-fire in the following rest period during SWR events (SWR co-firing; Pearson correlation of instantaneous firing counts in bins aligned to SWR events). Finally, reactivation strength was calculated as the similarity of the firing associations expressed during sleep compared to waking and was obtained by calculating the Pearson correlation between the SWR co-firing values and the theta co-firing values.

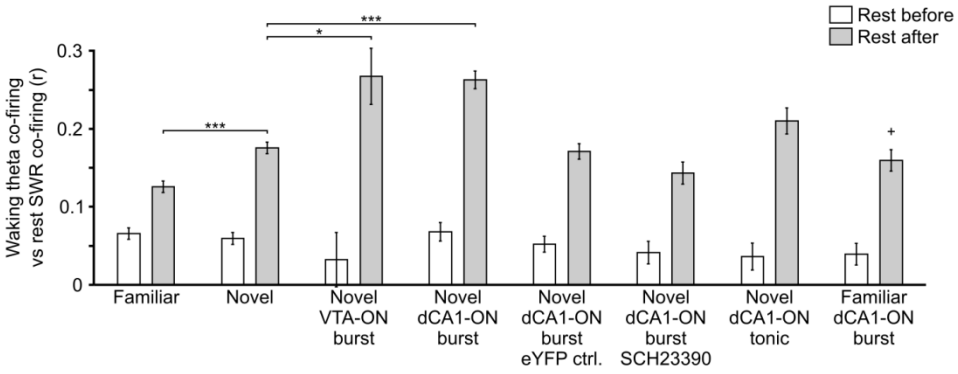

Figure 5.4 *Open field enhanced sleep reactivation after activation of dopamine*
Grey bars represent sleep reactivation after exploration in the open field across a number of conditions. White bars establish a baseline correlation level through comparison of waking activity in the various conditions to sleep recordings at the start of each day before exploration started. In all conditions reactivation strength was higher than the baseline comparison (all P < 0.0001, z-tests, Table 5.2). Reactivation strength was greater after exploration of a novel open field compared to a familiar open field (P = $1.7x10^{-6}$). This was further increased by burst mode photostimulation of midbrain dopaminergic neurons both at their cell bodies in the VTA (VTA-ON) and at the afferent dopaminergic fibres in the hippocampus (dCA1-ON), during exploration of a novel environment (VTA-ON: P = 0.011; dCA1-ON: P = $7.2x10^{-11}$). This enhanced reactivation was not seen in photostimulated control animals injected with a viral construct lacking the sequence coding for channelrhodopsin-2 (P = 0.70), nor was it present in animals injected with the dopamine antagonist SCH23390 prior to exploration in the presence of burst mode photostimulation (P = 0.42). Tonic mode photostimulation produced only a weak trend of increased reactivation (P = 0.052). Burst mode photostimulation also increased reactivation strength when delivered during exploration of a familiar open field when compared to the familiar non-stimulated condition (P = 0.030, '+' symbol in figure). z and P values from z-tests for all possible comparisons between reactivation strength in each of the conditions including those highlighted in this caption are reported in Table 5.3. All error bars are correlation coefficient ± standard error of the correlation coefficient.

Table 5.2 *Baseline correlations (Rest before) versus reactivation strength (Rest after)*

	Rest before correlation coefficient*	Rest after correlation coefficient*	Rest before vs Rest after Z-value	P-value
Familiar	0.066 ± 0.007	0.126 ± 0.007	-5.7	1.0E-08
Novel	0.059 ± 0.007	0.175 ± 0.007	-11.1	9.0E-29
Novel VTA-ON burst	0.032 ± 0.037	0.267 ± 0.036	-4.6	4.8E-06
Novel dCA1-ON burst	0.068 ± 0.012	0.263 ± 0.011	-11.9	6.9E-33
Novel dCA1-ON burst eYFP ctrl.	0.052 ± 0.010	0.171 ± 0.010	-8.2	1.6E-16
Novel dCA1-ON burst SCH23390	0.042 ± 0.014	0.143 ± 0.014	-5.1	3.9E-07
Novel dCA1-ON tonic	0.036 ± 0.017	0.210 ± 0.017	-7.3	2.3E-13
Familiar dCA1-ON burst	0.039 ± 0.014	0.159 ± 0.014	-6.2	6.2E-10

*Pearson correlation coefficient ± the standard error of the correlation coefficient

Table 5.3 *Comparison of reactivation strength (Rest after) across conditions*

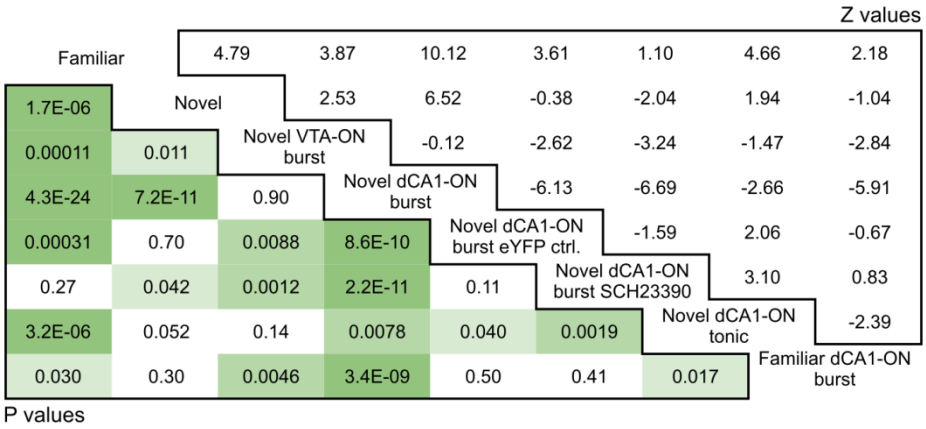

Hippocampal reactivation occurred in sleep after exploration under all conditions. When firing associations present during exploration were compared with firing associations in subsequent sleep, they always better matched than when the same waking firing associations were compared to firing associations in sleep recordings taken daily before exploration recordings began (all $P < 0.0001$, z-tests, Figure 5.4, Table 5.2). As previously reported in rats (O'Neill et al., 2008) and now replicated in mice, reactivation strength after exploration of a novel environment was higher than that seen after exploration of a familiar environment ($z = 4.79$, $P = 1.7 \times 10^{-6}$, z-test, Figure 5.4, Table 5.3). When applied during exploration of a novel environment, burst mode photostimulation of dopaminergic neurons both at their cell bodies in the VTA or at their afferent dopaminergic fibres in the hippocampus produced enhanced hippocampal reactivation in the subsequent sleep/rest (VTA-ON: $z = 2.53$, $P = 0.011$; dCA1-ON: $z = 6.52$, $P = 7.2 \times 10^{-11}$; z-tests, Figure 5.4). Additionally, dCA1-ON burst mode photostimulation during exploration of a familiar environment resulted in enhanced reactivation in comparison to the unstimulated condition ($z = 2.18$, $P = 0.030$, z-test, Figure 5.4). However, the enhanced reactivation seen after stimulation in the familiar environment remained lower than that seen after stimulation in the novel environment ($z = -5.91$, $P = 3.4 \times 10^{-9}$, z-test, Figure 5.4) and was similar in strength to that produced by novelty in the absence of stimulation ($z = -1.04$, $P = 0.30$, z-test, Figure 5.4). The enhanced reactivation produced by burst mode photostimulation in the novel environment was blocked when the D1/D5 antagonist SCH23390 was injected prior to exploration, with reactivation strength reducing to levels more near those seen for the familiar condition (compared to novel: $z = -2.04$, $P = 0.042$; compared with familiar: $z = 1.10$, P

= 0.27; z-tests, Figure 5.4). Enhanced reactivation was also not present in photostimulated DAT-IRES-Cre mice transfected with a viral construct coding for enhanced yellow florescent protein and lacking the light activated ion channel channelrhodopsin-2 (z = -0.38, P = 0.70, z-test, Figure 5.4). Finally, tonic mode stimulation consisting of the same number of light pulses (now equally spaced), when delivered in the novel environment, produced only a weak trend of increased reactivation (z = 1.94, P = 0.052, z-test, Figure 5.4).

5.6 Broader sleep physiology and associated estimates of arousal were unaltered post activation of dopamine

When placed in the sleep box during the recording days, mice generally quickly settled into an immobile state. The hippocampal local field potential recorded from the CA1 pyramidal cell layer visibly changed, with sharp wave ripples occurring in much greater abundancy being the most prominent change. Figure 5.5a shows instantaneous speed plots calculated in 820 ms bins across three recordings from the same day when the animal was in the sleep box, the first is rest before exploration, the second is rest after exploration of a novel environment in the absence of photostimulation and the third is rest after exploration of a novel environment with burst mode photostimulation enabled. Note the animal is mostly immobile with an instantaneous speed below 2 cm/s represented by the dashed dotted lines. However, occasionally there are times where the instantaneous speed is above 2 cm/s representing times where the animal moves its head or moves about within the box. These general properties of animal state and recorded field potential remained unaltered in sleep sessions after photostimulation of dopaminergic neurons. The portion of time spent immobile was similar across the data set for rest before exploration and rest after exploration in the absence of photostimulation, with VTA photostimulation and with dorsal hippocampus photostimulation (Figure 5.5b). The number of sharp wave ripples per second was also unaffected by photoactivation of dopaminergic neurons with rest before exploration, rest after exploration OFF, VTA-ON and dCA1-ON all having a similar number of SWR per second ($F_{3, 143}$ = 0.24, P = 0.86; Figure 5.5c). The final electrophysiological measure of arousal presented here is the theta/delta ratio. When the animal is awake and active in an environment, the local field potential shows higher power in the theta band (5-12 Hz), whereas during slow wave sleep a delta band (2-4 Hz) oscillation is present, thus allowing the theta/delta ratio to be used as an

indication of arousal (Csicsvari et al., 1999). Photostimulation in the previous exploration did not alter the theta/delta ratio in the subsequent rest session with, rest before exploration and rest after exploration OFF, VTA-ON and dCA1-ON all producing a similar theta/delta ratio ($F_{3, 143}$ = 0.24, P = 0.86, ANOVA; Figure 5.5d).

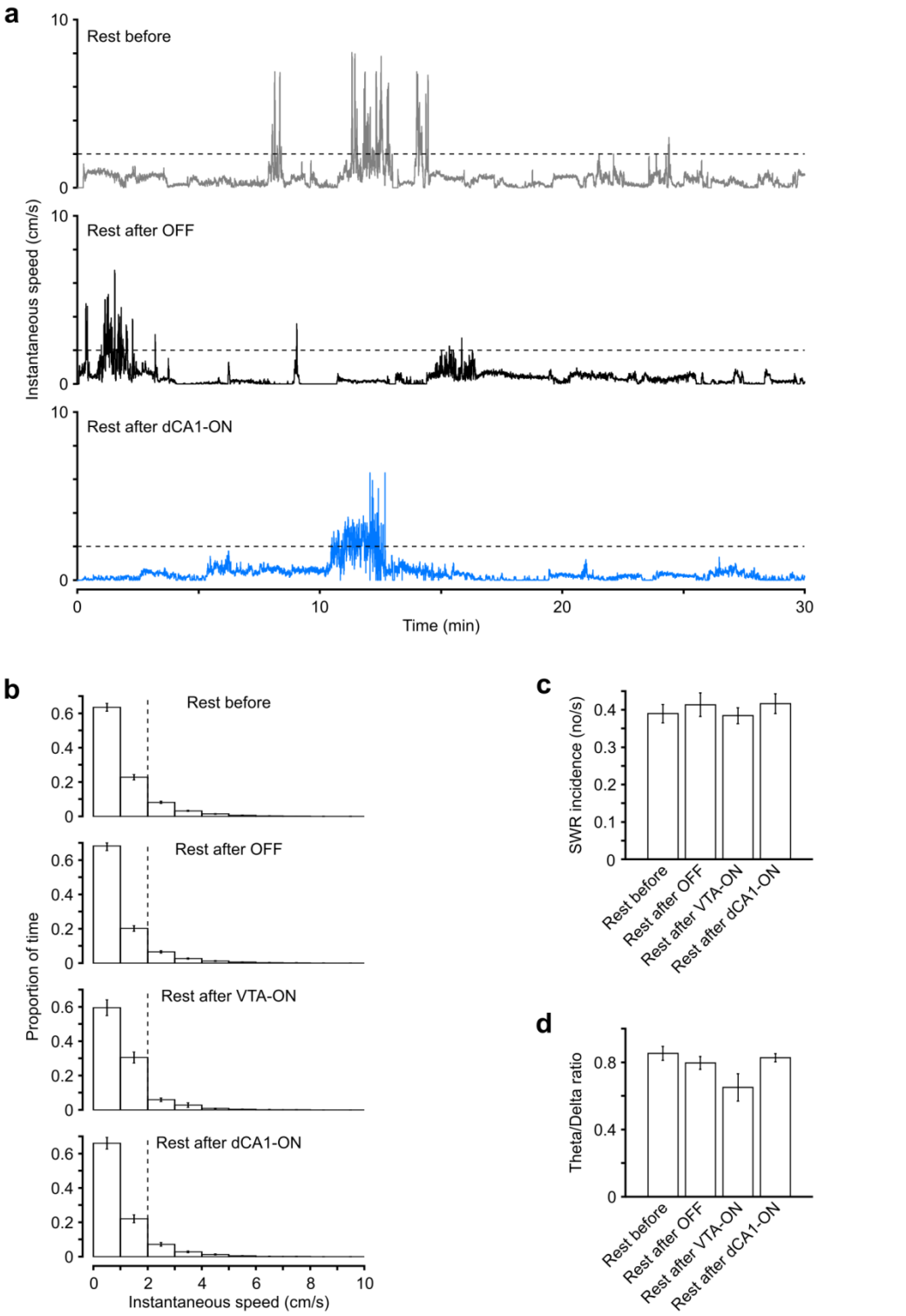

Figure 5.5 *Estimates of arousal state in rest sessions preceding and following exploration*
(a) *Example instantaneous speed plots (820 ms bins) of a DAT-IRES-Cre mouse during rest in the sleep box before open field explorations, after exploration of a novel open field and after exploration of a novel open field with dCA1-ON photostimulation. Note that the animal spent most of its time immobile (instantaneous speed < 2cm/s; dashed line) in all conditions.* ***(b)*** *The distributions of the instantaneous speed (means ± s.e.m.) across animals. The proportion of time spent immobile (left of the 2 cm/s dashed line) was similar during the sleep/immobility rest sessions before exploration and after exploration across conditions.* ***(c)*** *The number of SWRs per second was similar in rest before exploration and after exploration across conditions (means ± s.e.m.;* $F_{3, 143} = 0.24$, $P = 0.86$, *one way ANOVA).* ***(d)*** *The theta/delta band power ratio (means ± s.e.m.;* $F_{3, 143} = 2.10$, $P = 0.10$, *one way ANOVA) was not significantly different in rest before exploration and after exploration across conditions.*

5.7 Dorsal CA1 pyramidal cell discharge during sharp wave ripple events

During sharp wave ripple events the Schaffer collaterals of groups of CA3 pyramidal neurons provide a temporally concentrated depolarising glutamatergic input to CA1 pyramidal neurons (Csicsvari et al., 2000; Sullivan et al., 2011). This depolarisation is evident as a negative deflection of the LFP (sharp wave component) when recorded from stratum radiatum or the bottom of the pyramidal cell layer. The firing probability of pyramidal neurons in CA1 increases during SWR events due, in part, to this depolarising input (Csicsvari et al., 2000). Pyramidal cell firing locked to SWR events is evident in the simultaneously recorded raster plots of isolated pyramidal neurons in Figure 5.6a which are shown along with the wide band recording from one of the channels and the same trace band pass filtered in the ripple band (135-250 Hz). Note the vertical stripes of concentrated pyramidal neuron firing coinciding with the ripple events. Pyramidal cell participation in SWR events is also evident in the SWR triggered firing rate histograms of Figure 5.6c.

The mean field potential structure of sharp waves was unaltered in sessions following photostimulation. Figure 5.6b shows the mean SWR-triggered waveforms from three separate tetrodes, with waveforms from rest before exploration and rest after exploration with burst mode photostimulation superimposed. Additionally, broad metrics of CA1 pyramidal neuron participation in SWR events remained unaltered across rest sessions recorded before exploration, after non-stimulated exploration and after exploration with photoactivation of dopamine. The SWR triggered firing rate histograms were similar across conditions (Figure 5.6c). Firing rate histograms were calculated using 20 ms bins in reference to the peak ripple band power. The mean peak SWR firing rate (peak bin of the SWR triggered firing rate histograms) was not different across conditions ($F_{2, 2892}$ = 0.86, P = 0.42, one-way ANOVA, Figure 5.6c insert). Additionally, for each SWR event, the mean proportion of pyramidal cells discharging at least one action potential was not different in rest sessions before exploration, after exploration and after exploration with photoactivation of dopamine ($F_{2, 129}$ = 0.78, P = 0.46, one-way ANOVA, Figure 5.6d).

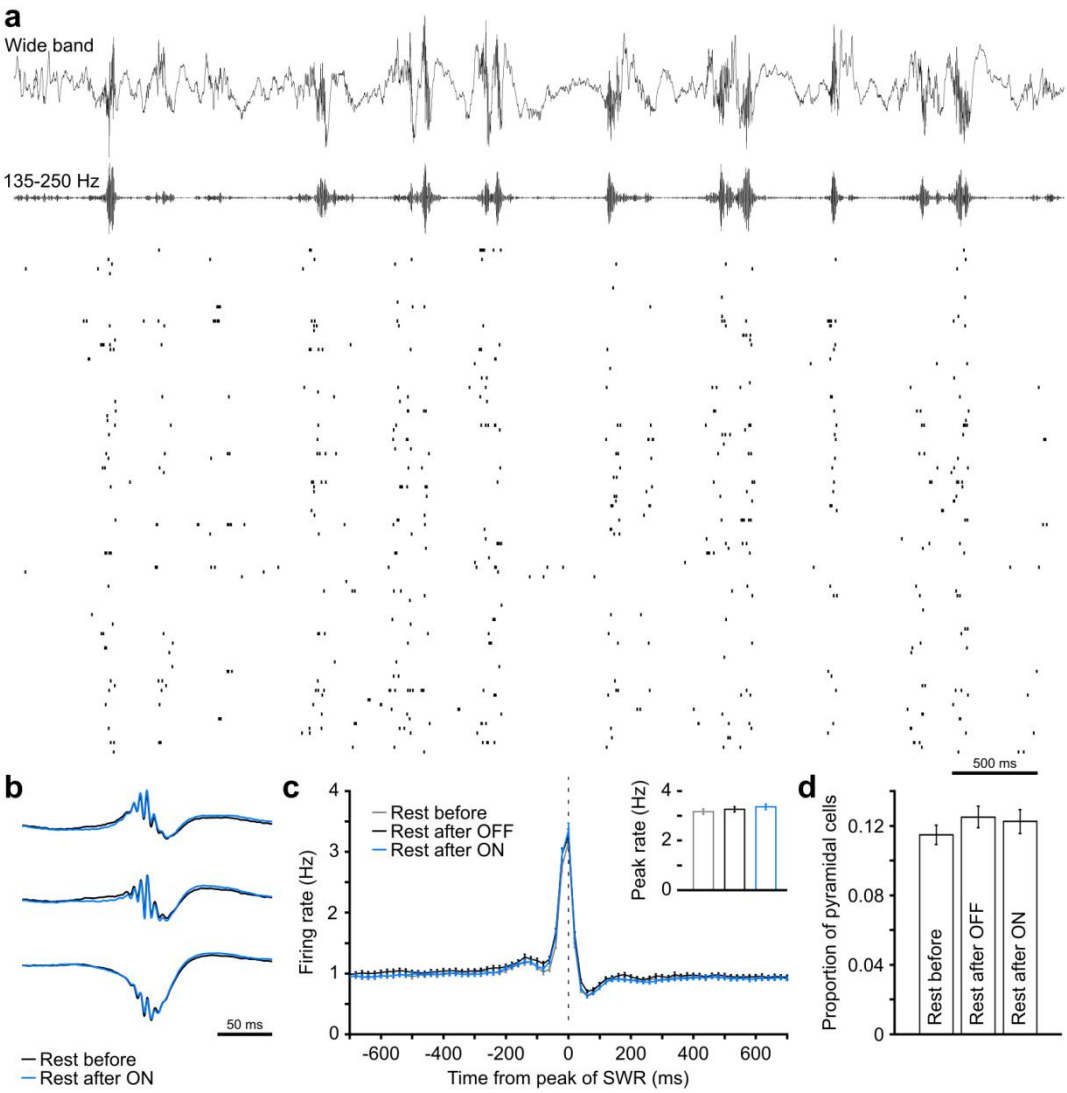

Figure 5.6 *Sharp wave ripple firing responses of dCA1 pyramidal cells during rest*
(a) *Top trace, wide band signal. Bottom trace, 135-250 Hz band pass filtered signal highlighting ripple frequency events. Raster plots, spike times of simultaneously recorded dCA1 pyramidal cells (one cell per row). Note the firing synchrony of pyramidal cells during ripple events.* ***(b)*** *Mean SWR-triggered waveforms from three separate tetrodes recorded during rest before and after dCA1-ON photostimulation. Traces obtained from the same tetrode (one channel displayed) are superimposed.* ***(c)*** *SWR-triggered firing rate histograms (means ± s.e.m.) of dCA1 pyramidal cells from mice during rest sessions preceding and following exploratory sessions with or without photostimulation. SWR firing rate histograms were calculated using 20 ms bins in reference to the SWR peak (i.e., peak of ripple-band power). The mean peak SWR firing rate was unaltered by photostimulation ($F_{2,\ 2892}$ = 0.86, P = 0.42, one way ANOVA).* ***(d)*** *The proportion of SWR-active pyramidal cells (i.e., for each SWR the proportion of cells discharging at least one spike) in rest sessions preceding and following exploratory sessions with or without photostimulation was similar (means ± s.e.m.; $F_{2,\ 129}$ = 0.78, P = 0.46, one way ANOVA). Note data recorded from DAT-IRES-Cre mice included in the next chapter were also included in this analysis.*

5.8 Discussion

In this chapter, I report results demonstrating that activation of midbrain dopaminergic neurons – both at their cell bodies in the VTA or at the afferent dopaminergic fibres within the hippocampus – during waking experience in an open field resulted in enhanced reactivation in subsequent sleep/rest of the dorsal CA1 waking firing activity which occurred during experience in that open field (see section 5.5). Reactivation was measured during LFP events called sharp wave ripples. This finding reveals a process capable of regulating which experiences are retained as memories and which are forgotten since hippocampal SWR reactivation is thought to aid memory consolidation through the strengthening (and perhaps reorganisation) of representations formed during waking experience (Buzsáki, 1989; Carr et al., 2011; O'Neill et al., 2010; O'Neill et al., 2008). Additionally, the effect was due to the activation of light activated ion channels targeted to dopaminergic neurons and not confounds due to virus transfection or the delivery of laser light to the brain since it was not seen in animals injected with a viral construct lacking the coding sequence for the light activated ion-channel. Mice injected with the D1/D5 receptor antagonist SCH23390 also did not show enhanced reactivation in subsequent rest/sleep indicating that the effect on reactivation was directly mediated through dopamine receptor activation. Furthermore, enhanced reactivation measured after photoactivation of dopaminergic neurons could not be explained due to a change in exploratory activity levels in the photostimulation enabled condition because the mean speeds of the animals were similar across conditions (see section 5.3). Nor can it be explained by changes in arousal level during the different sleep/rest periods since the animals showed similar levels of immobility, the theta/delta ratio was similar and the rate at which SWR events occurred was also similar, irrespective of whether photostimulation had been enabled in the preceding exploration (see section 5.6). Furthermore, enhanced reactivation was not due to a change in the extent of pyramidal cell participation in the SWR events (see section 5.7). Nor could it be attributed to a change in the waking firing of pyramidal cells because the spatial tuning properties of dorsal CA1 pyramidal cells and the reorganisation of dorsal CA1 pyramidal cell co-firing associations between environments was unaffected when photostimulation was enabled during exploration (see section 5.4).

It may have been expected that animals would have had increased locomotor activity in the novel environments or perhaps in exploratory sessions with photostimulation enabled. Mice did show high levels of locomotor activity in the novel environments. This, however, was not significantly different to movement levels in the familiar environment since in this study animals were also active in the familiar environments. The high levels of locomotor activity in the familiar environments were encouraged as part of the experimental design to remove differences in movement levels as a confounding factor in the analysis. Two factors potentially contributed to this. Firstly, it is possible that the mice tended to be more active in the open fields due to immediately previously being inactive in the relatively confined space of the sleep box. Secondly, increased locomotion was encouraged during pre-training; during the days before the recordings began, when the animals were familiarised with the familiar open field and sleep box, if the animal stopped moving for an extended period in the open field I would introduce my hand above the environment and this typically caused the animal to move about again. It is possible that experiments in less active animals or studies with increased duration of photostimulation would see a difference in locomotor activity across conditions.

The results of this chapter strongly implicate sleep reactivation as a means through which dopamine signalling capable of coding for value and novelty (see Chapter 4) can affect hippocampal network dynamics resulting in increased memory persistence, thus allowing dopamine signalling to modulate memory performance. However, a direct demonstration of optogenetic activation of dopamine on memory performance and an assessment of the effect of hippocampal dopamine activation on the stability of dCA1 firing patterns associated with spatial representations was still lacking and is addressed in experiments reported in the next chapter. The results of this chapter also raise questions about how enhanced reactivation fits with theories of hippocampal dopamine receptor activation 'tagging' synapses for enhanced potentiation through the activation of second systems (Redondo and Morris, 2011; Takeuchi et al., 2014; Wang et al., 2010) and is discussed in the final chapter.

Chapter 6 Memory persistence and dopamine in the hippocampus during a spatial learning task

6.1 Introduction

The open field experiments presented in Chapter 5 revealed that activation of midbrain derived dopaminergic afferents within the hippocampus during waking exploration resulted in enhanced reactivation in subsequent sleep. This result coupled with results from behavioural studies using pharmacological manipulation of dopamine receptors within the hippocampus (Bethus et al., 2010; O'Carroll et al., 2006; Wang et al., 2010) suggested that optogenetic activation of dopamine in the hippocampus would result in improved memory performance; however, a direct demonstration of this was still lacking. Importantly, it also remained unclear to what extent any effect of dopamine signalling on memory would be due to a direct effect on the ability or rate of learning as opposed to being aided by upregulation of processes occurring after acquisition aiding retention. In this chapter I present data addressing these questions based on recordings from a new spatial learning task developed in collaboration with lab members. In addition to allowing memory retention to be assessed in a probe test an important feature of this task is that it also allows the rate of learning to be assessed. This is because performance improves gradually over a number of learning trials resulting in a learning curve with potential to show either an increase or decrease in the rate of learning. I also investigate if changes in behaviourally assessed memory performance are accompanied by, and reflect changes in, the spatial representations within the brain measured by large scale recording from the CA1 pyramidal cell layer.

6.2 Experimental outline

To assess the effect of midbrain derived dopamine on hippocampal firing dynamics during learning, with the help of lab colleagues, we developed a new spatial learning task dubbed the

crossword maze (see section 2.11) based on a layout used previously by Tolman (1948). The maze consisted of four start boxes and eight intersecting tracks without side walls as shown in Figure 2.1. Movable barriers could be introduced across the tracks providing a blockade which the mouse was unable to pass. There were three stages in the experimental protocol, pre-learning, learning and probe, which were interspersed with rest periods during which time the mouse was placed in a small box containing home cage bedding. During the pre-learning stage, mice were allowed to freely explore the maze in the absence of barriers with the start boxes closed. For the learning stage the maze was setup with a new configuration each day. Two start boxes were selected as in use for that day and a reward location was chosen at the end of one of the tracks protruding from the maze. Barriers were introduced such that there was only one path from each of the in use start boxes to the reward location. Mice were given twenty trials to learn the maze configuration and reward location. Finally, in the probe stage a probe test was performed one hour after the end of the learning stage. For the probe test, the maze configuration was maintained from the learning stage but no reward was placed at the reward location and the mouse was placed in one of the in use start boxes and allowed to move freely on the maze. This was repeated four times to ensure the mouse covered the maze allowing the calculation of spatial firing rate maps for the probe recording stage.

A total of four DAT-IRES-Cre mice were recorded performing the crossword maze task. Mice received bilateral injections in the VTA of a Cre activated viral construct coding for channelrhodopsin-2 fused to enhanced yellow fluorescent protein. Mice also received a bilateral implant whereby an optic fibre was located at the top of the hippocampus on either side of the brain, with tetrode recordings also performed from the dorsal CA1 of both hippocampi. On about half of the recording days, burst mode photostimulation (trains of 20 light pulses 20 ms in duration with pulses at 50 ms intervals and a burst train delivered every 20 seconds) was enabled during the learning trials with the other days performed in the absence of photostimulation serving as a baseline for comparison. Recordings were performed in four mice providing 12 days (3, 3, 1 and 5 per animal) without photostimulation, yielding 244 pyramidal cells (16, 33, 4 and 191 per animal), giving 6061 simultaneously recorded cell pairs (52, 361, 6 and 5642 per animal), and 13 days with photostimulation enabled, yielding

316 pyramidal cells (53, 89, 18 and 156 per animal), giving 6011 simultaneously recorded cell pairs (598, 1398, 108 and 3907 per animal).

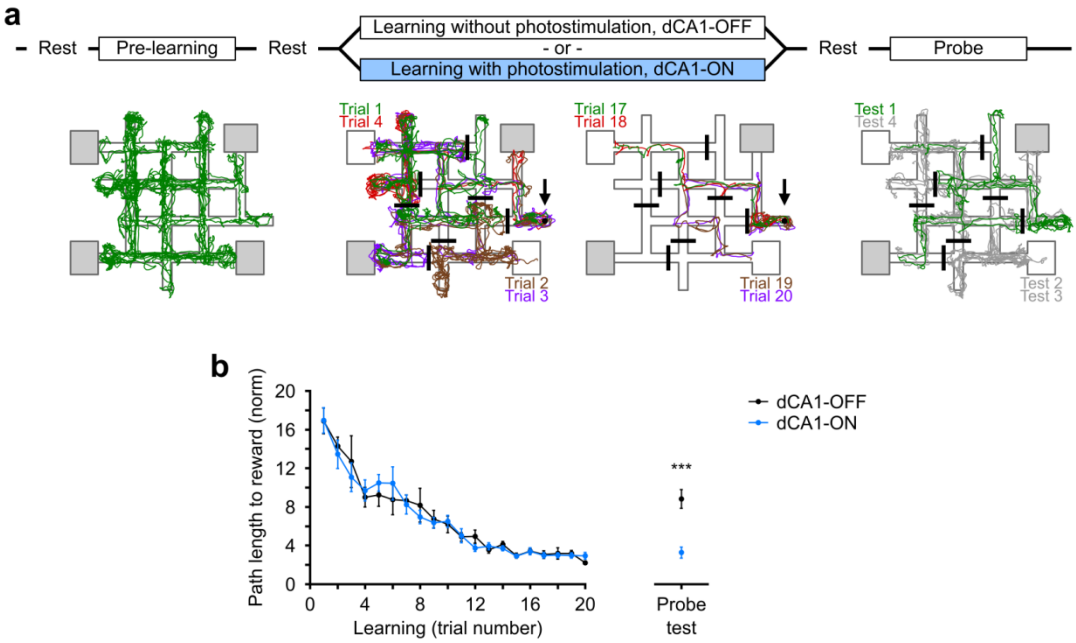

Figure 6.1 *Behavioural performance in the crossword maze task*
(a) *Recording protocol with example single-day single-animal trajectories for the pre-learning, learning and probe sessions. Arrows indicate reward location for that day and in-use start boxes are shown in white. Note the last learning trials are shorter and the mouse remembered the newly-learned goal location in the first probe test (green).* ***(b)*** *Left, photostimulation did not alter path shortening to reward across learning trials (means ± s.e.m. of per day values across animals, $F_{19, 405} = 0.40$, $P = 0.99$, between-within repeated ANOVA group x trial interaction). Right, photostimulation stabilised subsequent performance in the probe test preventing degradation in path length to reward seen on laser off days ($t_{23} = 4.99$, $P = 4.8x10^{-5}$, unpaired t-test).*

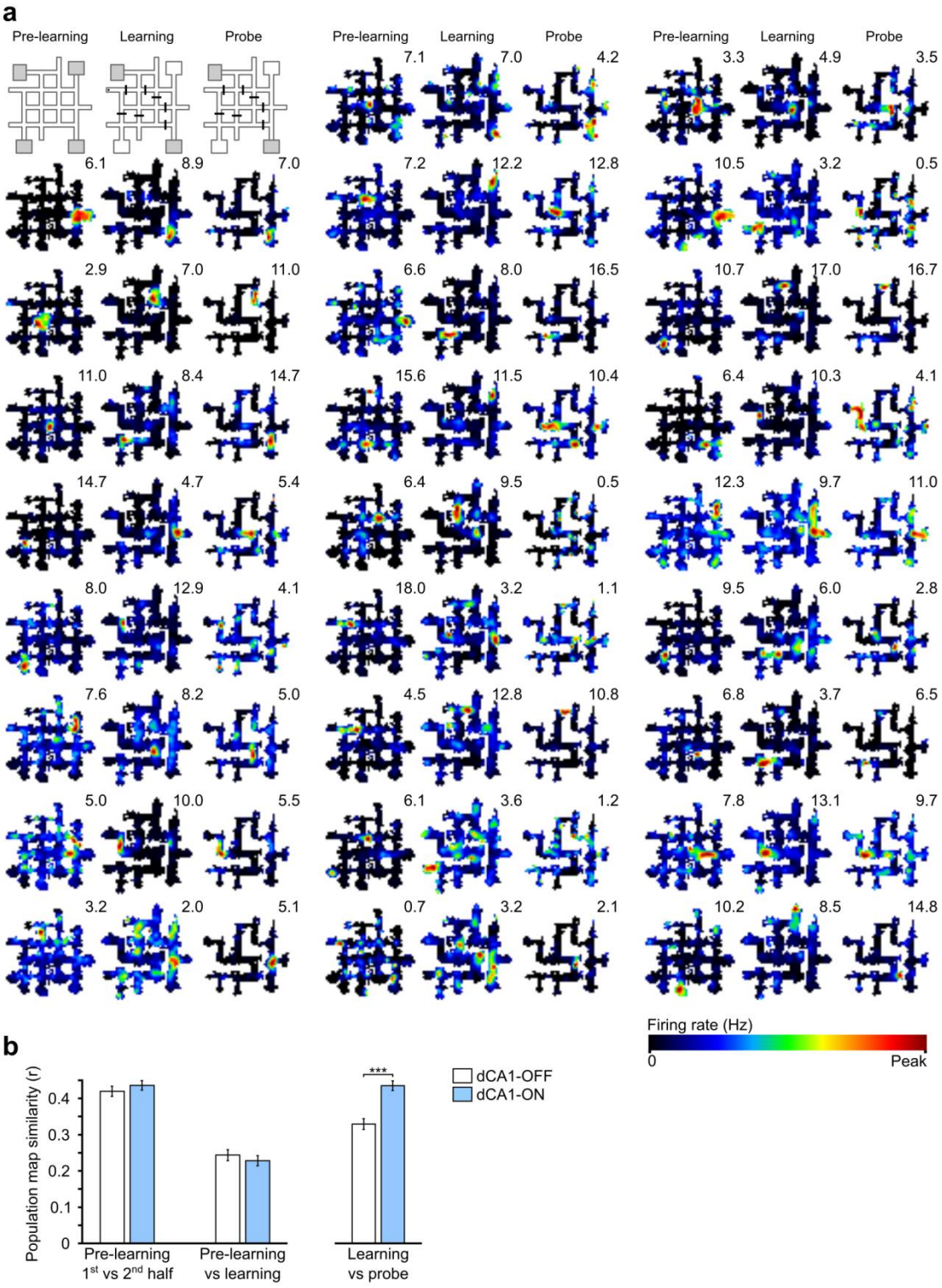

Figure 6.2 *Crossword maze spatial maps*

(a) *Spatial rate maps for a set of dCA1 pyramidal cells from the same recording day followed across the pre-learning, learning and probe stages. The peak firing rate (Hz) for each map is shown. The maze configuration for that day is depicted in the top left. Note that most cells established new firing fields in learning compared to pre-learning and many but not all reinstated the newly-established maps during the probe test.* ***(b)*** *Left, photostimulation did not affect the reorganization of dCA1 spatial maps between pre-learning and learning, with the*

pre-learning to learning comparison showing similarly lower correlation levels, in contrast to the within pre-learning comparison for both the photostimulated and non-stimulated conditions. Right, photostimulation promoted the reinstatement of newly-established maps during the probe test since comparison of learning to probe showed a higher correlation on photostimulated days over non-stimulated days (z = 5.90, P = 3.6x10^{-9}, z-test). Note how in the presence of dCA1 burst mode photostimulation the correlation levels reached the level seen in the within pre-learning comparison.

6.3 Behavioural performance

During the pre-learning stage, mice arbitrarily moved throughout the maze in much the same manner as animals in the open field did, generally covering the entirety of the maze. Performance during learning trials was assessed by measuring the path length from the start box to the rewarded location in each trial. During the learning trials, mice gradually learned the new maze layout and reward location with path length gradually shortening across trials (Figure 6.1). Photoactivation of afferent dopaminergic fibres within the hippocampus did not alter the rate of learning ($F_{19, 405}$ = 0.40, P = 0.99, between-within repeated ANOVA group x trial interaction, Figure 6.1). Importantly however, it did enhance memory performance in the probe test. Path length to the now no longer rewarded reward location was shorter in probe tests after learning with photoactivation of dopamine, than in probe tests after learning in the absence of photostimulation (t_{23} = 4.99, P = 4.8x10^{-5}, unpaired t-test; Figure 6.1). Interestingly, this enhanced memory performance maintained the path length at the level seen in the final learning trials, preventing the degradation in performance seen on non-stimulated days. Note photostimulation was only ever delivered during learning trials and not during the probe test or intervening sleep periods.

6.4 Reorganisation and reinstatement of spatial maps

Figure 6.2a shows spatial rate maps for a selection of simultaneously recorded dorsal CA1 pyramidal neurons calculated separately for the pre-learning, learning and probe stages. These maps depict the firing rate of the cell as a function of the position of the animal. Each cell can be seen to be more active in a sub-region of the environment or preferred firing field. The combined firing of these cells and the many others not recorded here are thought to collectively provide a representation of the environment within the brain (O'Keefe and Nadel, 1978). This representation remapped from the pre-learning exploration to the learning trials

on the introduction of the barriers as can be seen in Figure 6.2a, since the preferred firing fields of much of the recorded cells moved in location. This new representation was partially reinstated in the probe test with many of the cells reinstating their preferred firing fields in the new location established in the learning stage.

I used the population map similarity measure to quantify the similarity of this population representation of the environment from two different time periods (Dupret et al., 2010; O'Neill et al., 2008). It is based on comparing how cells which fired in similar regions of space during the first time period, fire in similar regions of space in the second time period, and how cells which fire in different regions of space still fire in different regions of space in the second time period (see section 2.17). In this manner, the relative spatial firing relationships between the cells can be compared. I first established the similarity expected of a within environment comparison by comparing the first half to the second half of the pre-learning exploration. The population map similarity calculated across days between the pre-learning and learning stages was much lower than the within-environment baseline similarity reflecting the remapping which occurred between the two stages (Figure 6.2b). The extent to which the population representation remapped from pre-learning to learning across days was not different when photoactivation of dopamine was enabled during the learning stage (Figure 6.2b). However, the reinstatement in the probe test of the newly established spatial maps (second half of the learning trials) was promoted following photoactivation of dorsal CA1 dopaminergic axons ($z = 5.90$, $P = 3.6 \times 10^{-9}$, z-test, Figure 6.2b). The population map similarity between learning (second half) and the probe test on days with photostimulation enabled was at level similar to the within-environment baseline comparison whereas for days without stimulation the similarity level reflected only partial reinstatement.

6.5 Sleep reactivation

As in the open field experiments, hippocampal reactivation occurred in sleep after each of the recording stages across conditions (reactivation strength was higher than a baseline level generated through comparison with sleep recordings taken daily directly before the pre-learning stage; comparison with sleep after pre-learning: $z = 4.1$, $P = 4.6 \times 10^{-5}$; after learning with photostimulation off: $z = 6.6$, $P = 3.3 \times 10^{-11}$; and after learning with photostimulation

enabled: z = 10.2, P = $1.7x10^{-24}$; z-tests, Figure 6.3). Hippocampal reactivation is the reoccurrence of firing associations between CA1 pyramidal neurons in rest and sleep matching those which occurred during previous waking activity. I have quantified hippocampal reactivation strength here as the similarity between waking co-firing of CA1 pyramidal cell pairs during theta cycles and the co-firing during SWR events of the same cells during subsequent sleep (see section 2.15). The higher the reactivation strength the better the firing associations during sleep reflect those which occurred during the previous waking. Reactivation strength in rest after the learning stage was higher than that observed after the pre-learning stage (z = 4.23, P = $2.3x10^{-5}$, z-test, Figure 6.3) suggesting that the introduction of the barriers or the learning itself may invoke similar mechanisms as recruited to produce enhanced reactivation in a novel open field compared to a familiar one (see Chapter 5). Similar to results seen in the open field experiments, photoactivation of dopamine during learning enhanced the reactivation of firing associations observed during the learning stage above the reactivation strength seen on days without photostimulation (z = 3.16, P = 0.0016, z-test, Figure 6.3). Importantly, this enhanced reactivation preceded enhanced memory retention coupled with better reinstatement of the newly learned maps present in the probe tests.

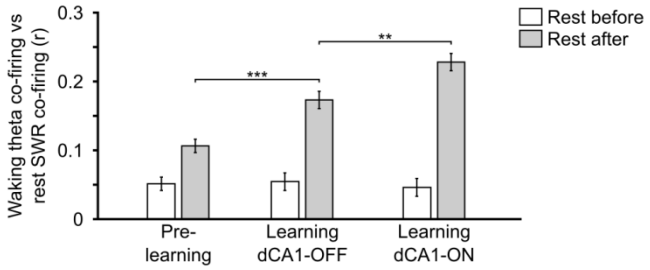

Figure 6.3 *Crossword maze enhanced sleep reactivation after activation of dopamine*
Grey bars represent reactivation strength in sleep/rest recordings after the stage indicated below the bar. White bars establish a baseline correlation level through comparison of waking activity in the various conditions to sleep recordings taken at the start of the day, before the pre-learning stage commenced. In all conditions, reactivation strength was higher than the baseline comparison (pre-learning: z = 4.1, P = $4.6x10^{-5}$; learning dCA1-OFF: z = 6.6, P = $3.3x10^{-11}$; learning dCA1-ON: z = 10.2, P = $1.7x10^{-24}$; z-tests). Reactivation strength seen after the learning stage was greater than that seen after the pre-learning stage (z = 4.23, P = $2.3x10^{-5}$, z-test). This increased further when burst mode photostimulation of the afferent dopaminergic fibres in the hippocampus was applied during the learning stage (z = 3.16, P = 0.0016, z-test).

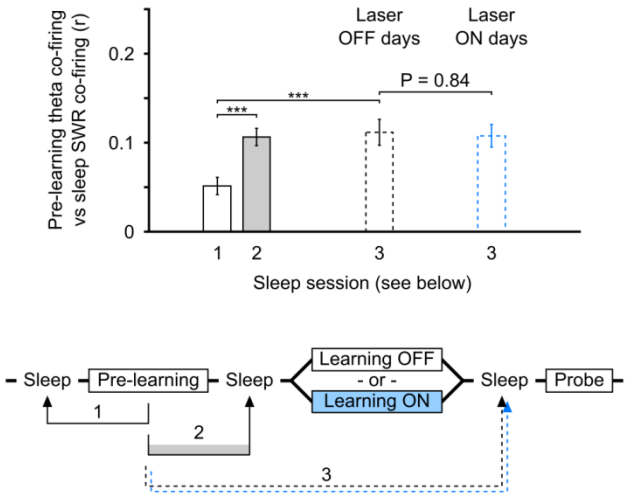

Figure 6.4 *Enhanced reactivation did not extend to recently expressed representations*
Pre-learning stage patterns were reactivated in the sleep after the pre-learning stage (grey bar, z = 4.1, P = 4.6x10^{-5}, z-test) and also in the sleep after the learning stage (black dashed bar, z = 3.5, P = 5.1x10^{-4}, z-test). However, reactivation of the pre-learning representation in the sleep/rest period after the learning stage was not enhanced by photostimulation delivered during the intervening learning stage (black dashed bar compared to blue dashed bar, z = 0.21, P = 0.84, z-test).

One additional insight about enhanced hippocampal reactivation due to photoactivation of dopamine revealed by the protocol used here is that only the actively expressed firing associations (and hence the active representation) were more strongly reactivated. The effect of photostimulation did not extend back in time to recently expressed representations despite those representations still being retained by the network. Consider the firing associations present during the pre-learning exploration. As stated already these pre-learning firing associations were reactivated in the subsequent rest period (z = 4.1, P = 4.6x10^{-5}, z-test, Figure 6.4). Additionally, on days with photostimulation disabled these same firing associations were also reactivated with similar strength in the later rest after the learning stage (z = 3.5, P = 5.1x10^{-4}, z-test, Figure 6.4) indicating that the pre-learning representation was still present in the hippocampal network during the learning stage despite not being actively expressed. Interestingly however, on days where the photostimulation was enabled the pre-learning firing associations were still only reactivated with this same strength in the rest after the learning stage despite the intervening photoactivation of dopamine during the learning stage (days with photostimulation compared to days without: z = 0.21, P = 0.84, z-test, Figure 6.4). Thus, photoactivation of dopamine during waking behaviour produces enhanced reactivation of the

concurrently actively expressed representations but the effect does not extend back to recently expressed and still retained representations.

6.6 Hippocampal dependence of the crossword maze task

The hippocampal dependency of the crossword maze learning task was established in a separate set of experiments as part of the development of the task with lab colleagues. Here an optogenetic approach was used to disrupt hippocampal function during learning. In these experiments, a total of five PV-IRES-Cre$^{+/+}$ mice were injected bilaterally in the dorsal hippocampi with the same Cre inducible viral construct used in the DAT-IRES-Cre mice (Figure 6.5). These mice also received a bilateral implant with optic fibres and tetrodes to the dorsal hippocampi. The injections resulted in expression of the light activated ion channel channelrhodopsin-2 fused to enhanced yellow fluorescent protein (ChR2-eYFP) in parvalbumin expressing interneurons in the dorsal CA1. Figure 6.5b shows this expression through the visualisation of the enhanced yellow florescent protein. The specificity of the expression can be seen in Figure 6.5c which shows immunoreactivity against parvalbumin co-localising with ChR2-eYFP expression. This approach was used in order to activate parvalbumin expressing interneurons which in turn inhibited CA1 pyramidal neurons creating an overall disruptive effect on the hippocampal network. The light pulse triggered raster plots in Figure 6.5d, isolated from a dorsal CA1 recording, show a putative parvalbumin expressing interneuron firing increased action potentials during application of laser light. The mean firing rate of dorsal CA1 pyramidal neurons was halved during photoactivation of parvalbumin expressing interneurons (n = 224, Figure 6.5e), demonstrating the disruptive effect of the photostimulation on the hippocampal network.

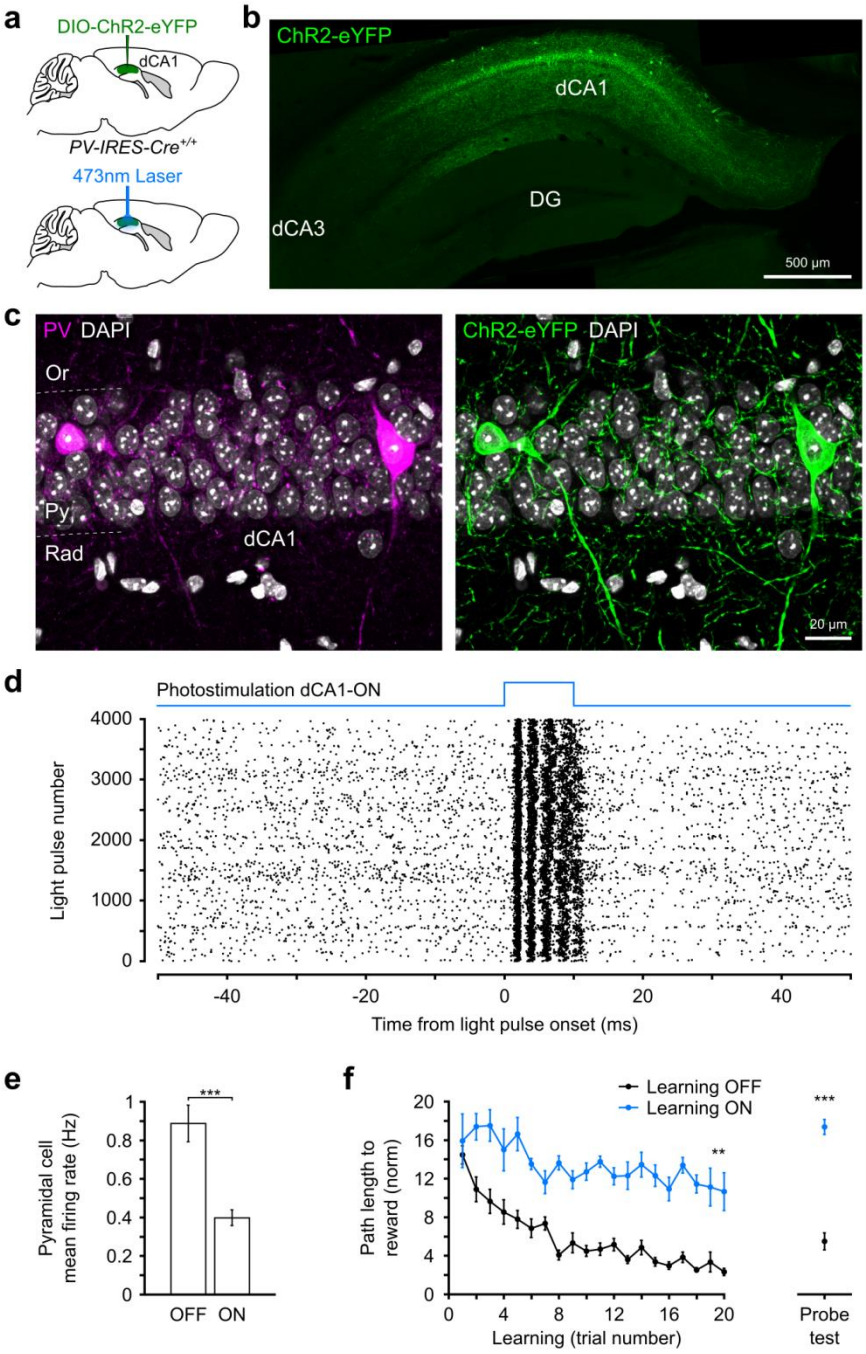

Figure 6.5 *Spatial learning on the crossword maze requires a functional hippocampus*
(a) *In order to disrupt locally the activity of dCA1 hippocampal pyramidal cells, a Cre-inducible viral construct coding for channelrhodopsin-2 (ChR2-eYFP) was injected into the dCA1 of parvalbumin PV-IRES-Cre$^{+/+}$ mice. To control and monitor dCA1 pyramidal cell activity these PV^{dCA1}::ChR2-eYFP mice were implanted in dCA1 for combined in vivo multichannel recordings with photostimulation.* ***(b)*** *Low magnification image showing the expression of ChR2-eYFP targeted to the dCA1 of a PV-IRES-Cre$^{+/+}$ mouse.* ***(c)*** *High magnification confocal image of the dCA1 showing expression of ChR2-eYFP in PV expressing interneurons (flattened 5 µm z-stack). Cell nuclei stained with DAPI.* ***(d)*** *Raster plot showing the spike times of one dCA1 interneuron recorded in a PV^{dCA1}::ChR2-eYFP mouse in relation to the onset of 10 ms light pulses in the dCA1-ON condition. Note the increased spiking activity with short latency (< 3 ms) induced by*

the laser and confined to the duration of the stimulation pulse. ***(e)*** *Photostimulation of dCA1 in these* PV^{dCA1}*::ChR2-eYFP mice led to a decrease in firing rate of dCA1 pyramidal cells* (t_{222} *= 5.01, P =* 1.1×10^{-6}*, t-test, n = 224).* ***(f)*** *Left, learning performance, as measured by distance travelled to reward, was impaired in days when the* PV^{dCA1}*::ChR2-eYFP mice received photostimulation* ($F_{19, 354}$ *= 2.08, P = 0.0054, between-within repeated ANOVA group x trial interaction). Right, photostimulation applied during learning was associated with subsequent degraded performance during the probe test* (t_{19} *= 9.81, P =* 7.1×10^{-9}*, t-test).*

The PV-IRES-Cre mice performed the task using the same experimental protocol as the DAT-IRES-Cre mice. Photostimulation was delivered during the learning phase on some days, while other days were recorded entirely in the absence of photostimulation. In these experiments using PV-IRES-Cre mice, when enabled, photostimulation was applied randomly to 80% of the learning trials using trains of 10 ms pulses every 16 ms. The laser was off during the inter-trial intervals. On days when photostimulation was disabled (n = 13 days, 12 probe tests) these mice learned the task in a similar fashion to the DAT-IRES-Cre mice with the path length to the reward location gradually shortening across learning trials. However, on days when photostimulation was active (n = 9 days) thus disrupting hippocampal network function, mice failed to learn the reward location, since path length to first reaching the reward location did not shorten across trials in the same manner as non-stimulated days ($F_{19, 354} = 2.08$, P = 0.0054, between-within repeated ANOVA group x trial interaction, Figure 6.5f). The slight drop in path length in the photostimulated condition evident in Figure 6.5f was due to a drop in the maximum time allowed before a trial was terminated. This was imposed after trial five for practicality reasons in conducting the experiment. Unsurprisingly, given the learning stage result, performance in the probe test was also impaired on days when photoactivation of parvalbumin expressing interneurons was enabled ($t_{19} = 9.81$, $P = 7.1 \times 10^{-9}$, t-test, Figure 6.5f).

6.7 Discussion

Results presented in this chapter show enhanced retention of learnt performance in the probe test of a spatial task, when burst mode photoactivation of the dopaminergic projection to the hippocampus was applied during learning. Enhanced reactivation of the dorsal CA1 firing associations present during learning occurred in the intervening rest/sleep period. In addition, I demonstrated that enhanced retention of learnt performance was accompanied by better

reinstatement of spatial maps present during learning, as assessed by the firing locations of the recorded place cells.

It has previously been shown that pharmacological manipulation of dopamine receptors within the hippocampus results in increased memory performance (Bethus et al., 2010; O'Carroll et al., 2006), however it has been recently suggested that the required dopamine may originate from noradrenergic fibres originating in the locus coeruleus (Smith and Greene, 2012). While this may also be the case, the demonstration here that photoactivation of midbrain derived dopaminergic fibres within the hippocampus produces increased memory performance, shows that midbrain dopaminergic neurons can provide the required dopamine, an insight pharmacological manipulation was unable to provide.

That enhanced reactivation occurred between the learning stage (when dopaminergic fibres were activated) and the resulting increased memory performance in the probe test, suggests that regulation of reactivation is one of the means through which dopamine action within the hippocampus can regulate memory performance. It must be conceded however, that a link on the basis of these experiments alone is correlative. However, coupled with findings of reduced memory performance due to disruption of sharp wave ripples (Ego-Stengel and Wilson, 2010; Girardeau et al., 2009) it is fair to assert a link. Additionally, the demonstration of enhanced reinstatement of spatial maps in the probe test further strengthens evidence for dopamine directly effecting dorsal CA1 pyramidal neurons resulting in firing activity relevant to memory performance.

Chapter 7 General discussion

7.1 Overview

The hippocampus (particularly the CA1 and CA3 subfields) and the midbrain dopaminergic system are among the more extensively studied and better understood brain systems. It is therefore somewhat surprising that there is limited understanding of whether information present in one system is used by the brain to inform the other (either directly or indirectly), and if so how. In particular, it seems that this question is worthy of further investigation since the roles suggested of each system are somewhat related. The error prediction signal produced by dopaminergic neurons of the ventral tegmental area (VTA) is believed to inform learning (Schultz et al., 1997; Steinberg et al., 2013). It is thought to do this by signalling mismatches between expectation, based on past experiences, and actual events with particular emphasis on value, novelty detection, and saliency (Bunzeck and Düzel, 2006; Cohen et al., 2012; Lak et al., 2014; Schultz et al., 1997). The hippocampus is attributed with the not too dissimilar property of performing an important role in the retention and recall of information relating to experiences, thus allowing experiences to guide future behaviour (Eichenbaum and Cohen, 2014; Moser et al., 2015; O'Neill et al., 2010; Squire et al., 2004). The hippocampus is also associated with novelty detection particularly in relation to context (Knight, 1996; Lisman and Otmakhova, 2001; O'Neill et al., 2008). However, there are also many differences between the midbrain dopaminergic system and the hippocampus. Dopaminergic signalling is associated with an ongoing expectation mismatch signal (Schultz et al., 1997). In contrast, the hippocampus is associated with the more detailed representation of information relating to the current experience such as location (O'Keefe and Nadel, 1978) within the environment, as well as odours (Igarashi et al., 2014; Manns et al., 2007), tactile information (Young et al., 1994) and the tracking of time (Hampson et al., 1993; MacDonald et al., 2013). It nonetheless seems as though information sharing between the two systems would be advantageous. In this thesis, I have focused on establishing improved understanding

of the projection of dopaminergic neurons to the hippocampus with a focus on spatial novelty and learning.

Through the experiments presented in this thesis I demonstrated:

- sustained increased firing of VTA neurons in response to spatial novelty in the absence of rewards,
- that midbrain dopaminergic neurons do project to the dorsal hippocampus,
- and that stimulation of these afferent dopaminergic fibres within the hippocampus leads to
  - enhanced reactivation in subsequent sleep,
  - better reinstatement of newly learnt spatial representations,
  - and enhanced memory assessed through behavioural performance.

These data support the idea that (1) dopaminergic signalling facilitates mechanisms which increase retention of information in the hippocampal network aiding future recall and (2) that in addition to more short term responses, the VTA is capable of providing sustained signalling to drive such an upregulation in hippocampal memory function.

Although not the focus of this thesis, it is also likely that VTA novelty responses are informed by hippocampal processing. A direct projection from the hippocampus to the VTA has not been reported. However, many areas which receive projections from the hippocampus do project to the VTA including, the medial prefrontal cortex, the nucleus accumbens, the lateral septal nucleus, and the amygdala (Lisman and Otmakhova, 2001; Luo et al., 2011).

7.2 Technical limitations

A number of the techniques used in this study come with some small technical limitations which it was important to make sure were properly considered when interpreting the data. Data acquired by large scale extracellular recording using tetrodes requires many careful steps of data processing described in section 2.12, in order to isolate the spiking activity of individual neurons. The isolated activity representing a cell is often referred to as a unit to reflect that the spike times generated from the recording are an accurate sampling of the action potential firing of the cell, but not necessarily a perfect measurement of this; some action potentials can

be missed and other spikes in the recordings can be misclassified due to natural variations in spike shape and spikes of multiple cells occurring at the same time (Harris et al., 2000). However, only well-isolated and stable units over the entire recording day (based on the criteria of section 2.12) were used in the subsequent analysis. A further drawback of this type of recording is that it is not fully possible to determine the identity of the recorded cells. The analysis of hippocampal recordings in this thesis was limited to principal cells. This was performed on the bases of their auto-correlogram and firing rate. While this is generally a good criteria for separating principal cells and interneurons and has been used previously (Csicsvari et al., 1999), it is likely that a number of low firing interneurons may have been included in the data set. It should be noted however, that any limitations in relation to unit isolation and cell type identification equally apply across all conditions and as such should have a minimal effect on the conclusions of this work since comparisons were made between conditions.

Using tetrodes allows for a large number of recording sites with minimal tissue damage. However, this comes with the drawback that the exact location of all of the recording sites is not precisely known to the same extent as is the case when labelling is performed after single cell recordings. To achieve a high level of accuracy, tetrode implantation was guided by a stereotaxic frame. Furthermore, in the case of recordings from the hippocampus, it was possible to have reasonable confidence that the tetrode tip was located in the pyramidal cell layer due to the profile of sharp wave ripple events and the presence of a large number of units. In Figure 5.6b, the negative deflection in the bottom mean SWR trace is indicative that the tetrode was located towards the bottom of the cell layer, whereas, the slight positive deflection in the top trace is suggestive of a tetrode located higher in the layer. If the tetrode was to be located further from the layer, the sharp wave deflection would be greater and the ripple less pronounced. In the VTA, there is no such laminar structure to guide electrode placement. However, since the expression of channelrhodopsin was specific to dopaminergic cells, the spiking and local field potential (LFP) response produced on the tetrode in response to pulses of laser light gave an indication that the tetrode was located near the channelrhodopsin expressing cells, and hence the dopaminergic cell groups.

A number of the recorded cells could be identified as dopaminergic on the basis that they had an increased probability of firing action potentials at low latency (< 3 ms) to laser pulse onset. It was only possible to confidently isolate five such cells from the recordings. This number is quite low and it may have been possible to isolate more cells if some aspects of the experiment were further optimised. The primary difficulty in obtaining such single units was that while many of the recordings showed low latency spiking it was not possible to match the light induced spike shape with spikes from other units in the recording. The problem being that in such cases it appeared as though the light pulse was consistently causing more than one cell within the recording range of the tetrode to discharge simultaneously, resulting in a spike shape reflecting the summed spike shape of the multiple cells. Indeed, the cases where it was possible to isolate a light driven unit, were instances where the probability of inducing a spike was relatively low, indicating that the cell was located towards the edge of the illuminated area. In order to improve the yield of light driven single units, it may have been possible to adjust the laser intensity in order to activate fewer cells allowing the recording of a single light responsive unit. However, for these experiments the goal was to consistently activate a large proportion of midbrain dopaminergic neurons in order to capture the effect on hippocampal network activity, so the laser intensity was not reduced. An additional approach, which may help in conjunction with adjusting the laser intensity in order to isolate individual light responsive cells, is to glue the tetrodes to the side of the optic fibre, thus allowing a fixed relationship between the light source and the recording sites.

Activation of midbrain dopaminergic neurons using channelrhodopsin-2 is a very advanced and effective way of achieving targeted activation with minimal side effects. Nonetheless, this approach is not without limitations. The virus did not transfect all midbrain dopaminergic cells and, more significantly, the light is not delivered with even intensity to all channelrhodopsin expressing cells. This means that cells near the tip of the optic fibre were more strongly activated than cells further from the light source. An even more important, and not often mentioned drawback of this type of activation is that, the population of cells is simultaneously activated, something which does not occur in the natural state. Given how much emphasis is placed on phasic responses in dopaminergic neurons, the simultaneous firing of many of the

cells could be considered a phasic event of very large magnitude. The exact implications of this remain unclear.

7.3 How might dopamine release in the hippocampus promote subsequent activity and enhance memory performance

There are potentially a number of possible means by which dopamine release within the hippocampus during active experience can affect the hippocampal network to produce an increase in subsequent reactivation and memory persistence. The presence of different types of dopamine receptors within the hippocampus (Ciliax et al., 2000; Goldsmith and Joyce, 1994; Kwon et al., 2008; Lemon and Manahan-Vaughan, 2006; Levey et al., 1993; Li et al., 2014; Meador-Woodruff et al., 1992; Savasta et al., 1986; van der Weide et al., 1987) allows for the idea that multiple molecular pathways may be activated by dopamine release. Changes in synaptic efficacy through long term potentiation (LTP) are thought to underlie network plasticity and memory formation (Bliss and Collingridge, 1993; Hebb, 1949). Induction of LTP activates numerous cell signalling cascades (Lynch, 2004). In broad terms, LTP can be viewed as having an early phase and late phase. In the early phase pre-synaptic and post-synaptic spiking with the required timing activates kinases, including αCaMKII, which drive specific AMPA receptor phosphorylation and insertion of GluR1-containing AMPA receptors into synapses (Malinow and Malenka, 2002). This is, in the main, triggered by calcium influx from postsynaptic NMDA receptors and does not require the synthesis of new protein. In the late phase, maintenance of the increased synaptic efficacy occurs through the capture of plasticity-related proteins and is dependent on the synthesis of new proteins (Frey et al., 1996; Frey and Morris, 1997; Nguyen et al., 1994; Rogerson et al., 2014). There is evidence that dopamine can have an effect on both early and late-LTP.

Pharmacological activation of D1/D5 type receptors at CA1 synapses in hippocampal slice preparations have been shown to lower the threshold required to produce LTP and increase the magnitude of early-LTP (Otmakhova and Lisman, 1996). Additionally, in an elegant set of experiments which directly speak to the work in this thesis, Li and colleagues (2003) demonstrated that five minutes exposure to a novel environment lowered the threshold required to produce LTP at CA1 synapses in freely behaving rats. This direct demonstration of

novelty exposure on early-LTP was also demonstrated to be dependent on dopamine receptor activation, as it was prevented by injection of a D1/D5 receptor antagonist. Furthermore, injection of a D1/D5 agonist mimicked novelty exposure in that it was sufficient to induce LTP at the lower threshold without exploration of the novel environment. Taken together, these experiments suggest that dopamine release in the hippocampus could facilitate the formation of new connections in the hippocampal network reflecting the structure of the incoming activity associated with the new event or environment. These new connections, enhanced by dopamine action at the time of formation during experience, can then be further strengthened by subsequent offline network activity during SWR events. The known structure of the SWR events seems suited to achieving this. Strong bursts of excitatory activity arises in the recurrent CA3 network (Csicsvari et al., 2000; Sullivan et al., 2011), providing excitatory drive to CA1 which could reactivate the recently potentiated synapses, further strengthening them through reactivation of early-LTP mechanisms. This activity is further facilitated during the SWR event by the changes in the distribution of inhibitory tone by interneurons across the different subcellular compartments (Klausberger and Somogyi, 2008) e.g. removal of inhibition to the axon initial segment allowing spiking at a lower threshold potentially allowing postsynaptic spikes aiding additional early-LTP.

The second mechanism through which dopamine action at the time of experience during the initial LTP events can enhance the persistence of memory is by setting a molecular state or 'tag' in potentiated synapses, which upregulates the capture of plasticity-related proteins (PRPs), thus enhancing late-LTP mechanisms (Rogerson et al., 2014; Takeuchi et al., 2014). Frequently cited evidence for this comes from behavioural studies using infusion of a D1/D5 receptor antagonist into the hippocampus and observing the time scale of the effect in relation to the memory performance of the animal (Bethus et al., 2010; O'Carroll et al., 2006; Wang et al., 2010). Such experiments found that the drug induced a decrease in the persistence of memory performance over longer time scales (e.g. 24 hours), yet encoding of the memory tested at short delay (e.g. half an hour) remained intact. Studies using hippocampal slice preparations have also shown indication of D1/D5 receptor activation as affecting late-LTP (Frey et al., 1991; Wang et al., 2010). It is difficult to fully interpret the results of these experiments investigating late-LTP due to the fact that it is difficult to remove the potential

effect of D1/D5 receptor activation on early-LTP as a confound. However, these studies do appear to show an effect size beyond that explained by the early-LTP component.

Data presented in this thesis adds a further dimension to this. The demonstration that increased hippocampal reactivation occurs in the time period between the initial learning and probe test can potentially explain the increased persistence of the memory beyond that arising through initial encoding. It could arise through reactivation of early-LTP mechanisms. Indeed, in the crossword maze experiments, enhanced performance in the probe test (Figure 6.1) could be viewed as evidence for an effect of dopamine on late-LTP if there was no intervening reactivation since there was no enhancement in the rate of learning. This is because, if initial memory formation was occurring with greater strength due to increased early-LTP then one might expect a faster rate of learning; (this would be evident as a sharper decline of the path length to reward across trials which could have been accommodated in these experiments given the gradual rate of learning). Importantly however, the demonstration of enhanced reactivation in the intervening rest period makes this logic unreliable. This is because the initial dopamine enhanced early-LTP could be amplified through additional activation of early-LTP mechanisms without the need for enhanced late-LTP to explain the increased memory in the probe test.

There is one additional piece of evidence for dopamine as acting to upregulate late-LTP. A possibly evolutionarily adaptive property of two stage LTP is that weakly potentiated synapses – which themselves were not sufficient to trigger upregulation of PRPs – can benefit from the capture of upregulated PRP synthesis triggered at a nearby synapse or occurring around the same time point (Frey and Morris, 1997; Redondo and Morris, 2011; Rogerson et al., 2014; Takeuchi et al., 2014). This can have the effect that superfluous details occurring around the time of an important event are remembered better due to their proximity to the event. This property has been demonstrated of dopamine mediated enhanced memory retention (Wang et al., 2010).

The findings of this thesis taken with the studies mentioned in this section suggest that dopamine action at the time of experience facilitates memory encoding by facilitating and lowering the threshold required to induce early-LTP. This plasticity in the hippocampal network

occurs in a fashion such that later during SWR events, when an excitatory signal spreads throughout the network, recently potentiated synapses are reactivated in a manner which further activates LTP strengthening the representation. Additionally, dopamine presence at the time of LTP induction during experience, enhances changes at the potentiated synapses which cause the capture of PRPs (late-LTP) also lending to an increase in the long term persistence of the underlying memory trace.

7.4 The noradrenergic system as a possible secondary source of dopamine

The observation that the noradrenergic innervation of the hippocampus is more dense than the dopaminergic innervation (in rodents), has led some to suggest noradrenergic fibres may be a potential and perhaps even a more relevant source of hippocampal dopamine release (Smith and Greene, 2012; Takeuchi et al., 2014). This assertion should be treated with caution as the current evidence is limited. In a mouse hippocampal slice preparation, amphetamine induced dopamine release from noradrenergic fibres, which was capable of acting on D1/D5 type receptors has been demonstrated (Smith and Greene, 2012). However, this is an artificial demonstration created by the presence of amphetamine. A potential mechanism through which this may occur is that amphetamine inhibits vesicular monoamine transporter 2 (VMAT2) and monoamine oxidase (MAO) function within noradrenergic fibres, preventing the timely transport of dopamine into vesicles for synthesis into noradrenalin. The resulting artificial build-up of dopamine in the cytosol may create a concentration gradient causing the reverse transport of dopamine by the norepinephrine transporter (NET), allowing it into the extracellular space where it can bind to dopamine receptors (Smith and Greene, 2012). While the demonstration that amphetamine can cause this effect provides an interesting insight into the action of the drug, it is still unclear to what extent, if at all, this can happen in the drug free brain. Furthermore, if it is demonstrated to occur, that the noradrenergic innervation is more dense than the dopaminergic innervation does not mean that it is more effective at activating dopamine receptors. Also, the relative density of the two innervations is more balanced in the cynomolgus monkey (Samson et al., 1990). Nonetheless, the noradrenergic system may provide a second source of dopamine within the hippocampus, which could mediate similar effects to those presented in this thesis through activation of dopamine receptors, and should

be investigated further. To this end, preliminary data presented by Takeuchi (2015) and colleagues indicated that optogenetic activation of the noradrenergic cells in the locus coeruleus can increase the persistence of a spatial memory.

7.5 Open questions and possible future investigations

Much is still to be understood about the extent to which reactivation is important for memory consolidation. Beyond the correlative evidence that the activity at this time reflects the previous waking experience the causal evidence to date has been provided by closed loop electrical stimulation locked to SWR onset (Ego-Stengel and Wilson, 2010; Girardeau et al., 2009). Electrical stimulation produces widespread non-specific effects on the network making the results more difficult to interpret; targeted optogenetic inhibition of principal cell firing during SWR events is one possible experiment to increase the causal evidence for SWR reactivation as important for memory stability. The demonstration in this thesis that artificially induced dopamine release produced enhanced reactivation and this ultimately increased memory persistence adds to the evidence implicating SWR reactivation as being causal to enhanced memory persistence. It is unfortunately limited by the fact that dopamine action may separately increase memory persistence and reactivation strength. Nonetheless, it is the first demonstration of artificially increased reactivation strength accompanied by increased memory persistence.

The precise means by which dopamine action at the time of experience causes the later effects on reactivation patterns, spatial representations and memory persistence require further investigation. To what extent is this explained as being mediated by stronger LTP at the time of the experience in the presence of dopamine or is it mediated by molecular pathways activated by dopamine receptors? The spatial firing properties of CA1 principal cells are broadly maintained when LTP is disrupted in CA1 pyramidal cells through specific knockout of the NMDAR1 gene in mice (McHugh et al., 1996). In these mice the same spatial representation was reinstated across repeated exposure to the same environment; however, the resulting place fields were slightly larger and less coherent. It may be revealing to investigate to what extent SWR reactivation is present in such mice and, particularly, is it stronger after exploration of a novel environment compared to a familiar environment. Similar transgenic

mice are capable of learning in the spatial reference memory water maze task but are impaired in tasks which involve discrimination of competing cues (Bannerman et al., 2012). Would optogenetic activation of hippocampal dopamine in such mice cause increased memory persistence and would this be accompanied with increased reactivation strength?

During these experiments, photostimulation was delivered during waking experience. I did not manage, in the time allotted, given all the conditions tested, to separately test if photostimulation delivered during sleep had an effect on memory persistence or indeed reactivation in the following sleep. Photoactivation of the dopaminergic innervation of the hippocampus during sleep could act in a similar fashion to that during waking experience, activating the same pathways resulting in upregulation of the persistence of activity occurring during the stimulation time window. Given that firing activity during sleep reflects that in previous waking experience, it could serve to enhance the persistence of the memory for the waking experience. The effect would perhaps be less specific, since patterns from previous waking experiences (beyond that of the immediately previous) are reactivated in a given sleep period (see Figure 6.4). This remains to be tested.

Another possible angle of investigation in relation to these experiments is to optogenetically inhibit the dopaminergic innervation of the hippocampus with ArchT (Han et al., 2011). This would allow further elucidation as to the extent to which the novelty induced increase in reactivation is solely mediated through dopaminergic signalling in the hippocampus. Systemic injection of D1/D5 receptor antagonist before exploration of a novel environment, in the presence of photoactivation of hippocampal dopamine, reduced reactivation strength below that associated with the novel environment reaching levels more close to that associated with the familiar environment (Figure 5.4, Table 5.3). This suggests that the novelty effect on hippocampal reactivation is mediated through dopamine action. However, systemic injection of dopamine receptor antagonist affects dopamine receptors throughout the CNS and body, so a more specific intervention may add additional evidence in this respect. Optogenetic silencing of the projection is not without confounds too; it would be difficult to assert full transfection of the projection and also full exposure of the CA1 with continuous laser light. Together, the same result shown separately, through pharmacological and optogenetic means, would add strength to the evidence.

Finally, it is still unclear how much of a role the activity of dopaminergic neurons plays in enhancing coupling between target brain areas. Enhanced coupling can be measured as increased gamma coherence, an increased number of cells showing correlated spiking or an increase in the strength of correlated firing between the two areas. Such an increase is taken to reflect increased information sharing and processing. The prefrontal cortex (PFC) is implicated in brain circuits associated with executive control, rule learning and working memory (Miller and Cohen, 2001; Wallis et al., 2001). It receives a large dopaminergic innervation consisting of fibres emanating from the midbrain (Björklund and Lindvall, 1984). There is increased theta frequency coherence between the hippocampus and PFC during behaviour that recruits spatial working memory requiring a rule based decision (Jones and Wilson, 2005). Indeed, phase biasing of local gamma oscillations, as well as pyramidal cell and interneuron firing in relation to hippocampal theta oscillations, has been demonstrated across numerous cortical areas (Sirota et al., 2008). Cell assemblies in the PFC that are active during times of high hippocampal-PFC theta coherence are more strongly reactivated during subsequent sleep (locked to hippocampal SWR events), in comparison to assemblies active at times of low coherence (Benchenane et al., 2010). Furthermore, local application of dopamine in the PFC produces increased hippocampal-PFC theta coherence (Benchenane et al., 2010). Does dopamine action somehow promote this coherence? Can it serve to promote the later reactivation in slow wave sleep of related associations, not just in the hippocampus but throughout the brain? Such a distributed representation would be capable of binding many types of information into a memory. This could be episodic in nature, but the representation could also share similar substrates to non-episodic declarative information, allowing similar information to be represented by similar means. Is the coordination across target brain structures promoted by the specific timed firing of dopaminergic neurons? Alternatively, is dopamine release without specific timing structure activating mechanisms within the target structures, which in turn promote the timing required for binding across the structures? To what extent are some of these functions mediated through co-release of other neurotransmitters (such as glutamate) from dopaminergic neurons? Also there is a non-dopaminergic projection from the VTA to the hippocampus (Gasbarri et al., 1994a; Gasbarri et al., 1994b), how significant is this in producing binding across structures? Fujisawa and

colleagues (2011) reported a 4 Hz LFP oscillation was present in the VTA and PFC which was phase coupled to hippocampal theta oscillation (typically 8 Hz). Local gamma oscillations and the firing of some of the cells recorded in the various structures also showed phase coupling to the oscillation. It remains for me to investigate such phenomena in the dual site (CA1 and VTA) recordings collected as part of this work. In the published studies to date, the cross area coordination was most prevalent during the working memory portion of the tasks involved. Dual site recordings taken as part of this DPhil were from animals freely exploring open fields with no particular task requirements so the degree to which cross area coupling is present remains to be determined.

7.6 Concluding remarks

Determining the network-level processes underpinning the specific stabilization of some newly-acquired engrams (while others fade) is critical for a comprehensive understanding of memory. The open field experiments demonstrated that dopaminergic activity at the time of formation of new hippocampal representations increases the subsequent off-line SWR reactivation of these representations. Such reactivation is thought to enable the incorporation of new memory engrams, especially those associated with novel and rewarded outcomes, into stable representations capable of informing future behaviour (Buzsáki, 1989; Dupret et al., 2010; Singer and Frank, 2009; Wilson and McNaughton, 1994). Accordingly, the crossword maze experiments showed that dopaminergic-enhanced reactivation prevents the degradation of learned behavioural performance while concurrently strengthening the reinstatement of the newly-acquired spatial representation. The body of work presented in this thesis thus provides novel insights into the relationship between midbrain dopaminergic neurons, encoding salient information about an environment (Cohen et al., 2012; Li et al., 2003; Lisman and Grace, 2005; Luo et al., 2011; Schultz et al., 1997), and hippocampal assemblies, providing representations of space (Moser et al., 2008; O'Keefe, 1976; Wilson and McNaughton, 1993), in modulating memory according to the value of the information to be remembered.

References

Abeles, M., and Goldstein, M.H., Jr. (1977). Multispike train analysis. Proc IEEE *65*, 762-773.

Acsády, L., Görcs, T.J., and Freund, T.F. (1996). Different populations of vasoactive intestinal polypeptide-immunoreactive interneurons are specialized to control pyramidal cells or interneurons in the hippocampus. Neuroscience *73*, 317-334.

Acsády, L., Kamondi, A., Sík, A., Freund, T., and Buzsáki, G. (1998). GABAergic Cells Are the Major Postsynaptic Targets of Mossy Fibers in the Rat Hippocampus. J Neurosci *18*, 3386-3403.

Ali, A.B., and Thomson, A.M. (1998). Facilitating pyramid to horizontal oriens-alveus interneurone inputs: dual intracellular recordings in slices of rat hippocampus. The Journal of Physiology *507*, 185-199.

Allen, K., Rawlins, J.N.P., Bannerman, D.M., and Csicsvari, J. (2012). Hippocampal Place Cells Can Encode Multiple Trial-Dependent Features through Rate Remapping. J Neurosci *32*, 14752-14766.

Alsiö, J., Nordenankar, K., Arvidsson, E., Birgner, C., Mahmoudi, S., Halbout, B., Smith, C., Fortin, G.M., Olson, L., Descarries, L.*, et al.* (2011). Enhanced Sucrose and Cocaine Self-Administration and Cue-Induced Drug Seeking after Loss of VGLUT2 in Midbrain Dopamine Neurons in Mice. J Neurosci *31*, 12593-12603.

Alvarez, P., Zola-Morgan, S., and Squire, L.R. (1994). The animal model of human amnesia: long-term memory impaired and short-term memory intact. Proc Natl Acad Sci USA *91*, 5637-5641.

Amaral, D., and Lavenex, P. (2006). Hippocampal Neuroanatomy. In The Hippocampus Book (New York, Oxford University Press).

Amaral, D.G., and Cowan, W.M. (1980). Subcortical afferents to the hippocampal formation in the monkey. J Comp Neurol *189*, 573-591.

Amaral, D.G., and Dent, J.A. (1981). Development of the mossy fibers of the dentate gyrus: I. A light and electron microscopic study of the mossy fibers and their expansions. J Comp Neurol *195*, 51-86.

Amaral, D.G., Dolorfo, C., and Alvarez-Royo, P. (1991). Organization of CA1 projections to the subiculum: A PHA-L analysis in the rat. Hippocampus *1*, 415-435.

Andersen, P., Bliss, T.V.P., and Skrede, K.K. (1971). Lamellar organization of hippocampal excitatory pathways. Experimental Brain Research *13*, 222-238.

Andersen, P., Morris, R., Amaral, D., Bliss, T., and O'Keefe, J. (2006). The Hippocampus Book (New York, Oxford University Press).

Bäckman, C.M., Malik, N., Zhang, Y., Shan, L., Grinberg, A., Hoffer, B.J., Westphal, H., and Tomac, A.C. (2006). Characterization of a mouse strain expressing Cre recombinase from the 3' untranslated region of the dopamine transporter locus. Genesis *44*, 383-390.

Bannerman, D.M., Bus, T., Taylor, A., Sanderson, D.J., Schwarz, I., Jensen, V., Hvalby, O., Rawlins, J.N.P., Seeburg, P.H., and Sprengel, R. (2012). Dissecting spatial knowledge from spatial choice by hippocampal NMDA receptor deletion. Nat Neurosci *15*, 1153-1159.

Bannerman, D.M., Rawlins, J.N.P., McHugh, S.B., Deacon, R.M.J., Yee, B.K., Bast, T., Zhang, W.N., Pothuizen, H.H.J., and Feldon, J. (2004). Regional dissociations within the hippocampus—memory and anxiety. Neuroscience & Biobehavioral Reviews *28*, 273-283.

Bannerman, D.M., Sprengel, R., Sanderson, D.J., McHugh, S.B., Rawlins, J.N.P., Monyer, H., and Seeburg, P.H. (2014). Hippocampal synaptic plasticity, spatial memory and anxiety. Nat Rev Neurosci *15*, 181-192.

Beason-Held, L.L., Rosene, D.L., Killiany, R.J., and Moss, M.B. (1999). Hippocampal formation lesions produce memory impairment in the rhesus monkey. Hippocampus *9*, 562-574.

Benchenane, K., Peyrache, A., Khamassi, M., Tierney, P.L., Gioanni, Y., Battaglia, F.P., and Wiener, S.I. (2010). Coherent Theta Oscillations and Reorganization of Spike Timing in the Hippocampal- Prefrontal Network upon Learning. Neuron *66*, 921-936.

Bentivoglio, M., and Morelli, M. (2005). Chapter I The organization and circuits of mesencephalic dopaminergic neurons and the distribution of dopamine receptors in the brain. In Handbook of Chemical Neuroanatomy, S.B. Dunnett, M. Bentivoglio, A. Björklund, and T. Hökfelt, eds. (Elsevier), pp. 1-107.

Berger, B., Gaspar, P., and Verney, C. (1991). Dopaminergic innervation of the cerebral cortex: unexpected differences between rodents and primates. Trends Neurosci *14*, 21-27.

Bertler, Å., and Rosengren, E. (1959). Occurrence and distribution of dopamine in brain and other tissues. Experientia *15*, 10-11.

Bethus, I., Tse, D., and Morris, R.G.M. (2010). Dopamine and Memory: Modulation of the Persistence of Memory for Novel Hippocampal NMDA Receptor-Dependent Paired Associates. J Neurosci *30*, 1610-1618.

Bezaire, M.J., and Soltesz, I. (2013). Quantitative assessment of CA1 local circuits: Knowledge base for interneuron-pyramidal cell connectivity. Hippocampus *23*, 751-785.

Björklund, A., and Dunnett, S.B. (2007a). Dopamine neuron systems in the brain: an update. Trends Neurosci *30*, 194-202.

Björklund, A., and Dunnett, S.B. (2007b). Fifty years of dopamine research. Trends Neurosci *30*, 185-187.

Björklund, A., and Lindvall, O. (1984). Chapter III Dopamine-containing systems in the CNS. In Handbook of Chemical Neuroanatomy, Volume 2: Classical Transmitters in the CNS, Part I, A. Björklund, and T. Hökfelt, eds. (Elsevier), pp. 55-122.

Blackstad, T.W., Brink, K., Hem, J., and June, B. (1970). Distribution of hippocampal mossy fibers in the rat. An experimental study with silver impregnation methods. J Comp Neurol *138*, 433-449.

Bland, B.H. (1986). The physiology and pharmacology of hippocampal formation theta rhythms. Progress in Neurobiology *26*, 1-54.

Bliss, T.V.P., and Collingridge, G.L. (1993). A synaptic model of memory: long-term potentiation in the hippocampus. Nature *361*, 31-39.

Bliss, T.V.P., and Lømo, T. (1973). Long-lasting potentiation of synaptic transmission in the dentate area of the anaesthetized rabbit following stimulation of the perforant path. The Journal of Physiology *232*, 331-356.

Boehm, S., and Betz, H. (1997). Somatostatin Inhibits Excitatory Transmission at Rat Hippocampal Synapses via Presynaptic Receptors. J Neurosci *17*, 4066-4075.

Brankačk, J., Stewart, M., and E. Fox, S. (1993). Current source density analysis of the hippocampal theta rhythm: associated sustained potentials and candidate synaptic generators. Brain Res *615*, 310-327.

Brown, E.N., Frank, L.M., Tang, D., Quirk, M.C., and Wilson, M.A. (1998). A Statistical Paradigm for Neural Spike Train Decoding Applied to Position Prediction from Ensemble Firing Patterns of Rat Hippocampal Place Cells. J Neurosci *18*, 7411-7425.

Bunzeck, N., and Düzel, E. (2006). Absolute Coding of Stimulus Novelty in the Human Substantia Nigra/VTA. Neuron *51*, 369-379.

Burwell, R.D., and Amaral, D.G. (1998a). Cortical afferents of the perirhinal, postrhinal, and entorhinal cortices of the rat. J Comp Neurol *398*, 179-205.

Burwell, R.D., and Amaral, D.G. (1998b). Perirhinal and postrhinal cortices of the rat: Interconnectivity and connections with the entorhinal cortex. J Comp Neurol *391*, 293-321.

Burwell, R.D., Witter, M.P., and Amaral, D.G. (1995). Perirhinal and postrhinal cortices of the rat: A review of the neuroanatomical literature and comparison with findings from the monkey brain. Hippocampus *5*, 390-408.

Buzsáki, G. (1986). Hippocampal sharp waves: Their origin and significance. Brain Res *398*, 242-252.

Buzsáki, G. (1989). Two-stage model of memory trace formation: A role for “noisy” brain states. Neuroscience *31*, 551-570.

Buzsáki, G. (2002). Theta Oscillations in the Hippocampus. Neuron *33*, 325-340.

Buzsáki, G. (2006). Rhythms of the Brain (New York, Oxford University Press).

Buzsáki, G., Anastassiou, C.A., and Koch, C. (2012). The origin of extracellular fields and currents — EEG, ECoG, LFP and spikes. Nat Rev Neurosci *13*, 407-420.

Buzsáki, G., Buhl, D.L., Harris, K.D., Csicsvari, J., Czéh, B., and Morozov, A. (2003). Hippocampal network patterns of activity in the mouse. Neuroscience *116*, 201-211.

Buzsáki, G., Horvath, Z., Urioste, R., Hetke, J., and Wise, K. (1992). High-frequency network oscillation in the hippocampus. Science *256*, 1025-1027.

Buzsáki, G., Lai-Wo S, L., and Vanderwolf, C.H. (1983). Cellular bases of hippocampal EEG in the behaving rat. Brain Research Reviews *6*, 139-171.

Caballero-Bleda, M., and Witter, M.P. (1993). Regional and laminar organization of projections from the presubiculum and parasubiculum to the entorhinal cortex: An anterograde tracing study in the rat. J Comp Neurol *328*, 115-129.

Cajal, R.y. (1909). Histologie du système nerveux de l'homme & des vertébrés, Vol 2 (Paris).

Cajal, S.R. (1893). Estructura del asta de Ammon y fascia dentata (tip. de Fortanet).

Canto, C.B., Wouterlood, F.G., and Witter, M.P. (2008). What Does the Anatomical Organization of the Entorhinal Cortex Tell Us? Neural Plasticity *2008*, 18.

Carlsson, A. (1959). The occurrence, distribution and physiological role of catecholamines in the nervous system. Pharmacological Reviews *11*, 490-493.

Carlsson, A., Falck, B., and Hillarp, N.A. (1962). Cellular localization of brain monoamines. Acta physiologica Scandinavica Supplementum *56*, 1-28.

Carlsson, A., Lindqvist, M., Magnusson, T., and Waldeck, B. (1958). On the Presence of 3-Hydroxytyramine in Brain. Science *127*, 471.

Carlsson, A., Lindqvist, M., and Magnusson, T.O.R. (1957). 3,4-Dihydroxyphenylalanine and 5-Hydroxytryptophan as Reserpine Antagonists. Nature *180*, 1200-1200.

Carr, M.F., Jadhav, S.P., and Frank, L.M. (2011). Hippocampal replay in the awake state: a potential substrate for memory consolidation and retrieval. Nat Neurosci *14*, 147-153.

Carr, Margaret F., Karlsson, Mattias P., and Frank, Loren M. (2012). Transient Slow Gamma Synchrony Underlies Hippocampal Memory Replay. Neuron *75*, 700-713.

Cenquizca, L.A., and Swanson, L.W. (2007). Spatial organization of direct hippocampal field CA1 axonal projections to the rest of the cerebral cortex. Brain Research Reviews *56*, 1-26.

Cetin, A., Komai, S., Eliava, M., Seeburg, P.H., and Osten, P. (2007). Stereotaxic gene delivery in the rodent brain. Nat Protoc *1*, 3166-3173.

Chrobak, J.J., and Buzsáki, G. (1996). High-Frequency Oscillations in the Output Networks of the Hippocampal–Entorhinal Axis of the Freely Behaving Rat. J Neurosci *16*, 3056-3066.

Chrobak, J.J., and Buzsáki, G. (1998). Operational Dynamics in the Hippocampal-entorhinal Axis. Neuroscience & Biobehavioral Reviews *22*, 303-310.

Chuhma, N., Choi, W.Y., Mingote, S., and Rayport, S. (2009). Dopamine neuron glutamate cotransmission: frequency-dependent modulation in the mesoventromedial projection. Neuroscience *164*, 1068-1083.

Chuhma, N., Zhang, H., Masson, J., Zhuang, X., Sulzer, D., Hen, R., and Rayport, S. (2004). Dopamine Neurons Mediate a Fast Excitatory Signal via Their Glutamatergic Synapses. J Neurosci *24*, 972-981.

Chung, C.Y., Seo, H., Sonntag, K.C., Brooks, A., Lin, L., and Isacson, O. (2005). Cell type-specific gene expression of midbrain dopaminergic neurons reveals molecules involved in their vulnerability and protection. Human Molecular Genetics *14*, 1709-1725.

Ciliax, B.J., Nash, N., Heilman, C., Sunahara, R., Hartney, A., Tiberi, M., Rye, D.B., Caron, M.G., Niznik, H.B., and Levey, A.I. (2000). Dopamine D5 receptor immunolocalization in rat and monkey brain. Synapse *37*, 125-145.

Claiborne, B.J., Amaral, D.G., and Cowan, W.M. (1986). A light and electron microscopic analysis of the mossy fibers of the rat dentate gyrus. J Comp Neurol *246*, 435-458.

Clemens, Z., Mölle, M., Erőss, L., Barsi, P., Halász, P., and Born, J. (2007). Temporal coupling of parahippocampal ripples, sleep spindles and slow oscillations in humans. Brain *130*, 2868-2878.

Clemens, Z., Mölle, M., Erőss, L., Jakus, R., Rásonyi, G., Halász, P., and Born, J. (2011). Fine-tuned coupling between human parahippocampal ripples and sleep spindles. European Journal of Neuroscience *33*, 511-520.

Cohen, J.Y., Haesler, S., Vong, L., Lowell, B.B., and Uchida, N. (2012). Neuron-type-specific signals for reward and punishment in the ventral tegmental area. Nature *482*, 85-88.

Collingridge, G.L., Kehl, S.J., and McLennan, H. (1983). Excitatory amino acids in synaptic transmission in the Schaffer collateral-commissural pathway of the rat hippocampus. The Journal of Physiology *334*, 33-46.

Colmers, W.F., Lukowiak, K., and Pittman, Q.J. (1985). Neuropeptide Y reduces orthodromically evoked population spike in rat hippocampal CA1 by a possibly presynaptic mechanism. Brain Res *346*, 404-408.

Corkin, S. (1968). Acquisition of motor skill after bilateral medial temporal-lobe excision. Neuropsychologia *6*, 255-265.

Corkin, S., Amaral, D.G., González, R.G., Johnson, K.A., and Hyman, B.T. (1997). H. M.'s Medial Temporal Lobe Lesion: Findings from Magnetic Resonance Imaging. J Neurosci *17*, 3964-3979.

Cotzias, G.C., Van Woert, M.H., and Schiffer, L.M. (1967). Aromatic Amino Acids and Modification of Parkinsonism. New England Journal of Medicine *276*, 374-379.

Csicsvari, J., Hirase, H., Czurkó, A., Mamiya, A., and Buzsáki, G. (1999). Oscillatory Coupling of Hippocampal Pyramidal Cells and Interneurons in the Behaving Rat. J Neurosci *19*, 274-287.

Csicsvari, J., Hirase, H., Mamiya, A., and Buzsáki, G. (2000). Ensemble Patterns of Hippocampal CA3-CA1 Neurons during Sharp Wave-Associated Population Events. Neuron *28*, 585-594.

Csicsvari, J., Jamieson, B., Wise, K.D., and Buzsáki, G. (2003). Mechanisms of Gamma Oscillations in the Hippocampus of the Behaving Rat. Neuron *37*, 311-322.

Dahlstroem, A., and Fuxe, K. (1964). Evidence for the existence of monoamine-containing neurons in the central nervous system. I. Demonstration of monoamines in the cell bodies of brain stem neurons. Acta physiologica Scandinavica Supplementum, SUPPL 232:231-255.

Davidson, T.J., Kloosterman, F., and Wilson, M.A. (2009). Hippocampal Replay of Extended Experience. Neuron *63*, 497-507.

Deuchars, J., and Thomson, A.M. (1996). CA1 pyramid-pyramid connections in rat hippocampus in vitro: Dual intracellular recordings with biocytin filling. Neuroscience *74*, 1009-1018.

Diba, K., and Buzsaki, G. (2007). Forward and reverse hippocampal place-cell sequences during ripples. Nat Neurosci *10*, 1241-1242.

Double, K.L., Reyes, S., Werry, E.L., and Halliday, G.M. (2010). Selective cell death in neurodegeneration: Why are some neurons spared in vulnerable regions? Progress in Neurobiology *92*, 316-329.

Draguhn, A., Traub, R.D., Schmitz, D., and Jefferys, J.G.R. (1998). Electrical coupling underlies high-frequency oscillations in the hippocampus in vitro. Nature *394*, 189-192.

Dupret, D., O'Neill, J., Pleydell-Bouverie, B., and Csicsvari, J. (2010). The reorganization and reactivation of hippocampal maps predict spatial memory performance. Nat Neurosci *13*, 995-1002.

Dupret, D., O'Neill, J., and Csicsvari, J. (2013). Dynamic Reconfiguration of Hippocampal Interneuron Circuits during Spatial Learning. Neuron *78*, 166-180.

Ego-Stengel, V., and Wilson, M.A. (2010). Disruption of ripple-associated hippocampal activity during rest impairs spatial learning in the rat. Hippocampus *20*, 1-10.

Ehringer, H., and Hornykiewicz, O. (1960). Verteilung Von Noradrenalin Und Dopamin (3-Hydroxytyramin) Im Gehirn Des Menschen Und Ihr Verhalten Bei Erkrankungen Des Extrapyramidalen Systems. Klin Wochenschr *38*, 1236-1239.

Eichenbaum, H., and Cohen, Neal J. (2014). Can We Reconcile the Declarative Memory and Spatial Navigation Views on Hippocampal Function? Neuron *83*, 764-770.

Ellender, T.J., Nissen, W., Colgin, L.L., Mann, E.O., and Paulsen, O. (2010). Priming of Hippocampal Population Bursts by Individual Perisomatic-Targeting Interneurons. J Neurosci *30*, 5979-5991.

Falck, B., Hillarp, N.-Å., Thieme, G., and Torp, A. (1962). Fluorescence of catechol amines and related compounds condensed with formaldehyde. Journal of Histochemistry & Cytochemistry *10*, 348-354.

Fallon, J.H., and Loughlin, S.E. (1982). Monoamine innervation of the forebrain: Collateralization. Brain Research Bulletin *9*, 295-307.

Fallon, J.H., and Moore, R.Y. (1978). Catecholamine innervation of the basal forebrain IV. Topography of the dopamine projection to the basal forebrain and neostriatum. J Comp Neurol *180*, 545-579.

Fell, J., Klaver, P., Lehnertz, K., Grunwald, T., Schaller, C., Elger, C.E., and Fernandez, G. (2001). Human memory formation is accompanied by rhinal-hippocampal coupling and decoupling. Nat Neurosci *4*, 1259-1264.

Felleman, D.J., and Van Essen, D.C. (1991). Distributed Hierarchical Processing in the Primate Cerebral Cortex. Cerebral Cortex *1*, 1-47.

Ferbinteanu, J., and Shapiro, M.L. (2003). Prospective and Retrospective Memory Coding in the Hippocampus. Neuron *40*, 1227-1239.

Ferraguti, F., Klausberger, T., Cobden, P., Baude, A., Roberts, J.D.B., Szucs, P., Kinoshita, A., Shigemoto, R., Somogyi, P., and Dalezios, Y. (2005). Metabotropic Glutamate Receptor 8-Expressing Nerve Terminals Target Subsets of GABAergic Neurons in the Hippocampus. J Neurosci *25*, 10520-10536.

Fortin, G.M., Bourque, M.-J., Mendez, J.A., Leo, D., Nordenankar, K., Birgner, C., Arvidsson, E., Rymar, V.V., Bérubé-Carrière, N., Claveau, A.-M*., et al.* (2012). Glutamate Corelease Promotes Growth and Survival of Midbrain Dopamine Neurons. J Neurosci *32*, 17477-17491.

Foster, D.J., and Wilson, M.A. (2006). Reverse replay of behavioural sequences in hippocampal place cells during the awake state. Nature *440*, 680-683.

Frank, L.M., Brown, E.N., and Wilson, M. (2000). Trajectory Encoding in the Hippocampus and Entorhinal Cortex. Neuron *27*, 169-178.

Frank, L.M., Stanley, G.B., and Brown, E.N. (2004). Hippocampal Plasticity across Multiple Days of Exposure to Novel Environments. J Neurosci *24*, 7681-7689.

Franklin, K.B.J., and Paxinos, G. (2008). The mouse brain in stereotaxic coordinates (Academic Press).

Fremeau, R.T., Duncan, G.E., Fornaretto, M.G., Dearry, A., Gingrich, J.A., Breese, G.R., and Caron, M.G. (1991). Localization of D1 dopamine receptor mRNA in brain supports a role in cognitive, affective, and neuroendocrine aspects of dopaminergic neurotransmission. Proc Natl Acad Sci USA *88*, 3772-3776.

Freund, T.F., and Antal, M. (1988). GABA-containing neurons in the septum control inhibitory interneurons in the hippocampus. Nature *336*, 170-173.

Frey, U., Frey, S., Schollmeier, F., and Krug, M. (1996). Influence of actinomycin D, a RNA synthesis inhibitor, on long-term potentiation in rat hippocampal neurons in vivo and in vitro. The Journal of Physiology *490*, 703-711.

Frey, U., Matthies, H., Reymann, K.G., and Matthies, H. (1991). The effect of dopaminergic D1 receptor blockade during tetanization on the expression of long-term potentiation in the rat CA1 region in vitro. Neurosci Lett *129*, 111-114.

Frey, U., and Morris, R.G.M. (1997). Synaptic tagging and long-term potentiation. Nature *385*, 533-536.

Fries, P., Reynolds, J.H., Rorie, A.E., and Desimone, R. (2001). Modulation of Oscillatory Neuronal Synchronization by Selective Visual Attention. Science *291*, 1560-1563.

Fu, Y., Yuan, Y., Halliday, G., Rusznák, Z., Watson, C., and Paxinos, G. (2012). A cytoarchitectonic and chemoarchitectonic analysis of the dopamine cell groups in the substantia nigra, ventral tegmental area, and retrorubral field in the mouse. Brain Struct Funct *217*, 591-612.

Fuchs, H., and Hauber, W. (2004). Dopaminergic innervation of the rat globus pallidus characterized by microdialysis and immunohistochemistry. Experimental Brain Research *154*, 66-75.

Fuentealba, P., Begum, R., Capogna, M., Jinno, S., Márton, L.F., Csicsvari, J., Thomson, A., Somogyi, P., and Klausberger, T. (2008). Ivy Cells: A Population of Nitric-Oxide-Producing, Slow-Spiking GABAergic Neurons and Their Involvement in Hippocampal Network Activity. Neuron *57*, 917-929.

Fujisawa, S., and Buzsáki, G. (2011). A 4 Hz Oscillation Adaptively Synchronizes Prefrontal, VTA, and Hippocampal Activities. Neuron *72*, 153-165.

Gaarskjaer, F.B. (1978). Organization of the mossy fiber system of the rat studied in extended hippocampi. II. Experimental analysis of fiber distribution with silver impregnation methods. J Comp Neurol *178*, 73-88.

Gangarossa, G., Longueville, S., De Bundel, D., Perroy, J., Hervé, D., Girault, J.-A., and Valjent, E. (2012). Characterization of dopamine D1 and D2 receptor-expressing neurons in the mouse hippocampus. Hippocampus, n/a-n/a.

García-Cabezas, M.Á., Martínez-Sánchez, P., Sánchez-González, M.Á., Garzón, M., and Cavada, C. (2009). Dopamine Innervation in the Thalamus: Monkey versus Rat. Cerebral Cortex *19*, 424-434.

Gasbarri, A., Packard, M.G., Campana, E., and Pacitti, C. (1994a). Anterograde and retrograde tracing of projections from the ventral tegmental area to the hippocampal formation in the rat. Brain Research Bulletin *33*, 445-452.

Gasbarri, A., Packard, M.G., Sulli, A., Pacitti, C., Innocenzi, R., and Perciavalle, V. (1996). The projections of the retrorubral field A8 to the hippocampal formation in the rat. Experimental Brain Research *112*, 244-252.

Gasbarri, A., Verney, C., Innocenzi, R., Campana, E., and Pacitti, C. (1994b). Mesolimbic dopaminergic neurons innervating the hippocampal formation in the rat: a combined retrograde tracing and immunohistochemical study. Brain Res *668*, 71-79.

Gauthier, J., Parent, M., Lévesque, M., and Parent, A. (1999). The axonal arborization of single nigrostriatal neurons in rats. Brain Res *834*, 228-232.

Girardeau, G., Benchenane, K., Wiener, S.I., Buzsáki, G., and Zugaro, M.B. (2009). Selective suppression of hippocampal ripples impairs spatial memory. Nat Neurosci *12*, 1222-1223.

Goldsmith, S.K., and Joyce, J.N. (1994). Dopamine D2 receptor expression in hippocampus and parahippocampal cortex of rat, cat, and human in relation to tyrosine hydroxylase-immunoreactive fibers. Hippocampus *4*, 354-373.

Grace, A., and Bunney, B. (1984a). The control of firing pattern in nigral dopamine neurons: burst firing. J Neurosci *4*, 2877-2890.

Grace, A., and Bunney, B. (1984b). The control of firing pattern in nigral dopamine neurons: single spike firing. J Neurosci *4*, 2866-2876.

Gray, C. (1994). Synchronous oscillations in neuronal systems: Mechanisms and functions. J Comput Neurosci *1*, 11-38.

Gray, C.M., Maldonado, P.E., Wilson, M., and McNaughton, B. (1995). Tetrodes markedly improve the reliability and yield of multiple single-unit isolation from multi-unit recordings in cat striate cortex. Journal of Neuroscience Methods *63*, 43-54.

Green, J.D., and Arduini, A.A. (1954). Hippocampal electrical activity in arousal. J Neurophysiol *17*, 533-557.

Gulyás, A.I., Hájos, N., and Freund, T.F. (1996). Interneurons Containing Calretinin Are Specialized to Control Other Interneurons in the Rat Hippocampus. J Neurosci *16*, 3397-3411.

Gulyás, A.I., Hájos, N., Katona, I., and Freund, T.F. (2003). Interneurons are the local targets of hippocampal inhibitory cells which project to the medial septum. European Journal of Neuroscience *17*, 1861-1872.

Halliday, G.M., and Törk, I. (1986). Comparative anatomy of the ventromedial mesencephalic tegmentum in the rat, cat, monkey and human. J Comp Neurol *252*, 423-445.

Hampson, R.E., Heyser, C.J., and Deadwyler, S.A. (1993). Hippocampal cell firing correlates of delayed-match-to-sample performance in the rat. Behavioral Neuroscience *107*, 715-739.

Han, X., Chow, B.Y., Zhou, H., Klapoetke, N.C., Chuong, A., Rajimehr, R., Yang, A., Baratta, M.V., Winkle, J., Desimone, R*., et al.* (2011). A high-light sensitivity optical neural silencer: development, and application to optogenetic control of nonhuman primate cortex. Frontiers in Systems Neuroscience *5*.

Harris, K.D., Csicsvari, J., Hirase, H., Dragoi, G., and Buzsaki, G. (2003). Organization of cell assemblies in the hippocampus. Nature *424*, 552-556.

Harris, K.D., Henze, D.A., Csicsvari, J., Hirase, H., and Buzsáki, G. (2000). Accuracy of Tetrode Spike Separation as Determined by Simultaneous Intracellular and Extracellular Measurements. J Neurophysiol *84*, 401-414.

Harris, K.D., Hirase, H., Leinekugel, X., Henze, D.A., and Buzsáki, G. (2001). Temporal Interaction between Single Spikes and Complex Spike Bursts in Hippocampal Pyramidal Cells. Neuron *32*, 141-149.

Hassani, O.-K., François, C., Yelnik, J., and Féger, J. (1997). Evidence for a dopaminergic innervation of the subthalamic nucleus in the rat. Brain Res *749*, 88-94.

Hasselmo, M.E., and Bower, J.M. (1993). Acetylcholine and memory. Trends Neurosci *16*, 218-222.

Hebb, D.O. (1949). The organization of behavior: a neuropsychological theory (New York, Wiley).

Hill, A.J. (1978). First occurrence of hippocampal spatial firing in a new environment. Exp Neurol *62*, 282-297.

Hnasko, T.S., Chuhma, N., Zhang, H., Goh, G.Y., Sulzer, D., Palmiter, R.D., Rayport, S., and Edwards, R.H. (2010). Vesicular Glutamate Transport Promotes Dopamine Storage and Glutamate Corelease In Vivo. Neuron *65*, 643-656.

Hnasko, T.S., Hjelmstad, G.O., Fields, H.L., and Edwards, R.H. (2012). Ventral Tegmental Area Glutamate Neurons: Electrophysiological Properties and Projections. J Neurosci *32*, 15076-15085.

Höglinger, G.U., Arias-Carrión, O., Ipach, B., and Oertel, W.H. (2014). Origin of the dopaminergic innervation of adult neurogenic areas. Journal of Comparative Neurology *522*, 2336-2348.

Hoglinger, G.U., Rizk, P., Muriel, M.P., Duyckaerts, C., Oertel, W.H., Caille, I., and Hirsch, E.C. (2004). Dopamine depletion impairs precursor cell proliferation in Parkinson disease. Nat Neurosci *7*, 726-735.

Hok, V., Lenck-Santini, P.-P., Roux, S., Save, E., Muller, R.U., and Poucet, B. (2007). Goal-Related Activity in Hippocampal Place Cells. J Neurosci *27*, 472-482.

Hökfelt, T., Martensson, R., Björklund, A., Kleinau, S., and Goldstein, M. (1984). Chapter VI Distributional maps of tyrosine hydroxylase-immunoreactive neurons in the rat brain. In Handbook of Chemical Neuroanatomy, Volume 2: Classical Transmitters in the CNS, Part I, A. Björklund, and T. Hökfelt, eds. (Elsevier), pp. 277-379.

Hollup, S.A., Molden, S., Donnett, J.G., Moser, M.-B., and Moser, E.I. (2001). Accumulation of Hippocampal Place Fields at the Goal Location in an Annular Watermaze Task. J Neurosci *21*, 1635-1644.

Holt, G.R., Softky, W.R., Koch, C., and Douglas, R.J. (1996). Comparison of discharge variability in vitro and in vivo in cat visual cortex neurons. J Neurophysiol *75*, 1806-1814.

Igarashi, K.M., Lu, L., Colgin, L.L., Moser, M.-B., and Moser, E.I. (2014). Coordination of entorhinal-hippocampal ensemble activity during associative learning. Nature *510*, 143-147.

Iordanova, M.D., Westbrook, R.F., and Killcross, A.S. (2006). Dopamine activity in the nucleus accumbens modulates blocking in fear conditioning. European Journal of Neuroscience *24*, 3265-3270.

Ishikawa, K., Ott, T., and McGaugh, J.L. (1982). Evidence for dopamine as a transmitter in dorsal hippocampus. Brain Res *232*, 222-226.

Ishizuka, N., Weber, J., and Amaral, D.G. (1990). Organization of intrahippocampal projections originating from CA3 pyramidal cells in the rat. J Comp Neurol *295*, 580-623.

Isomura, Y., Sirota, A., Özen, S., Montgomery, S., Mizuseki, K., Henze, D.A., and Buzsáki, G. (2006). Integration and Segregation of Activity in Entorhinal-Hippocampal Subregions by Neocortical Slow Oscillations. Neuron *52*, 871-882.

Iversen, L., Iversen, S., Dunnett, S., and Bjorklund, A. (2009). Dopamine Handbook (New York, Oxford University Press).

Jackson, J.C., Johnson, A., and Redish, A.D. (2006). Hippocampal Sharp Waves and Reactivation during Awake States Depend on Repeated Sequential Experience. J Neurosci *26*, 12415-12426.

Jinno, S., Klausberger, T., Marton, L.F., Dalezios, Y., Roberts, J.D.B., Fuentealba, P., Bushong, E.A., Henze, D., Buzsáki, G., and Somogyi, P. (2007). Neuronal Diversity in GABAergic Long-Range Projections from the Hippocampus. J Neurosci *27*, 8790-8804.

Johnson, A., and Redish, A.D. (2007). Neural Ensembles in CA3 Transiently Encode Paths Forward of the Animal at a Decision Point. J Neurosci *27*, 12176-12189.

Jones, M.W., and Wilson, M.A. (2005). Theta Rhythms Coordinate Hippocampal–Prefrontal Interactions in a Spatial Memory Task. PLoS Biol *3*, e402.

Joyce, M.P., and Rayport, S. (2000). Mesoaccumbens dopamine neuron synapses reconstructed in vitro are glutamatergic. Neuroscience *99*, 445-456.

Karlsson, M.P., and Frank, L.M. (2009). Awake replay of remote experiences in the hippocampus. Nat Neurosci *12*, 913-918.

Katona, L., Lapray, D., Viney, Tim J., Oulhaj, A., Borhegyi, Z., Micklem, Benjamin R., Klausberger, T., and Somogyi, P. (2014). Sleep and Movement Differentiates Actions of Two Types of Somatostatin-Expressing GABAergic Interneuron in Rat Hippocampus. Neuron *82*, 872-886.

Kentros, C.G., Agnihotri, N.T., Streater, S., Hawkins, R.D., and Kandel, E.R. (2004). Increased Attention to Spatial Context Increases Both Place Field Stability and Spatial Memory. Neuron *42*, 283-295.

Kepecs, A., and Fishell, G. (2014). Interneuron cell types are fit to function. Nature *505*, 318-326.

Kirwan, C.B., Bayley, P.J., Galván, V.V., and Squire, L.R. (2008). Detailed recollection of remote autobiographical memory after damage to the medial temporal lobe. Proc Natl Acad Sci USA *105*, 2676-2680.

Klausberger, T., Magill, P.J., Marton, L.F., Roberts, J.D.B., Cobden, P.M., Buzsaki, G., and Somogyi, P. (2003). Brain-state- and cell-type-specific firing of hippocampal interneurons in vivo. Nature *421*, 844-848.

Klausberger, T., Marton, L.F., Baude, A., Roberts, J.D.B., Magill, P.J., and Somogyi, P. (2004). Spike timing of dendrite-targeting bistratified cells during hippocampal network oscillations in vivo. Nat Neurosci *7*, 41-47.

Klausberger, T., Marton, L.F., O'Neill, J., Huck, J.H.J., Dalezios, Y., Fuentealba, P., Suen, W.Y., Papp, E., Kaneko, T., Watanabe, M.*, et al.* (2005). Complementary Roles of Cholecystokinin- and Parvalbumin-Expressing GABAergic Neurons in Hippocampal Network Oscillations. J Neurosci *25*, 9782-9793.

Klausberger, T., and Somogyi, P. (2008). Neuronal Diversity and Temporal Dynamics: The Unity of Hippocampal Circuit Operations. Science *321*, 53-57.

Klitenick, M.A., Deutch, A.Y., Churchill, L., and Kalivas, P.W. (1992). Topography and functional role of dopaminergic projections from the ventral mesencephalic tegmentum to the ventral pallidum. Neuroscience *50*, 371-386.

Kloosterman, F., Witter, M.P., and Van Haeften, T. (2003). Topographical and laminar organization of subicular projections to the parahippocampal region of the rat. J Comp Neurol *455*, 156-171.

Knight, R.T. (1996). Contribution of human hippocampal region to novelty detection. Nature *383*, 256-259.

Ko, D., Wilson, C.J., Lobb, C.J., and Paladini, C.A. (2012). Detection of bursts and pauses in spike trains. Journal of Neuroscience Methods *211*, 145-158.

Köhler, C. (1985). Intrinsic projections of the retrohippocampal region in the rat brain. I. The subicular complex. J Comp Neurol *236*, 504-522.

Kwon, O.B., Paredes, D., Gonzalez, C.M., Neddens, J., Hernandez, L., Vullhorst, D., and Buonanno, A. (2008). Neuregulin-1 regulates LTP at CA1 hippocampal synapses through activation of dopamine D4 receptors. Proc Natl Acad Sci USA *105*, 15587-15592.

Lak, A., Stauffer, W.R., and Schultz, W. (2014). Dopamine prediction error responses integrate subjective value from different reward dimensions. Proc Natl Acad Sci USA *111*, 2343-2348.

Lammel, S., Lim, B.K., and Malenka, R.C. (2014). Reward and aversion in a heterogeneous midbrain dopamine system. Neuropharmacology *76, Part B*, 351-359.

Lapray, D., Lasztoczi, B., Lagler, M., Viney, T.J., Katona, L., Valenti, O., Hartwich, K., Borhegyi, Z., Somogyi, P., and Klausberger, T. (2012). Behavior-dependent specialization of identified hippocampal interneurons. Nat Neurosci *15*, 1265-1271.

Lasztóczi, B., and Klausberger, T. (2014). Layer-Specific GABAergic Control of Distinct Gamma Oscillations in the CA1 Hippocampus. Neuron *81*, 1126-1139.

Laurier, L.G., O'Dowd, B.F., and George, S.R. (1994). Heterogeneous tissue-specific transcription of dopamine receptor subtype messenger RNA in rat brain. Molecular Brain Research *25*, 344-350.

Lawson, V.H., and Bland, B.H. (1993). The Role of the Septohippocampal Pathway in the Regulation of Hippocampal Field Activity and Behavior: Analysis by the Intraseptal Microinfusion of Carbachol, Atropine, and Procaine. Exp Neurol *120*, 132-144.

Lee, A.K., and Wilson, M.A. (2002). Memory of Sequential Experience in the Hippocampus during Slow Wave Sleep. Neuron *36*, 1183-1194.

Lee, M.G., Chrobak, J.J., Sik, A., Wiley, R.G., and Buzsáki, G. (1994). Hippocampal theta activity following selective lesion of the septal cholinergic systeM. Neuroscience *62*, 1033-1047.

Legendy, C.R., and Salcman, M. (1985). Bursts and recurrences of bursts in the spike trains of spontaneously active striate cortex neurons. J Neurophysiol *53*, 926-939.

Lemon, N., and Manahan-Vaughan, D. (2006). Dopamine D1/D5 Receptors Gate the Acquisition of Novel Information through Hippocampal Long-Term Potentiation and Long-Term Depression. J Neurosci *26*, 7723-7729.

Léránth, C., and Frotscher, M. (1987). Cholinergic innervation of hippocampal GAD- and somatostatin-immunoreactive commissural neurons. J Comp Neurol *261*, 33-47.

Leung, L.S., Martin, L.-A., and Stewart, D.J. (1994). Hippocampal theta rhythm in behaving rats following ibotenic acid lesion of the septum. Hippocampus *4*, 136-147.

Leutgeb, S., Leutgeb, J.K., Barnes, C.A., Moser, E.I., McNaughton, B.L., and Moser, M.-B. (2005). Independent Codes for Spatial and Episodic Memory in Hippocampal Neuronal Ensembles. Science *309*, 619-623.

Levey, A.I., Hersch, S.M., Rye, D.B., Sunahara, R.K., Niznik, H.B., Kitt, C.A., Price, D.L., Maggio, R., Brann, M.R., and Ciliax, B.J. (1993). Localization of D1 and D2 dopamine receptors in brain with subtype-specific antibodies. Proc Natl Acad Sci USA *90*, 8861-8865.

Lewis, D.A., and Sesack, S.R. (1997). Chapter VI Dopamine systems in the primate brain. In Handbook of Chemical Neuroanatomy, F.E. Bloom, A. Björklund, and T. Hökfelt, eds. (Elsevier), pp. 263-375.

Li, S.-B., Du, D., Hasan, M.T., and Köhr, G. (2014). D4 Receptor Activation Differentially Modulates Hippocampal Basal and Apical Dendritic Synapses in Freely Moving Mice. Cerebral Cortex.

Li, S., Cullen, W.K., Anwyl, R., and Rowan, M.J. (2003). Dopamine-dependent facilitation of LTP induction in hippocampal CA1 by exposure to spatial novelty. Nat Neurosci *6*, 526-531.

Li, X.G., Somogyi, P., Ylinen, A., and Buzsáki, G. (1994). The hippocampal CA3 network: An in vivo intracellular labeling study. J Comp Neurol *339*, 181-208.

Lindvall, O. (1975). Mecencephalic dopaminergic afferents to the lateral septal nucleus of the rat. Brain Res *87*, 89-95.

Lindvall, O., and Björklund, A. (1979). Dopaminergic innervation of the globus pallidus by collaterals from the nigrostriatal pathway. Brain Res *172*, 169-173.

Lindvall, O., Björklund, A., and Divac, I. (1978). Organization of catecholamine neurons projecting to the frontal cortex in the rat. Brain Res *142*, 1-24.

Lisman, J.E., and Grace, A.A. (2005). The Hippocampal-VTA Loop: Controlling the Entry of Information into Long-Term Memory. Neuron *46*, 703-713.

Lisman, J.E., and Otmakhova, N.A. (2001). Storage, recall, and novelty detection of sequences by the hippocampus: Elaborating on the SOCRATIC model to account for normal and aberrant effects of dopamine. Hippocampus *11*, 551-568.

Ljungberg, T., Apicella, P., and Schultz, W. (1992). Responses of monkey dopamine neurons during learning of behavioral reactions. J Neurophysiol *67*, 145-163.

Loughlin, S.E., and Fallon, J.H. (1984). Substantia nigra and ventral tegmental area projections to cortex: Topography and collateralization. Neuroscience *11*, 425-435.

Lovett-Barron, M., Turi, G.F., Kaifosh, P., Lee, P.H., Bolze, F., Sun, X.-H., Nicoud, J.-F., Zemelman, B.V., Sternson, S.M., and Losonczy, A. (2012). Regulation of neuronal input transformations by tunable dendritic inhibition. Nat Neurosci *15*, 423-430.

Luo, A.H., Tahsili-Fahadan, P., Wise, R.A., Lupica, C.R., and Aston-Jones, G. (2011). Linking Context with Reward: A Functional Circuit from Hippocampal CA3 to Ventral Tegmental Area. Science *333*, 353-357.

Lynch, M.A. (2004). Long-Term Potentiation and Memory. Physiological Reviews *84*, 87-136.

Ma, S.Y., Röytta, M., Rinne, J.O., Collan, Y., and Rinne, U.K. (1995). Single section and disector counts in evaluating neuronal loss from the substantia nigra in patients with Parkinson's disease. Neuropathology and Applied Neurobiology *21*, 341-343.

MacDonald, C.J., Carrow, S., Place, R., and Eichenbaum, H. (2013). Distinct Hippocampal Time Cell Sequences Represent Odor Memories in Immobilized Rats. J Neurosci *33*, 14607-14616.

MacDonald, Christopher J., Lepage, Kyle Q., Eden, Uri T., and Eichenbaum, H. (2011). Hippocampal “Time Cells” Bridge the Gap in Memory for Discontiguous Events. Neuron *71*, 737-749.

Magee, J.C., and Johnston, D. (1997). A Synaptically Controlled, Associative Signal for Hebbian Plasticity in Hippocampal Neurons. Science *275*, 209-213.

Malinow, R., and Malenka, R.C. (2002). AMPA RECEPTOR TRAFFICKING AND SYNAPTIC PLASTICITY. Annu Rev Neurosci *25*, 103-126.

Manns, J.R., Hopkins, R.O., and Squire, L.R. (2003). Semantic Memory and the Human Hippocampus. Neuron *38*, 127-133.

Manns, J.R., Howard, M.W., and Eichenbaum, H. (2007). Gradual Changes in Hippocampal Activity Support Remembering the Order of Events. Neuron *56*, 530-540.

Marín, F., Herrero, M.-T., Vyas, S., and Puelles, L. (2005). Ontogeny of tyrosine hydroxylase mRNA expression in mid- and forebrain: Neuromeric pattern and novel positive regions. Developmental Dynamics *234*, 709-717.

Marinelli, M., and McCutcheon, J.E. (2014). Heterogeneity of dopamine neuron activity across traits and states. Neuroscience *282*, 176-197.

Markus, E., Qin, Y., Leonard, B., Skaggs, W., McNaughton, B., and Barnes, C. (1995). Interactions between location and task affect the spatial and directional firing of hippocampal neurons. J Neurosci *15*, 7079-7094.

Marslen-Wilson, W.D., and Teuber, H.-L. (1975). Memory for remote events in anterograde amnesia: Recognition of public figures from newsphotographs. Neuropsychologia *13*, 353-364.

Matsuda, W., Furuta, T., Nakamura, K.C., Hioki, H., Fujiyama, F., Arai, R., and Kaneko, T. (2009). Single Nigrostriatal Dopaminergic Neurons Form Widely Spread and Highly Dense Axonal Arborizations in the Neostriatum. J Neurosci *29*, 444-453.

Matsumoto, M., and Hikosaka, O. (2009). Two types of dopamine neuron distinctly convey positive and negative motivational signals. Nature *459*, 837-841.

Maurer, A.P., Cowen, S.L., Burke, S.N., Barnes, C.A., and McNaughton, B.L. (2006). Phase Precession in Hippocampal Interneurons Showing Strong Functional Coupling to Individual Pyramidal Cells. J Neurosci *26*, 13485-13492.

McHugh, T.J., Blum, K.I., Tsien, J.Z., Tonegawa, S., and Wilson, M.A. (1996). Impaired Hippocampal Representation of Space in CA1-Specific NMDAR1 Knockout Mice. Cell *87*, 1339-1349.

McNamara, C.G., Tejero-Cantero, A., Trouche, S., Campo-Urriza, N., and Dupret, D. (2014). Dopaminergic neurons promote hippocampal reactivation and spatial memory persistence. Nat Neurosci *17*, 1658-1660.

McNaughton, B.L., O'Keefe, J., and Barnes, C.A. (1983). The stereotrode: A new technique for simultaneous isolation of several single units in the central nervous system from multiple unit records. Journal of Neuroscience Methods *8*, 391-397.

McRitchie, D.A., Hardman, C.D., and Halliday, G.M. (1996). Cytoarchitectural distribution of calcium binding proteins in midbrain dopaminergic regions of rats and humans. J Comp Neurol *364*, 121-150.

Meador-Woodruff, J.H., Mansour, A., Grandy, D.K., Damask, S.P., Civelli, O., and Watson Jr, S.J. (1992). Distribution of D5 dopamine receptor mRNA in rat brain. Neurosci Lett *145*, 209-212.

Mendez, I., Sanchez-Pernaute, R., Cooper, O., Viñuela, A., Ferrari, D., Björklund, L., Dagher, A., and Isacson, O. (2005). Cell type analysis of functional fetal dopamine cell suspension transplants in the striatum and substantia nigra of patients with Parkinson's disease. Brain *128*, 1498-1510.

Mendez, J.A., Bourque, M.-J., Bo, G.D., Bourdeau, M.L., Danik, M., Williams, S., Lacaille, J.-C., and Trudeau, L.-E. (2008). Developmental and Target-Dependent Regulation of Vesicular Glutamate Transporter Expression by Dopamine Neurons. J Neurosci *28*, 6309-6318.

Meunier, M., Bachevalier, J., Mishkin, M., and Murray, E. (1993). Effects on visual recognition of combined and separate ablations of the entorhinal and perirhinal cortex in rhesus monkeys. J Neurosci *13*, 5418-5432.

Miller, E.K., and Cohen, J.D. (2001). An integrative theory of prefrontal cortex function. Annu Rev Neurosci *24*, 167-202.

Milner, B., Corkin, S., and Teuber, H.L. (1968). Further analysis of the hippocampal amnesic syndrome: 14-year follow-up study of H.M. Neuropsychologia *6*, 215-234.

Mirenowicz, J., and Schultz, W. (1994). Importance of unpredictability for reward responses in primate dopamine neurons. J Neurophysiol *72*, 1024-1027.

Mishkin, M. (1978). Memory in monkeys severely impaired by combined but not by separate removal of amygdala and hippocampus. Nature *273*, 297-298.

Mitra, P.P., and Pesaran, B. (1999). Analysis of Dynamic Brain Imaging Data. Biophys J *76*, 691-708.

Mizuseki, K., Sirota, A., Pastalkova, E., and Buzsáki, G. (2009). Theta Oscillations Provide Temporal Windows for Local Circuit Computation in the Entorhinal-Hippocampal Loop. Neuron *64*, 267-280.

Monaco, J.D., Rao, G., Roth, E.D., and Knierim, J.J. (2014). Attentive scanning behavior drives one-trial potentiation of hippocampal place fields. Nat Neurosci *17*, 725-731.

Montagu, K.A. (1957). Catechol Compounds in Rat Tissues and in Brains of Different Animals. Nature *180*, 244-245.

Montague, P.R., Dayan, P., Person, C., and Sejnowski, T.J. (1995). Bee foraging in uncertain environments using predictive hebbian learning. Nature *377*, 725-728.

Montgomery, S.M., Betancur, M.I., and Buzsáki, G. (2009). Behavior-Dependent Coordination of Multiple Theta Dipoles in the Hippocampus. J Neurosci *29*, 1381-1394.

Morales, M., and Root, D.H. (2014). Glutamate neurons within the midbrain dopamine regions. Neuroscience *282*, 60-68.

Morris, R. (1984). Developments of a water-maze procedure for studying spatial learning in the rat. Journal of Neuroscience Methods *11*, 47-60.

Morris, R. (2006). Theories of Hippocampal Function. In The Hippocampus Book (New York, Oxford University Press), pp. 581-713.

Morris, R.G.M., Garrud, P., Rawlins, J.N.P., and O'Keefe, J. (1982). Place navigation impaired in rats with hippocampal lesions. Nature *297*, 681-683.

Morris, R.G.M., Schenk, F., Tweedie, F., and Jarrard, L.E. (1990). Ibotenate Lesions of Hippocampus and/or Subiculum: Dissociating Components of Allocentric Spatial Learning. European Journal of Neuroscience *2*, 1016-1028.

Moser, E.I., Kropff, E., and Moser, M.-B. (2008). Place Cells, Grid Cells, and the Brain's Spatial Representation System. Annu Rev Neurosci *31*, 69-89.

Moser, M.-B., Rowland, D.C., and Moser, E.I. (2015). Place Cells, Grid Cells, and Memory. Cold Spring Harbor Perspectives in Biology *7*.

Mu, Y., Zhao, C., and Gage, F.H. (2011). Dopaminergic Modulation of Cortical Inputs during Maturation of Adult-Born Dentate Granule Cells. J Neurosci *31*, 4113-4123.

Muller, R. (1996). A Quarter of a Century of Place Cells. Neuron *17*, 813-822.

Muller, R., and Kubie, J. (1987). The effects of changes in the environment on the spatial firing of hippocampal complex-spike cells. J Neurosci *7*, 1951-1968.

Muller, R., Kubie, J., and Ranck, J. (1987). Spatial firing patterns of hippocampal complex-spike cells in a fixed environment. J Neurosci *7*, 1935-1950.

Muller, R.U., and Kubie, J.L. (1989). The firing of hippocampal place cells predicts the future position of freely moving rats. J Neurosci *9*, 4101-4110.

Murray, E.A., and Mishkin, M. (1998). Object Recognition and Location Memory in Monkeys with Excitotoxic Lesions of the Amygdala and Hippocampus. J Neurosci *18*, 6568-6582.

Naber, P.A., Lopes da Silva, F.H., and Witter, M.P. (2001). Reciprocal connections between the entorhinal cortex and hippocampal fields CA1 and the subiculum are in register with the projections from CA1 to the subiculum. Hippocampus *11*, 99-104.

Nair-Roberts, R.G., Chatelain-Badie, S.D., Benson, E., White-Cooper, H., Bolam, J.P., and Ungless, M.A. (2008). Stereological estimates of dopaminergic, GABAergic and glutamatergic neurons in the ventral tegmental area, substantia nigra and retrorubral field in the rat. Neuroscience *152*, 1024-1031.

Nguyen, P., Abel, T., and Kandel, E. (1994). Requirement of a critical period of transcription for induction of a late phase of LTP. Science *265*, 1104-1107.

O'Carroll, C.M., Martin, S.J., Sandin, J., Frenguelli, B., and Morris, R.G.M. (2006). Dopaminergic modulation of the persistence of one-trial hippocampus-dependent memory. Learn Mem *13*, 760-769.

O'Keefe, J. (1976). Place units in the hippocampus of the freely moving rat. Exp Neurol *51*, 78-109.

O'Keefe, J., and Dostrovsky, J. (1971). The hippocampus as a spatial map. Preliminary evidence from unit activity in the freely-moving rat. Brain Res *34*, 171-175.

O'Keefe, J., and Nadel, L. (1978). The hippocampus as a cognitive map (Clarendon Press).

O'Keefe, J., and Recce, M.L. (1993). Phase relationship between hippocampal place units and the EEG theta rhythm. Hippocampus *3*, 317-330.

O'Keefe, J., and Speakman, A. (1987). Single unit activity in the rat hippocampus during a spatial memory task. Experimental Brain Research *68*, 1-27.

O'Mara, S.M., Commins, S., Anderson, M., and Gigg, J. (2001). The subiculum: a review of form, physiology and function. Progress in Neurobiology *64*, 129-155.

O'Neill, J., Pleydell-Bouverie, B., Dupret, D., and Csicsvari, J. (2010). Play it again: reactivation of waking experience and memory. Trends Neurosci *33*, 220-229.

O'Neill, J., Senior, T., and Csicsvari, J. (2006). Place-Selective Firing of CA1 Pyramidal Cells during Sharp Wave/Ripple Network Patterns in Exploratory Behavior. Neuron *49*, 143-155.

O'Neill, J., Senior, T.J., Allen, K., Huxter, J.R., and Csicsvari, J. (2008). Reactivation of experience-dependent cell assembly patterns in the hippocampus. Nat Neurosci *11*, 209-215.

O'Tuathaigh, C.M.P., Salum, C., Young, A.M.J., Pickering, A.D., Joseph, M.H., and Moran, P.M. (2003). The effect of amphetamine on Kamin blocking and overshadowing. Behavioural Pharmacology *14*, 315-322.

Otmakhova, N.A., and Lisman, J.E. (1996). D1/D5 Dopamine Receptor Activation Increases the Magnitude of Early Long-Term Potentiation at CA1 Hippocampal Synapses. J Neurosci *16*, 7478-7486.

Overman, W.H., Ormsby, G., and Mishkin, M. (1990). Picture recognition vs. picture discrimination learning in monkeys with medial temporal removals. Experimental Brain Research *79*, 18-24.

Overton, P.G., and Clark, D. (1997). Burst firing in midbrain dopaminergic neurons. Brain Research Reviews *25*, 312-334.

Pakkenberg, B., Møller, A., Gundersen, H.J., Mouritzen Dam, A., and Pakkenberg, H. (1991). The absolute number of nerve cells in substantia nigra in normal subjects and in patients with Parkinson's disease estimated with an unbiased stereological method. Journal of Neurology, Neurosurgery & Psychiatry *54*, 30-33.

Pan, W.-X., and McNaughton, N. (2004). The supramammillary area: its organization, functions and relationship to the hippocampus. Progress in Neurobiology *74*, 127-166.

Penfield, W., and Milner, B. (1958). Memory deficit produced by bilateral lesions in the hippocampal zone. AMA Archives of Neurology & Psychiatry *79*, 475-497.

Perez, F., and Granger, B.E. (2007). IPython: A System for Interactive Scientific Computing. Computing in Science & Engineering *9*, 21-29.

Petsche, H., Stumpf, C., and Gogolak, G. (1962). The significance of the rabbit's septum as a relay station between the midbrain and the hippocampus I. The control of hippocampus arousal activity by the septum cells. Electroencephalography and Clinical Neurophysiology *14*, 202-211.

Phillipson, O.T. (1979a). The cytoarchitecture of the interfascicular nucleus and ventral tegmental area of tsai in the rat. J Comp Neurol *187*, 85-98.

Phillipson, O.T. (1979b). A Golgi study of the ventral tegmental area of Tsai and interfascicular nucleus in the rat. J Comp Neurol *187*, 99-115.

Pinault, D. (1996). A novel single-cell staining procedure performed in vivo under electrophysiological control: morpho-functional features of juxtacellularly labeled thalamic cells and other central neurons with biocytin or Neurobiotin. Journal of Neuroscience Methods *65*, 113-136.

Price, C.J., Cauli, B., Kovacs, E.R., Kulik, A., Lambolez, B., Shigemoto, R., and Capogna, M. (2005). Neurogliaform Neurons Form a Novel Inhibitory Network in the Hippocampal CA1 Area. J Neurosci *25*, 6775-6786.

Ramon y Cajal, S. (1893). Estructura del asta de Ammon y fascia dentata. Anal Soc Espan Historia Natural, 53-114.

Ranck Jr, J.B. (1973). Studies on single neurons in dorsal hippocampal formation and septum in unrestrained rats: Part I. Behavioral correlates and firing repertoires. Exp Neurol *41*, 462-531.

Rayport, S. (2001). Glutamate is a cotransmitter in ventral midbrain dopamine neurons. Parkinsonism & Related Disorders *7*, 261-264.

Redondo, R.L., and Morris, R.G.M. (2011). Making memories last: the synaptic tagging and capture hypothesis. Nat Rev Neurosci *12*, 17-30.

Reyes, S., Fu, Y., Double, K., Thompson, L., Kirik, D., Paxinos, G., and Halliday, G.M. (2012). GIRK2 expression in dopamine neurons of the substantia nigra and ventral tegmental area. J Comp Neurol *520*, 2591-2607.

Roeper, J. (2013). Dissecting the diversity of midbrain dopamine neurons. Trends Neurosci *36*, 336-342.

Rogerson, T., Cai, D.J., Frank, A., Sano, Y., Shobe, J., Lopez-Aranda, M.F., and Silva, A.J. (2014). Synaptic tagging during memory allocation. Nat Rev Neurosci *15*, 157-169.

Romo, R., and Schultz, W. (1990). Dopamine neurons of the monkey midbrain: contingencies of responses to active touch during self-initiated arm movements. J Neurophysiol *63*, 592-606.

Rossato, J.I., Bevilaqua, L.R.M., Izquierdo, I., Medina, J.H., and Cammarota, M. (2009). Dopamine Controls Persistence of Long-Term Memory Storage. Science *325*, 1017-1020.

Royer, S., Zemelman, B.V., Losonczy, A., Kim, J., Chance, F., Magee, J.C., and Buzsaki, G. (2012). Control of timing, rate and bursts of hippocampal place cells by dendritic and somatic inhibition. Nat Neurosci *15*, 769-775.

Salat, D.H., van der Kouwe, A.J.W., Tuch, D.S., Quinn, B.T., Fischl, B., Dale, A.M., and Corkin, S. (2006). Neuroimaging H.M.: A 10-year follow-up examination. Hippocampus *16*, 936-945.

Samson, Y., Wu, J.J., Friedman, A.H., and Davis, J.N. (1990). Catecholaminergic innervation of the hippocampus in the cynomolgus monkey. J Comp Neurol *298*, 250-263.

Savasta, M., Dubois, A., and Scatton, B. (1986). Autoradiographic localization of D1 dopamine receptors in the rat brain with [3H]SCH 23390. Brain Res *375*, 291-301.

Scatton, B., Simon, H., Le Moal, M., and Bischoff, S. (1980). Origin of dopaminergic innervation of the rat hippocampal formation. Neurosci Lett *18*, 125-131.

Schein, J.C., Hunter, D.D., and Roffler-Tarlov, S. (1998). Girk2 Expression in the Ventral Midbrain, Cerebellum, and Olfactory Bulb and Its Relationship to the Murine Mutationweaver. Developmental Biology *204*, 432-450.

Schmitt, W.B., Deacon, R.M.J., Seeburg, P.H., Rawlins, J.N.P., and Bannerman, D.M. (2003). A Within-Subjects, Within-Task Demonstration of Intact Spatial Reference Memory and Impaired Spatial Working Memory in Glutamate Receptor-A-Deficient Mice. J Neurosci *23*, 3953-3959.

Schmitz, D., Schuchmann, S., Fisahn, A., Draguhn, A., Buhl, E.H., Petrasch-Parwez, E., Dermietzel, R., Heinemann, U., and Traub, R.D. (2001). Axo-Axonal Coupling: A Novel Mechanism for Ultrafast Neuronal Communication. Neuron *31*, 831-840.

Schomburg, Erik W., Fernández-Ruiz, A., Mizuseki, K., Berényi, A., Anastassiou, Costas A., Koch, C., and Buzsáki, G. (2014). Theta Phase Segregation of Input-Specific Gamma Patterns in Entorhinal-Hippocampal Networks. Neuron *84*, 470-485.

Schultz, W. (1998). Predictive Reward Signal of Dopamine Neurons. J Neurophysiol *80*, 1-27.

Schultz, W. (2007). Behavioral dopamine signals. Trends Neurosci *30*, 203-210.

Schultz, W., Dayan, P., and Montague, P.R. (1997). A Neural Substrate of Prediction and Reward. Science *275*, 1593-1599.

Scoville, W.B., and Milner, B. (1957). Loss of recent memory after bilateral hippocampal lesions. Journal of neurology, neurosurgery, and psychiatry *20*, 11-21.

Shepherd, G.M. (2004). The Synaptic Organization of the Brain, 5 edn (New York, Oxford University Press).

Siapas, A.G., Lubenov, E.V., and Wilson, M.A. (2005). Prefrontal Phase Locking to Hippocampal Theta Oscillations. Neuron *46*, 141-151.

Sik, A., Penttonen, M., Ylinen, A., and Buzsaki, G. (1995). Hippocampal CA1 interneurons: an in vivo intracellular labeling study. J Neurosci *15*, 6651-6665.

Singer, A.C., and Frank, L.M. (2009). Rewarded Outcomes Enhance Reactivation of Experience in the Hippocampus. Neuron *64*, 910-921.

Singer, W. (1993). Synchronization of Cortical Activity and its Putative Role in Information Processing and Learning. Annual Review of Physiology *55*, 349-374.

Sirota, A., Montgomery, S., Fujisawa, S., Isomura, Y., Zugaro, M., and Buzsáki, G. (2008). Entrainment of Neocortical Neurons and Gamma Oscillations by the Hippocampal Theta Rhythm. Neuron *60*, 683-697.

Skaggs, W.E., and McNaughton, B.L. (1996). Replay of Neuronal Firing Sequences in Rat Hippocampus During Sleep Following Spatial Experience. Science *271*, 1870-1873.

Skaggs, W.E., McNaughton, B.L., Wilson, M.A., and Barnes, C.A. (1996). Theta phase precession in hippocampal neuronal populations and the compression of temporal sequences. Hippocampus *6*, 149-172.

Smeets, W.J.A.J., and González, A. (2000). Catecholamine systems in the brain of vertebrates: new perspectives through a comparative approach. Brain Research Reviews *33*, 308-379.

Smidt, M.P., van Schaick, H.S.A., Lanctôt, C., Tremblay, J.J., Cox, J.J., van der Kleij, A.A.M., Wolterink, G., Drouin, J., and Burbach, J.P.H. (1997). A homeodomain gene Ptx3 has highly restricted brain expression in mesencephalic dopaminergic neurons. Proc Natl Acad Sci USA *94*, 13305-13310.

Smith, C.C., and Greene, R.W. (2012). CNS Dopamine Transmission Mediated by Noradrenergic Innervation. J Neurosci *32*, 6072-6080.

Somogyi, P., Katona, L., Klausberger, T., Lasztóczi, B., and Viney, T.J. (2013). Temporal redistribution of inhibition over neuronal subcellular domains underlies state-dependent rhythmic change of excitability in the hippocampus. Philosophical Transactions of the Royal Society of London B: Biological Sciences *369*.

Somogyi, P., Nunzi, M.G., Gorio, A., and Smith, A.D. (1983). A new type of specific interneuron in the monkey hippocampus forming synapses exclusively with the axon initial segments of pyramidal cells. Brain Res *259*, 137-142.

Spruston, N., and Johnston, D. (1992). Perforated patch-clamp analysis of the passive membrane properties of three classes of hippocampal neurons. J Neurophysiol *67*, 508-529.

Squire, L.R. (2004). Memory systems of the brain: A brief history and current perspective. Neurobiology of Learning and Memory *82*, 171-177.

Squire, L.R. (2009a). The Legacy of Patient H.M. for Neuroscience. Neuron *61*, 6-9.

Squire, L.R. (2009b). Memory and Brain Systems: 1969–2009. J Neurosci *29*, 12711-12716.

Squire, L.R., Stark, C.E.L., and Clark, R.E. (2004). The Medial Temporal Lobe. Annu Rev Neurosci *27*, 279-306.

Stamatakis, Alice M., Jennings, Joshua H., Ung, Randall L., Blair, Grace A., Weinberg, Richard J., Neve, Rachael L., Boyce, F., Mattis, J., Ramakrishnan, C., Deisseroth, K.*, et al.* (2013). A Unique Population of Ventral Tegmental Area Neurons Inhibits the Lateral Habenula to Promote Reward. Neuron *80*, 1039-1053.

Stauffer, William R., Lak, A., and Schultz, W. (2014). Dopamine Reward Prediction Error Responses Reflect Marginal Utility. Current Biology *24*, 2491-2500.

Steinberg, E.E., Keiflin, R., Boivin, J.R., Witten, I.B., Deisseroth, K., and Janak, P.H. (2013). A causal link between prediction errors, dopamine neurons and learning. Nat Neurosci *16*, 966-973.

Steinvorth, S., Levine, B., and Corkin, S. (2005). Medial temporal lobe structures are needed to re-experience remote autobiographical memories: evidence from H.M. and W.R. Neuropsychologia *43*, 479-496.

Steward, O., and Scoville, S.A. (1976). Cells of origin of entorhinal cortical afferents to the hippocampus and fascia dentata of the rat. J Comp Neurol *169*, 347-370.

Stuber, G.D., Hnasko, T.S., Britt, J.P., Edwards, R.H., and Bonci, A. (2010). Dopaminergic Terminals in the Nucleus Accumbens But Not the Dorsal Striatum Corelease Glutamate. J Neurosci *30*, 8229-8233.

Sullivan, D., Csicsvari, J., Mizuseki, K., Montgomery, S., Diba, K., and Buzsáki, G. (2011). Relationships between Hippocampal Sharp Waves, Ripples, and Fast Gamma Oscillation: Influence of Dentate and Entorhinal Cortical Activity. J Neurosci *31*, 8605-8616.

Sutton, R.S., and Barto, A.G. (1998). Reinforcement Learning: An Introduction (MIT Press).

Suzuki, W., Zola-Morgan, S., Squire, L., and Amaral, D. (1993). Lesions of the perirhinal and parahippocampal cortices in the monkey produce long-lasting memory impairment in the visual and tactual modalities. J Neurosci *13*, 2430-2451.

Swanson, L.W. (1982). The projections of the ventral tegmental area and adjacent regions: A combined fluorescent retrograde tracer and immunofluorescence study in the rat. Brain Research Bulletin *9*, 321-353.

Swanson, L.W., Wyss, J.M., and Cowan, W.M. (1978). An autoradiographic study of the organization of intrahippocampal association pathways in the rat. J Comp Neurol *181*, 681-715.

Takács, V.T., Klausberger, T., Somogyi, P., Freund, T.F., and Gulyás, A.I. (2012). Extrinsic and local glutamatergic inputs of the rat hippocampal CA1 area differentially innervate pyramidal cells and interneurons. Hippocampus *22*, 1379-1391.

Takada, M., and Hattori, T. (1987). Organization of ventral tegmental area cells projecting to the occipital cortex and forebrain in the rat. Brain Res *418*, 27-33.

Takahashi, Y.K., Roesch, M.R., Stalnaker, T.A., Haney, R.Z., Calu, D.J., Taylor, A.R., Burke, K.A., and Schoenbaum, G. (2009). The Orbitofrontal Cortex and Ventral Tegmental Area Are Necessary for Learning from Unexpected Outcomes. Neuron *62*, 269-280.

Takeuchi, T., Duszkiewicz, A., Tse, D., Spooner, P., Deisseroth, K., and Morris, R. (2015). Catecholaminergic control of initial memory consolidation in mice. . Paper presented at: British Neurosci Assoc Abstr (Edinburgh, BNA).

Takeuchi, T., Duszkiewicz, A.J., and Morris, R.G.M. (2014). The synaptic plasticity and memory hypothesis: encoding, storage and persistence. Philosophical Transactions of the Royal Society B: Biological Sciences *369*.

Tallent, M.K., and Siggins, G.R. (1997). Somatostatin Depresses Excitatory but not Inhibitory Neurotransmission in Rat CA1 Hippocampus. J Neurophysiol *78*, 3008-3018.

Thompson, L., Barraud, P., Andersson, E., Kirik, D., and Björklund, A. (2005). Identification of Dopaminergic Neurons of Nigral and Ventral Tegmental Area Subtypes in Grafts of Fetal Ventral Mesencephalon Based on Cell Morphology, Protein Expression, and Efferent Projections. J Neurosci *25*, 6467-6477.

Thompson, L.T., and Best, P.J. (1990). Long-term stability of the place-field activity of single units recorded from the dorsal hippocampus of freely behaving rats. Brain Res *509*, 299-308.

Thomson, D.J. (1982). Spectrum estimation and harmonic analysis. Proc IEEE *70*, 1055-1096.

Tobler, P.N., Dickinson, A., and Schultz, W. (2003). Coding of Predicted Reward Omission by Dopamine Neurons in a Conditioned Inhibition Paradigm. J Neurosci *23*, 10402-10410.

Tokdar, S., Xi, P., Kelly, R.C., and Kass, R.E. (2010). Detection of bursts in extracellular spike trains using hidden semi-Markov point process models. J Comput Neurosci *29*, 203-212.

Tolman, E.C. (1948). Cognitive maps in rats and men. Psychol Rev *55*, 189-208.

Traub, R.D., and Bibbig, A. (2000). A Model of High-Frequency Ripples in the Hippocampus Based on Synaptic Coupling Plus Axon–Axon Gap Junctions between Pyramidal Neurons. J Neurosci *20*, 2086-2093.

Tricoire, L., Pelkey, K.A., Erkkila, B.E., Jeffries, B.W., Yuan, X., and McBain, C.J. (2011). A Blueprint for the Spatiotemporal Origins of Mouse Hippocampal Interneuron Diversity. J Neurosci *31*, 10948-10970.

Tritsch, N.X., Ding, J.B., and Sabatini, B.L. (2012). Dopaminergic neurons inhibit striatal output through non-canonical release of GABA. Nature *490*, 262-266.

Tsai, H.-C., Zhang, F., Adamantidis, A., Stuber, G.D., Bonci, A., de Lecea, L., and Deisseroth, K. (2009). Phasic Firing in Dopaminergic Neurons Is Sufficient for Behavioral Conditioning. Science *324*, 1080-1084.

Ungless, M.A., and Grace, A.A. (2012). Are you or aren't you? Challenges associated with physiologically identifying dopamine neurons. Trends Neurosci *35*, 422-430.

Ungless, M.A., Magill, P.J., and Bolam, J.P. (2004). Uniform Inhibition of Dopamine Neurons in the Ventral Tegmental Area by Aversive Stimuli. Science *303*, 2040-2042.

van der Weide, J., Camps, M., Horn, A.S., and Palacios, J. (1987). Autoradiographic localization of dopamine D2 receptors in the rat brain using the new agonist [3H]N-0437. Neurosci Lett *83*, 259-263.

van den Pol, Anthony N. (2012). Neuropeptide Transmission in Brain Circuits. Neuron *76*, 98-115.

Vandecasteele, M., Varga, V., Berényi, A., Papp, E., Barthó, P., Venance, L., Freund, T.F., and Buzsáki, G. (2014). Optogenetic activation of septal cholinergic neurons suppresses sharp wave ripples and enhances theta oscillations in the hippocampus. Proc Natl Acad Sci USA *111*, 13535-13540.

Vanderwolf, C.H. (1969). Hippocampal electrical activity and voluntary movement in the rat. Electroencephalography and Clinical Neurophysiology *26*, 407-418.

Varga, C., Golshani, P., and Soltesz, I. (2012). Frequency-invariant temporal ordering of interneuronal discharges during hippocampal oscillations in awake mice. Proc Natl Acad Sci USA *109*, E2726-E2734.

Varga, C., Oijala, M., Lish, J., Szabo, G.G., Bezaire, M., Marchionni, I., Golshani, P., and Soltesz, I. (2014). Functional fission of parvalbumin interneuron classes during fast network events. eLife *3*.

Verney, C., Baulac, M., Berger, B., Alvarez, C., Vigny, A., and Helle, K.B. (1985). Morphological evidence for a dopaminergic terminal field in the hippocampal formation of young and adult rat. Neuroscience *14*, 1039-1052.

Vertes, R.P.K., B. (1997). Brainstem–diencephalo-septohippocampal systems controlling the theta rhythm of the hippocampus. Neuroscience *81*, 893-926.

Verwer, R.W.H., Meijer, R.J., Van Uum, H.F.M., and Witter, M.P. (1997). Collateral projections from the rat hippocampal formation to the lateral and medial prefrontal cortex. Hippocampus *7*, 397-402.

Viney, T.J., Lasztoczi, B., Katona, L., Crump, M.G., Tukker, J.J., Klausberger, T., and Somogyi, P. (2013). Network state-dependent inhibition of identified hippocampal CA3 axo-axonic cells in vivo. Nat Neurosci *16*, 1802-1811.

Waelti, P., Dickinson, A., and Schultz, W. (2001). Dopamine responses comply with basic assumptions of formal learning theory. Nature *412*, 43-48.

Wallis, J.D., Anderson, K.C., and Miller, E.K. (2001). Single neurons in prefrontal cortex encode abstract rules. Nature *411*, 953-956.

Wang, S.-H., Redondo, R.L., and Morris, R.G.M. (2010). Relevance of synaptic tagging and capture to the persistence of long-term potentiation and everyday spatial memory. Proc Natl Acad Sci USA *107*, 19537-19542.

Wikenheiser, A.M., and Redish, A.D. (2013). The balance of forward and backward hippocampal sequences shifts across behavioral states. Hippocampus *23*, 22-29.

Wilson, M., and McNaughton, B. (1994). Reactivation of hippocampal ensemble memories during sleep. Science *265*, 676-679.

Wilson, M.A., and McNaughton, B.L. (1993). Dynamics of the hippocampal ensemble code for space. Science *261*, 1055-1058.

Witter, M.P. (1993). Organization of the entorhinal—hippocampal system: A review of current anatomical data. Hippocampus *3*, 33-44.

Witter, M.P., Griffioen, A.W., Jorritsma-Byham, B., and Krijnen, J.L.M. (1988). Entorhinal projections to the hippocampal CA1 region in the rat: An underestimated pathway. Neurosci Lett *85*, 193-198.

Wood, E.R., Dudchenko, P.A., Robitsek, R.J., and Eichenbaum, H. (2000). Hippocampal Neurons Encode Information about Different Types of Memory Episodes Occurring in the Same Location. Neuron *27*, 623-633.

Wyass, J.M., and Van Groen, T. (1992). Connections between the retrosplenial cortex and the hippocampal formation in the rat: A review. Hippocampus *2*, 1-11.

Wyss, J.M., Swanson, L.W., and Cowan, W.M. (1980). The organization of the fimbria, dorsal fornix and ventral hippocampal commissure in the rat. Anat Embryol *158*, 303-316.

Yamaguchi, T., Qi, J., Wang, H.-L., Zhang, S., and Morales, M. (2015). Glutamatergic and dopaminergic neurons in the mouse ventral tegmental area. European Journal of Neuroscience, n/a-n/a.

Yamaguchi, T., Sheen, W., and Morales, M. (2007). Glutamatergic neurons are present in the rat ventral tegmental area. European Journal of Neuroscience *25*, 106-118.

Yamaguchi, T., Wang, H.-L., Li, X., Ng, T.H., and Morales, M. (2011). Mesocorticolimbic Glutamatergic Pathway. J Neurosci *31*, 8476-8490.

Yamaguchi, T., Wang, H.-L., and Morales, M. (2013). Glutamate neurons in the substantia nigra compacta and retrorubral field. European Journal of Neuroscience *38*, 3602-3610.

Yamamoto, J., Suh, J., Takeuchi, D., and Tonegawa, S. (2014). Successful Execution of Working Memory Linked to Synchronized High-Frequency Gamma Oscillations. Cell *157*, 845-857.

Yetnikoff, L., Lavezzi, H.N., Reichard, R.A., and Zahm, D.S. (2014). An update on the connections of the ventral mesencephalic dopaminergic complex. Neuroscience *282*, 23-48.

Ylinen, A., Bragin, A., Nadasdy, Z., Jando, G., Szabo, I., Sik, A., and Buzsaki, G. (1995). Sharp wave-associated high-frequency oscillation (200 Hz) in the intact hippocampus: network and intracellular mechanisms. J Neurosci *15*, 30-46.

Young, B., Fox, G., and Eichenbaum, H. (1994). Correlates of hippocampal complex-spike cell activity in rats performing a nonspatial radial maze task. J Neurosci *14*, 6553-6563.

Young, C.K., and McNaughton, N. (2009). Coupling of Theta Oscillations between Anterior and Posterior Midline Cortex and with the Hippocampus in Freely Behaving Rats. Cerebral Cortex *19*, 24-40.

Zar, J.H. (1999). Biostatistical Analysis (Prentice Hall).

Zhang, K., Ginzburg, I., McNaughton, B.L., and Sejnowski, T.J. (1998). Interpreting Neuronal Population Activity by Reconstruction: Unified Framework With Application to Hippocampal Place Cells. J Neurophysiol *79*, 1017-1044.

Zola-Morgan, S., Squire, L., and Amaral, D. (1986). Human amnesia and the medial temporal region: enduring memory impairment following a bilateral lesion limited to field CA1 of the hippocampus. J Neurosci *6*, 2950-2967.

Zweifel, L.S., Parker, J.G., Lobb, C.J., Rainwater, A., Wall, V.Z., Fadok, J.P., Darvas, M., Kim, M.J., Mizumori, S.J.Y., Paladini, C.A.*, et al.* (2009). Disruption of NMDAR-dependent burst firing by dopamine neurons provides selective assessment of phasic dopamine-dependent behavior. Proc Natl Acad Sci USA *106*, 7281-7288.